STUDY ON HIGH GAIN NON-ISOLATED BIDIRECTIONAL DC-DC CONVERTER FOR EV APPLICATION

A Master's Thesis submitted to the

Department of Electrical Engineering

in fulfillment of the requirement for the degree

MASTER OF ELECTRICAL ENGINEERING

2024

by

Sanju Sardar

Examination Roll No. **M4ELE24014**

Registration No. **163489** of **2022-23**

under the guidance of

Professor Dr. Debashis Chatterjee

Assoc. Prof. Nikhil Mondal

Asst. Prof. Mihir Hembram

DEPARTMENT OF ELECTRICAL ENGINEERING

FACULTY OF ENGINEERING AND TECHNOLOGY

JADAVPUR UNIVERSITY

KOLKATA-700032

Acknowledgements

I believe that only a 'thank you' message cannot express enough gratitude to those who contribute to our process of learning. But it is the conventional way that we acquiesce in doing so.

One of the momentous things that we must learn in our life is to think in simple way and I am mesmerized to learn this thing from my guide Prof. Debashis Chatterjee, co-guides Prof. Nikhil Mondal and Prof. Mihir Hembram who have the ability to sort out complicated and grave issues in simple yet logical way. Their sound knowledge of technology and sincerity towards work amaze me. Despite their busy schedule, they helped me every time I was in need of them.

I want to thank prof. Debashis Chatterjee for providing me with the appropriate ambience to carry out my degree in Master of Electrical Engineering.

I would also like to ventilate my gratitude to the research scholar, Subinay Sarkar, without whom, the project would not have been completed successfully. Moreover, I thank all the library assistants for their cooperation.

Last but not least, I owe my gratitude to my friends Supravat Saren and Susnata Kanjilal for their suggestions; to Amit Pal for his encouragement; to Panchasree Chandra for constant emotional support; and to my family members who have sacrificed a lot to make me reach the position I am at today.

Date - 29/08/2024

Sanju Sardar

Department of Electrical Engineering

Jadavpur University, Kolkata-700032

CERTIFICATE

JADAVPUR UANIVERSITY

Faculty of Engineering and Technology

CERTIFICATE

We hereby recommend the thesis entitled **"Study on High Gain Non-Isolated Bidirectional DC-DC Converter for EV Application"** prepared by **Sanju Sardar**, under our supervision and guidance, to be accepted in fulfillment of the requirements for conferring the degree of **"Master of Electrical Engineering"** at Jadavpur university. The project, in our opinion, is worthy of its acceptance.

Supervisors

Debashis Chatterjee 29/08/2024

Dr. Debashis Chatterjee
Professor
Department of Electrical Engineering

Professor
Electrical Engineering Department
JADAVPUR UNIVERSITY
Kolkata - 700 032

Nikhil Mondal 29.08.24

Mr. Nikhil Mondal
Associate Professor
Department of Electrical Engineering

Associate Professor
Electrical Engg. Dept.
Jadavpur University
Kolkata - 700 032

29/08/24

Mr. Mihir Hembram
Assistant Professor
Department of Electrical Engineering

Assistant Professor
Electrical Engg. Dept.
Jadavpur University
Kolkata - 700 032

countersigned by

Biswanath 29/08/2024

Head of the Department
Department of Electrical Engineering
Jadavpur University
Kolkata-70032

Head
Electrical Engineering Department
JADAVPUR UNIVERSITY
Kolkata - 700 032

Dipak Lala 29.8.24

Dean
Faculty of Engineering and Technology
Jadavpur University
Kolkata- 70032

DEAN
Faculty of Engineering & Technology
JADAVPUR UNIVERSITY
KOLKATA-700 032

Page | II

Faculty of Engineering and Technology

Jadavpur University, Kolkata- 700032

Certificate of Approval

The thesis entitled **"Study on High Gain Non-Isolated Bidirectional DC-DC Converter for EV Application"** is hereby approved as a creditable study of an Engineering subject carried out and presented in a manner that fulfils its acceptance as a prerequisite to the degree for which it is submitted. It is understood that by this approval, the undersigned does not necessarily endorse or approve of any statement made, opinion expressed, or conclusion drawn therein but approves of the thesis only for the purpose for which it is submitted.

BOARD OF EXAMINERS

The final examination for evaluation of the thesis _____

_____

_____

_____

(Signature of Examiners)

Declaration of Originality and Compliance with Academic Ethics

I hereby declare that this thesis contains original work done by me, as a part of his degree in Master of Electrical Engineering. All the information in this document has been obtained and presented according to academic rules and ethical conduct.

I also declare that, as required by these rules and conduct, I have cited and referenced all materials and results that are not original to this work.

Name: Sanju Sardar

Examination Roll No: M4ELE24014

University Registration No: 163489 of 2022-23

Thesis Title: Study on High Gain Non-Isolated Bidirectional DC-DC Converter for EV Application

Date - 29/08/2024

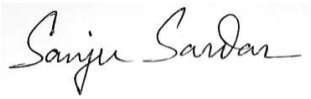

Signature of the student

Table of Contents

List of symbols

$\mathbf{D}$	**:** Duty ratio
$\mathbf{f_s}$	**:** Switching frequency
$\mathbf{I_{in}}$	**:** Input current of converter
$\mathbf{I_o}$	**:** Output current of converter
$\mathbf{I_{LV}}$	**:** Current at low voltage side
$\mathbf{I_{HV}}$	**:** Current at high voltage side
$\mathbf{I_{L1}}$	**:** Current through 'L1' inductor
$\mathbf{I_{L2}}$	**:** Current through 'L2' inductor
$\mathbf{I_{CH}}$	**:** Charging current
$\mathbf{P_{in}}$	**:** Input Power
$\mathbf{P_O}$	**:** Output Power
$\mathbf{T_{ON}}$	**:** The switch is on for a time period T
$\mathbf{T_{OFF}}$	**:** The switch is off for a time period T
$\mathbf{V_i}$	**:** Input voltage of converter
$\mathbf{V_o}$	**:** Output voltage of converter
$\mathbf{V_L}$	**:** Voltage at low voltage side
$\mathbf{V_H}$	**:** Voltage at high voltage side
$\mathbf{V_D}$	**:** Voltage across diode
$\mathbf{V_{L1}}$	**:** Voltage across inductor 'L1'
$\mathbf{V_{L2}}$	**:** Voltage across inductor 'L2'
$\mathbf{V_{Sx}}$	: Voltage across $(MOSFET)_x$ or S_x ; for x=1,2,3,4….
$\boldsymbol{\eta}$	: Efficiency

ABSTRACT

This study introduces a novel non-isolated high-gain bidirectional DC-DC converter designed for the efficient integration of energy storage systems with electric vehicles. The proposed converter achieves high voltage gain through a dual duty cycle operation while employing fewer components, thereby optimizing circuit design. The innovative topology utilizes dual current path inductor structures, reducing inductor size and eliminating the need for additional clamping circuits. Unlike traditional methods that rely on voltage multiplier cells or hybrid switched-capacitor approaches, this converter achieves significant voltage gain without these complexities. The performance of converter is analysed through MATLAB/Simulink simulations under various driving conditions. During forward motoring, the converter power delivers the motor from the battery; while during regenerative braking, the motor functions as a generator and the energy is transferred back through converter to battery where it is stored. This converter is contributing to energy recovery and enhancing overall efficiency.

1

Introduction

The use of renewable energy resources has recently increased to save the environment and conserve remaining fossil fuels, leading to a higher demand for energy storage solutions. In applications such as electric vehicles, interfacing energy storage with both the load and source is crucial for creating reliable and efficient systems. Bidirectional DC-DC converters play a key role in interfacing batteries and supercapacitors as storage devices, enhancing system reliability.

The automobile industry is focusing on developing new technologies for powertrains, batteries, and charging infrastructure in response to the growing demand for vehicles with improved fuel efficiency and reduced environmental impact. The integration of high-energy battery packs and regenerative braking systems helps extend the driving range and battery life of electric vehicles.

Power electronic converters play a crucial role in the drivetrain of electric and hybrid vehicles, where they manage the power flow from the battery to the propulsion motors and enable regenerative braking. To enhance efficiency and power density, the drivetrain motor and propulsion inverter are designed to operate at higher voltages. A boost converter is used to elevate the battery voltage to the required level, which also improves the overall performance of the drivetrain by decoupling the battery voltage from the inverter's DC link voltage.

The DC-DC converter must be bidirectional to handle both forward and reverse power flow. In forward mode, it manages transient and overload conditions by transferring power from the battery to the load. In reverse mode, it ensures that the battery pack is recharged during regenerative braking or other scenarios where power needs to flow back to the battery. This bidirectional capability is essential for maintaining efficient and flexible energy management within the vehicle's drivetrain.

Providing a Bidirectional DC-DC Converter (BDC) between the battery and the inverter offers several benefits. It reduces the stress on the inverter by adding an additional DC stage, adjusts the inverter supply voltage to enhance motor output, allows for a reduction in the cost and size of the battery due to a lower cell count requirement, and enables manufacturers to design the system voltage and battery independently.

These technological advancements are crucial in meeting the growing demand for vehicles that offer better fuel efficiency and reduced environmental impact, making them essential components in the future of sustainable transportation.

1.1 Literature Review

In the paper [1] titled "Bidirectional DC-DC Power Converters: A Review of Topologies and Control Schemes" presents a comprehensive analysis of bidirectional DC-DC power converters, which are increasingly used in applications requiring power flow in both forward and reverse directions, such as energy storage systems, electric vehicles, and renewable energy systems. The paper categorizes these converters into two main types: non-isolated and isolated topologies, each further divided into eight groups with respective schematics and summaries. The review also delves into various control schemes commonly applied to DC-DC converters, including PID, sliding mode, fuzzy, model predictive, and digital control. Special attention is given to switching strategies designed specifically for isolated bidirectional converters, like single phase shift, dual phase shift, and triple phase shift, which aim to enhance performance. The paper discusses the features, applications, and research trends of each topology and control scheme, emphasizing the ongoing efforts to optimize converter design by minimizing weight, volume, losses, and cost while maximizing reliability and power density. Additionally, the review highlights the importance of advanced solid-state semiconductors, wireless power transfer, and the development of soft-switching control strategies that achieve zero-voltage switching across all operation modes.

In the paper [2] titled "DC–DC Converter for Dual-Voltage Automotive Systems Based on Bidirectional Hybrid Switched-Capacitor Architectures" by D. Flores Cortez, G. Waltrich, J. Fraigneaud, H. Miranda, and I. Barbi, published in IEEE Transactions on Industrial Electronics, addresses the growing demand for advanced power electronic converters in automotive embedded electronic systems, which are increasing in power and complexity. The authors propose a bidirectional high-efficiency converter with a reduced number of components compared to traditional architectures. This innovative converter combines a switched-capacitor converter with a conventional bidirectional converter, resulting in a hybrid topology where the voltage across the semiconductors is equal to half of the highest voltage source value. The design features only one inductor to manage power flow between the two voltage sources, and the prototype implementation achieved a maximum efficiency of 97.5%. The study presents detailed analyses and experimental validation for both buck and boost operation modes, showing efficiencies of 97.5% and approximately 96.3%, respectively, at a switching frequency of 70 kHz. The converter's low current ripple on the low voltage and high current side makes it particularly suitable for automotive applications. The authors suggest that the proposed topology can achieve even higher efficiencies when designed for higher power levels.

In the paper [3] titled "A Bidirectional DC–DC Converter With High Voltage Conversion Ratio and Zero Ripple Current for Battery Energy Storage System" by Z. Wang, P. Wang, B. Li, X. Ma, and P. Wang, published in IEEE Transactions on Power Electronics, introduces an innovative bidirectional DC–DC converter (BDC) tailored for battery energy storage systems (BESS). This novel BDC incorporates an active switched-inductor (A-SL) cell, a zero current ripple cell, and an auxiliary capacitor cell, achieving high voltage conversion ratios and low voltage stresses on power switches. Additionally, it maintains a constant potential difference between the grounds of the low voltage side (LVS) and high voltage side, which is crucial for system stability. The synchronous rectification technology further enhances the efficiency of

the proposed BDC. The authors present comprehensive operating principles, characteristics analysis, and parameter design, demonstrating the BDC's superiority through comparison with other BDCs. Experimental validation using a 1000 W prototype showcases maximum conversion efficiencies of 96.43% in step-up mode and 96.67% in step-down mode. The proposed BDC's low LVS current ripple effectively protects the BESS, extending its service life and making it an excellent interface for linking BESS to the DC bus of the grid without requiring extreme duty cycles. These attributes underscore the BDC's suitability for BESS applications, enhancing both dynamic performance and conversion efficiency.

In the paper [4] titled "A Switched-Capacitor Bidirectional DC–DC Converter With Wide Voltage Gain Range for Electric Vehicles With Hybrid Energy Sources" by Y. Zhang, Y. Gao, L. Zhou, and M. Sumner, published in IEEE Transactions on Power Electronics, presents a novel switched-capacitor bidirectional DC–DC converter designed for electric vehicles with hybrid energy source systems. This converter is distinguished by its simplicity, reduced component count, wide voltage gain range, low voltage stress, and common ground configuration. The incorporation of synchronous rectifiers enables zero voltage switching (ZVS) turn-on and turn-off without additional hardware, thereby enhancing efficiency. Experimental validation with a 300 W prototype demonstrates the converter's capability to handle a variable low-voltage side (40–100 V) while maintaining a constant high-voltage side (300 V), achieving a maximum efficiency of 94.45% in step-down mode and 94.39% in step-up mode. The proposed topology's ability to rapidly respond to load step changes makes it effective for interfacing low-voltage supercapacitors with the high-voltage DC bus in hybrid energy storage systems (HESS) for electric vehicles. The converter's high step-up/step-down ratio, reduced voltage stress, and efficient ZVS operation meet the dynamic response requirements and protect the battery from current step changes, making it an ideal solution for power interfacing in EV applications.

In the paper [5] titled "A Wide Voltage Gain Bidirectional DC–DC Converter Based on Quasi Z-Source and Switched Capacitor Network" by A. Kumar, X. Xiong, X. Pan, M. Reza, A. R. Beig, and K. A. Jaafari, published in IEEE Transactions on Circuits and Systems II: Express Briefs, introduces a novel bidirectional DC-DC converter designed to integrate energy storage units with hybrid electric vehicles. This converter leverages the quasi Z-source and switched capacitor network to achieve higher voltage gain at lower duty cycles, thereby avoiding inductor core saturation problems commonly seen in other converters. Additionally, it exhibits lower voltage stress across capacitors. The paper provides an in-depth discussion of the converter's operation, steady-state analysis, and voltage and current stress analysis, alongside a comparative analysis with existing converters. Experimental and simulation setups validate the proposed converter's feasibility, demonstrating its effectiveness in both directions. The converter achieves a maximum efficiency of 96.5% and a minimum efficiency of 91.3%. The analysis confirms that the proposed topology outperforms other reported converters in terms of achieving high voltage gain in the boost stage without significantly increasing passive elements and maintaining the lowest voltage stress across capacitors. These features make it an ideal solution for high voltage gain applications in hybrid electric vehicles.

In the paper [6] titled "A Switched-Capacitor Interleaved Bidirectional Converter With Wide Voltage-Gain Range for Super Capacitors in EVs" by Y. Zhang, W. Zhang, F. Gao, S. Gao, and D. J. Rogers, published in IEEE Transactions on Power Electronics, presents a novel switched-capacitor interleaved bidirectional DC–DC converter designed for integrating supercapacitors in electric vehicles (EVs). The proposed converter combines a three-phase interleaved structure with switched-capacitor cells, offering a wide voltage-gain range, low current ripple on the low-voltage side (LVS), and reduced voltage stress across power switches. It maintains an absolute common ground between input and output, enhancing system stability and scalability. The paper provides detailed analysis of the converter's operating principles and stresses, and experimental validation with an 800 W prototype shows impressive performance, achieving maximum efficiencies of 95.8% in step-up mode and 95.9% in step-down mode. The converter's ability to handle a high voltage (400 V) and variable low voltage (30–100 V), along with its low ripple and voltage stress characteristics, makes it an excellent choice for interfacing supercapacitor banks with a constant high-voltage DC bus in hybrid energy source EVs.

In the paper [7] titled "Interleaved Switched-Capacitor Bidirectional DC-DC Converter With Wide Voltage-Gain Range for Energy Storage Systems" by Y. Zhang, Y. Gao, J. Li, and M. Sumner, published in IEEE Transactions on Power Electronics, introduces a bidirectional DC–DC converter designed to efficiently manage energy storage systems with a wide voltage-gain range. This converter utilizes an interleaved switched-capacitor structure on the low-voltage side to reduce current ripple and a series-connected structure on the high-voltage side to achieve high step-up/step-down voltage gains. The bidirectional synchronous rectification is implemented without additional hardware, enhancing overall efficiency. The paper details the converter's operating principles, voltage and current stresses, and current ripple characteristics. Experimental validation with a 1 kW prototype demonstrates the converter's capability to handle a variable low-voltage side (50–120 V) and a constant high-voltage side (400 V), achieving maximum efficiencies of 95.21% in step-up mode and 95.30% in step-down mode. The converter's benefits include high voltage gain, low voltage stress on power semiconductors and capacitors, and reduced current ripple. Its design allows for ZVS (zero-voltage switching) turn-on and turn-off, and the self-balancing function of capacitors and inductor currents enhances dynamic and steady-state performance. This topology is well-suited for interfacing low-voltage battery packs with high-voltage DC buses in various new energy storage systems.

In the paper [8] titled "Hybrid Switched-Capacitor/Switched-Quasi-Z-Source Bidirectional DC–DC Converter With a Wide Voltage Gain Range for Hybrid Energy Sources EVs" by Y. Zhang, Q. Liu, Y. Gao, J. Li, and M. Sumner, published in IEEE Transactions on Industrial Electronics, presents an advanced bidirectional DC–DC converter tailored for electric vehicles (EVs) with hybrid energy sources. This novel converter combines a switched-capacitor cell with a switched-quasi-Z-source topology, offering a wide voltage gain range and reduced voltage stresses on power switches compared to traditional quasi-Z-source converters. The design improves performance by repositioning the main power switch and integrating the switched-capacitor cell on the high-voltage side, resulting in lower voltage stress across the power switches. The paper provides a thorough analysis of the converter's operating principles, voltage and current stresses, and compares it with existing converters. It also details the

parameter design, dynamic modelling, and voltage control scheme. Experimental results from a 400 W prototype validate the converter's theoretical analysis, demonstrating its effective balance of voltage gain, component count, and stress levels. The proposed converter's simple structure, robust dynamic and static performance, and ease of control make it a viable solution for hybrid energy source EV applications.

In the paper [9] titled "Analysis and Implementation of a Novel Bidirectional DC–DC Converter" by L.-S. Yang and T.-J. Liang, published in IEEE Transactions on Industrial Electronics, introduces a novel bidirectional DC–DC converter distinguished by its simple circuit configuration and high performance. The converter utilizes a coupled inductor with identical winding turns on both primary and secondary sides, enabling high voltage gains in both step-up and step-down modes. In step-up mode, the primary and secondary windings are operated in parallel charge and series discharge, while in step-down mode, they are operated in series charge and parallel discharge, achieving greater voltage gains compared to conventional bidirectional boost/buck converters. The proposed converter also features a lower average switch current under the same electrical specifications. The paper details the operating principles, steady-state analysis, and presents experimental results from a 14/42-V prototype, demonstrating efficiencies of 92.7% in step-up mode and 93.7% in step-down mode, with a range of 92.7%–96.2% and 93.7%–96.7% respectively. These results highlight the proposed converter's improved efficiency and performance over traditional bidirectional converters.

In the paper [10] titled "Non-Isolated High Gain DC–DC Converter for DC Microgrids" by M. Lakshmi and S. Hemamalini, published in the IEEE Transactions on Industrial Electronics, addresses the need for high-efficiency, high-gain DC–DC converters essential for integrating low output voltage renewable energy sources like solar photovoltaics and fuel cells into DC microgrids. The authors propose a novel converter topology that eschews the traditional voltage multiplier cell and hybrid switched-capacitor techniques, instead employing two non-isolated inductors connected in series/parallel during their discharging/charging phases. This innovative approach allows the converter to achieve high voltage gain through the operation of switches with two different duty ratios, avoiding the drawbacks of extreme duty ratios. The paper provides a thorough steady-state analysis of the converter's performance with these dual duty ratios. Experimental validation is conducted using a 100 W, 20/200 V prototype circuit, demonstrating an efficiency of 93.6% at full load, which aligns closely with the theoretical efficiency. Although the converter showed a 2.5% output voltage variation under open-loop conditions due to load changes, the authors suggest that implementing a closed-loop control strategy could effectively regulate this variation, making the converter highly suitable for microgrid applications.

In the paper [11] titled "Performance Analysis of a High Gain Bidirectional DC-DC Converter Fed Drive for an Electric Vehicle With Battery Charging Capability During Braking" by C. P. Ragasudha and S. Hemamalini, published in IEEE Access, introduces a novel non-isolated high gain bidirectional DC–DC converter (HGBDC) designed for electric vehicles (EVs). This converter achieves high voltage gain through a dual duty cycle operation while employing

fewer components compared to conventional designs. It utilizes a dual current path inductor structure, eliminating the need for additional clamping circuits and avoiding voltage multiplier cells or hybrid switched-capacitor techniques. The proposed converter is evaluated using MATLAB/Simulink and real-time simulations, demonstrating its capability to power the motor during driving and recover energy during regenerative braking, which is then transferred back to the battery. The study highlights the converter's effective balancing of voltage gain and component count, making it a viable solution for interfacing storage devices with the DC link in EVs. The converter's performance in motoring and regenerative braking modes shows potential for further improvement with SiC power switches and soft switching to enhance efficiency at higher frequencies.

1.2 Motivation of the proposed work

Governments and organizations are tightening regulations on fuel consumption and emissions due to increasing oil use in transportation and concerns about global warming and energy depletion. With forecasts indicating that annual sales of electric vehicles and hybrid electric vehicles will exceed those of conventional petrol and diesel vehicles, the automotive industry is prioritizing advancements in powertrain technology, battery development, and charging infrastructure. This shift is driven by a rising demand for vehicles that offer superior fuel efficiency and a reduced environmental footprint. The motivation for developing a high-gain bidirectional DC-DC converter for an electric vehicle with battery charging capability during regenerative braking is driven by several key factors related to efficiency, performance, and overall vehicle effectiveness. Here is a breakdown of the primary motivations:

During regenerative braking, the bidirectional converter facilitates the conversion of the recovered energy into a suitable form for battery charging. This is particularly important for optimizing the use of regenerative braking to not only enhance vehicle performance but also to maintain battery charge and health.

By efficiently managing and converting energy between the battery and the drive system, a high-gain bidirectional converter helps in maximizing the driving range of vehicle. Effective use of regenerative braking and energy management contributes to a more efficient use of the battery capacity.

2

Basics of DC-DC Converter

2.1 Power Electronic Converter

Power electronics is the study of controlled conversion of electrical energy from one form to another in an efficient, clean, compact and robust manner for its better utilization. This conversation is done using a combination of power semiconductor devices and passive component such as transformer, inductor, capacitor etc. the system used for this conversation utilizing various electrical components.

Development in the field power semiconductor and solid-state devices with very high voltage and current ratings have made power electronic converters well equipped for use in versatile applications ranging from very low power to very high power.

The main classes of power electronic converters include-

I.AC to DC converters called rectifiers
II. DC to AC converters called inverters
III. AC to AC converters
IV. DC to DC converters

DC to DC converters change the DC voltage and current levels using the switching mode operation of semiconductor devices.

For controlling power flow to load, semiconductor devices used in power electronic converters are either fully on or fully off. With switches fully on, a power semiconductor device handles large current with negligible voltage drop across it. When the switch is off, they allow negligible current with full voltage across them. This phenomenon facilities with low power loss as in switches.

Due to this reason power electronic converters are considered to be much more efficient. Advantages of power electronic converters includes-

(a) Higher efficiency due to losses.

(b) Higher reliability due to low losses.

(c) Low maintenance

(d) Fast dynamics response.

(e) smaller size

(f) less weight

(g) Lower cost

Generalized semiconductor-based power electronic converter can be described, as shown in figure 2.1.

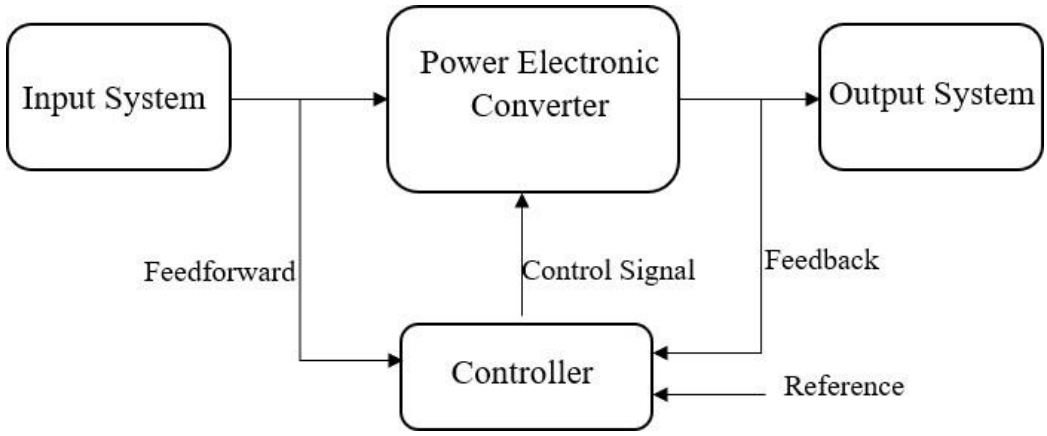

Figure 2.1 Block diagram of Power electronic converter

2.2 DC to DC Converters

A DC to DC converter converts a fixed/variable DC input to a controllable dc output. These converters mainly consist of switching circuits and filter sections and sometimes a transformer for steeping up or stepping down voltage.

DC to DC converters are generally used for regulated DC power supply in computers, various medical instruments, communication devices, television receivers, battery chargers and many more. They are also used to provide regulated variable DC voltage for DC motor speed control applications.

Several methods exist to achieve DC to DC voltage conversions which include using popular non-isolated converters such as buck, boost, buck-boost, cuck converters. Each of these converters has its specific benefits and drawbacks depending on operating modes and specifications such as voltage conversion ratio range, output power, power conversion efficiency, number of components etc. There also are isolated converters like, forward, flyback, push pull etc. However, in some applications isolation is a not mandatory requirement and non-isolated converters meeting required specifications can be employed. This simplifies design and implementation processes.

The processes requiring voltage gain cannot employ buck converters. Besides, buck-boost converter is not usually chosen in these cases, as the output voltage polarity in buck-boost converter is inverted with respect to input. Therefore, boost converter is the best option.

A step up or boost converter produces higher output voltage than the input. Here inductor is placed between input source and switch. Energy stored in inductor is used to increase or boost the voltage when the switch is off.

2.2.1 Buck converter

The Buck converter is a switch mode power device that outputs a DC voltage that is lower than the input DC voltage. A simplified version of the Buck converter can be seen in figure 2.2. The Buck converter requires a power switch, a power diode, a capacitor and an inductor.

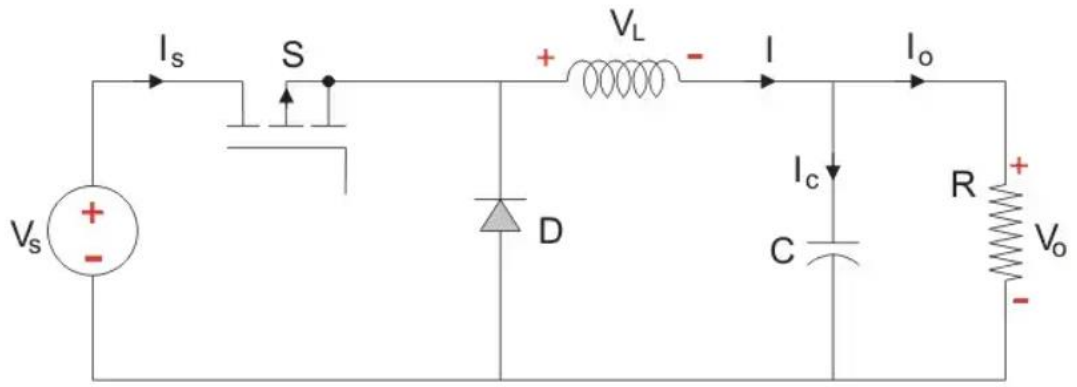

Figure 2.2 Buck converter

During normal operation, the Buck converter can operate in two states: the on-state and the off-state are explained below.

- **<u>On-state</u>**

The on-state circuit diagram as shown in figure 2.3. Whilst in the on-state, current is supplied from the voltage source, charging the inductor and supplying a current to the load. The stored energy in the inductor also increases and the magnetic field around it expands. In this mode the diode is reverse biased, meaning that it doesn't conduct current and is considered to be turned off.

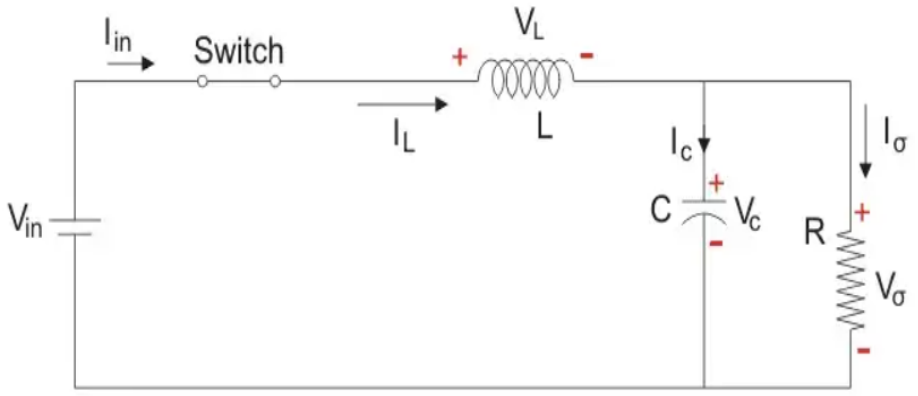

Figure 2.3 Buck converter operation in on-state

Let, the switch is on for a time T_{ON} and off for time T_{OFF}.

We define the time period T as, $T = T_{ON} + T_{OFF}$

And the switching frequency, $f_{switching} = \frac{1}{T}$

The duty cycle, $D = \frac{T_{ON}}{T}$

$T_{ON} = DT$

$T_{OFF} = T - T_{OFF} = T - DT = (1 - D)T$

- Steady state operation for ON state by using KVL

$$V_{in} = V_L + V_o$$
$$V_L = L\frac{di_L}{dt} = V_{in} - V_o$$
$$\frac{di_L}{dt} = \frac{\Delta i_L}{\Delta t} = \frac{\Delta i_L}{DT} = \frac{V_{in} - V_o}{L}$$

So, $(\Delta i_L)_{ON} = \left(\frac{V_{in} - V_o}{L}\right) DT$ (1)

- **Off-state**

Whilst in the off-state, the switch is turned off and the magnetic field around the inductor starts to collapse, reinserting the stored energy to the circuit. The back e.m.f causes the voltage polarity of the inductor to become reversed. Due to the reversed voltage polarity, the diode becomes forward biased and it begins to conduct. During the off-state both the inductor and the capacitor supplies the load with current.

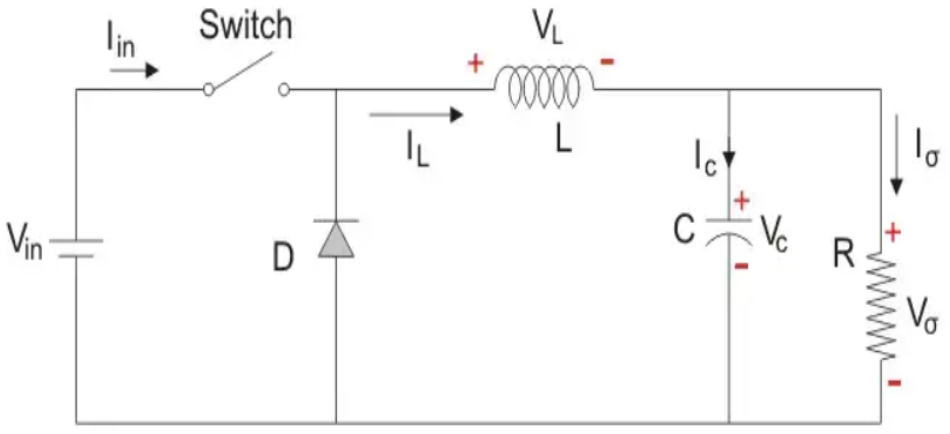

Figure 2.4 Buck converter operation in off-state

- Steady state operation for OFF state by using KVL

$$0 = V_L + V_o$$
$$V_L = L\frac{di_L}{dt} = -V_o$$
$$\frac{di_L}{dt} = \frac{\Delta i_L}{\Delta t} = \frac{\Delta i_L}{(1-D)T} = \frac{-V_o}{L}$$

So, $(\Delta i_L)_{OFF} = \left(\frac{-V_o}{L}\right)(1 - D)T$ (2)

We know, the net change of the inductor current over complete cycle is zero. So, equation (1) & (2) are combined and get equation (3).

$$(\Delta i_L)_{ON} + (\Delta i_L)_{OFF} = 0$$

$$\left(\frac{V_{in} - V_o}{L}\right) DT + \left(\frac{-V_o}{L}\right)(1 - D)T = 0$$

Finally, $\frac{V_o}{V_{in}} = D$ (3)

A desired output voltage can be produced by controlling the power switch of the Buck converter with pulse width modulation. The relationship between the voltages and the duty cycle, D, can be seen in equation (3).

Conversion Ratio: $\mathbf{D = \frac{V_{out}}{V_{in}}}$

When designing a Buck converter, the following equations are useful.

Inductor current ripple: $\Delta i_L = \frac{V_{in} * D(1-D)T}{L}$ (4)

Capacitor Ripple Voltage: $\Delta V_c = \frac{V_o(1-D)T^2}{8LC}$ (5)

Critical Inductance: $L_c = \frac{(1-D)T * R}{2}$ (6)

Critical Capacitance: $C_c = \frac{(1-D)T^2}{16 * L}$ (7)

2.2.2 Boost converter

The Boost converter requires the same components as the Buck converter but in a different configuration, as can be seen in figure 2.5. The Boost converter, as the name suggests, outputs a voltage that is higher than the input voltage.

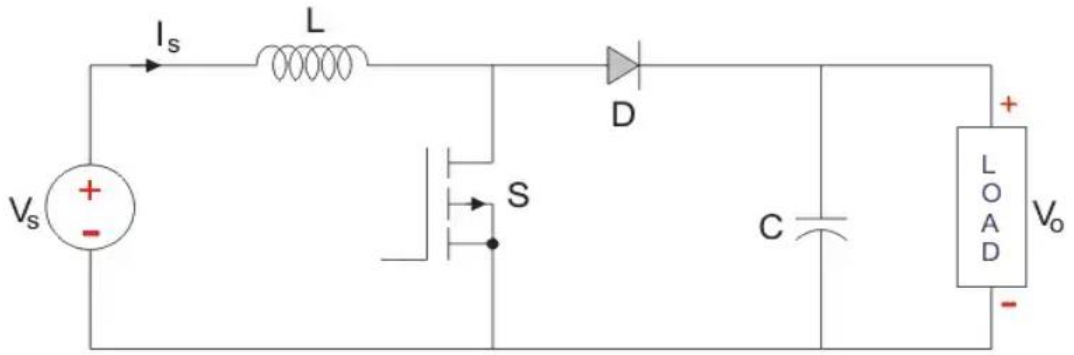

Figure 2.5 Boost Converter

During normal operation, the Boost converter has two states: the on-state and the off-state are explained below.

- **On-state**

During the on-state, The polarity of the left side of the inductor is positive and the current through the inductor increases its stored energy by generating magnetic field. In this mode the diode is reverse biased which separates the two sides of the converter, the inductor side and load side. Whilst the diode isn't conducting, the energy stored in the capacitor is being supplied to the load.

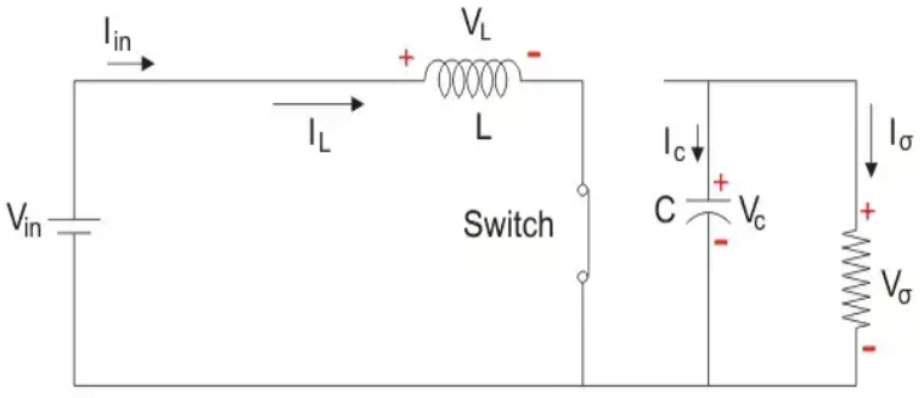

Figure 2.6 Boost Converter operation in on-state

Let, the switch is on for a time T_{ON} and off for time T_{OFF}.

We define the time period T as, $T = T_{ON} + T_{OFF}$

And the switching frequency, $f_{switching} = \frac{1}{T}$

The duty cycle, $D = \frac{T_{ON}}{T}$

$T_{ON} = DT$

$T_{OFF} = T - T_{OFF} = T - DT = (1 - D)T$

- Steady state operation for ON state by using KVL

$$V_{in} = V_L$$
$$V_L = L\frac{di_L}{dt} = V_{in}$$
$$\frac{di_L}{dt} = \frac{\Delta i_L}{\Delta t} = \frac{\Delta i_L}{DT} = \frac{V_{in}}{L}$$

So, $(\Delta i_L)_{ON} = \left(\frac{V_{in}}{L}\right)DT$ (8)

- **Off-state**

In the off-state the power switch is turned off. During the off-state the magnetic field previously created will be reduced in energy to maintain the current through the inductor. For this, The polarity of the inductor will be reversed, which means the left side of the inductor will become

negative and the diode becomes forward biased. The stored energy in the inductor results in a current flowing to the capacitor and the load. Unlike the Buck converter, the inductor of the Boost converter is always connected to the power supply. This means that its always being charged and that is how the converter can produce a voltage higher than the input voltage.

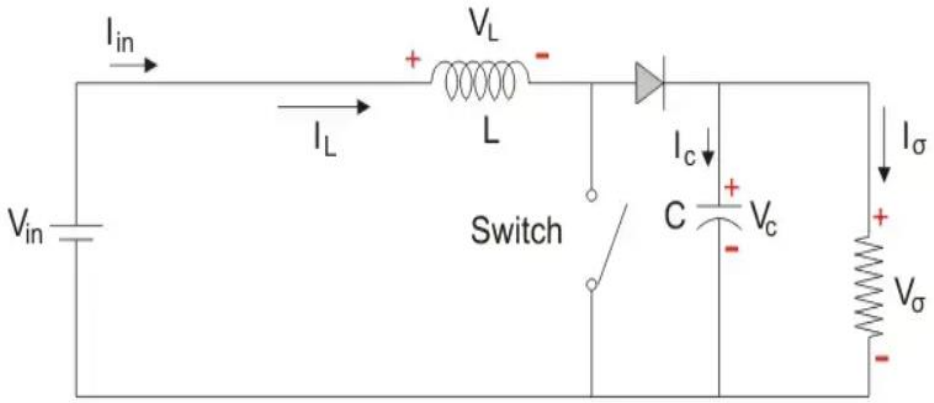

Figure 2.7 Boost converter operation in off-state

- Steady state operation for OFF state by using KVL

$$V_{in} = V_L + V_o$$
$$V_L = L\frac{di_L}{dt} = V_{in} - V_o$$
$$\frac{di_L}{dt} = \frac{\Delta i_L}{\Delta t} = \frac{\Delta i_L}{(1-D)T} = \frac{V_{in} - V_o}{L}$$

So, $(\Delta i_L)_{OFF} = \left(\frac{V_{in} - V_o}{L}\right)(1 - D)T$ (9)

We know, the net change of the inductor current over complete cycle is zero. So, equation (8) & (9) are combined and get equation (10).

$$(\Delta i_L)_{ON} + (\Delta i_L)_{OFF} = 0$$
$$\left(\frac{V_{in} - V_o}{L}\right)(1 - D)T + \left(\frac{-V_o}{L}\right)DT = 0$$

Finally, $\frac{V_o}{V_{in}} = \frac{1}{1-D}$ (10)

By controlling the power switch of the Boost converter with PWM, a desired output voltage can be produced. The relationship between the voltages and the duty cycle, D, can be seen in equation (10).

Conversion Ratio: $\mathbf{\frac{V_{out}}{V_{in}} = \frac{1}{1-D}}$

When designing a Boost converter, the following equations are useful

Inductor current ripple: $\Delta i_L = \frac{V_{in} * DT}{L}$ (11)

Capacitor Ripple Voltage: $\Delta V_c = \frac{V_o\, DT}{RC}$ (12)

Critical Inductance: $L_c = \frac{D(1-D)T * R}{2}$ (13)

Critical Capacitance: $C_c = \frac{DT}{2R}$ (14)

2.2.3 Buck Boost Converter

The buck boost converter is a type DC to DC converter, The output voltage of this converter is either less than or greater than the input voltage. The output voltage of the magnitude depends on the duty cycle denoted as D. These converters are also known as the step up and step down DC-DC converter and these names are coming from the analogous step up and step down transformer. By using the low conversion energy, the input power is equal to the output power. The following expression shows the low of a conversion.

Input Power (P_{in}) = Output Power (P_{out})

For step up mode, the input voltage is less than the output voltage ($V_{in} < V_{out}$). It shows that the output current is the less than the input current. Hence the buck booster is a step up mode.

$V_{in} < V_{out}$ and $I_{in} > I_{out}$

In the step down mode the input voltage is greater than output voltage ($V_{in} > V_{out}$). It follows that the output current is greater the input current. Hence the buck boost converter is a step down mode.

$V_{in} > V_{out}$ and $I_{in} < I_{out}$

A typical Buck-Boost converter circuit is shown below figure 2.8. The input voltage source is connected to a solid-state device. The second switch used is a diode. The diode is connected, in reverse to the direction of power flow from source, to a capacitor and the load and the two are connected in parallel.

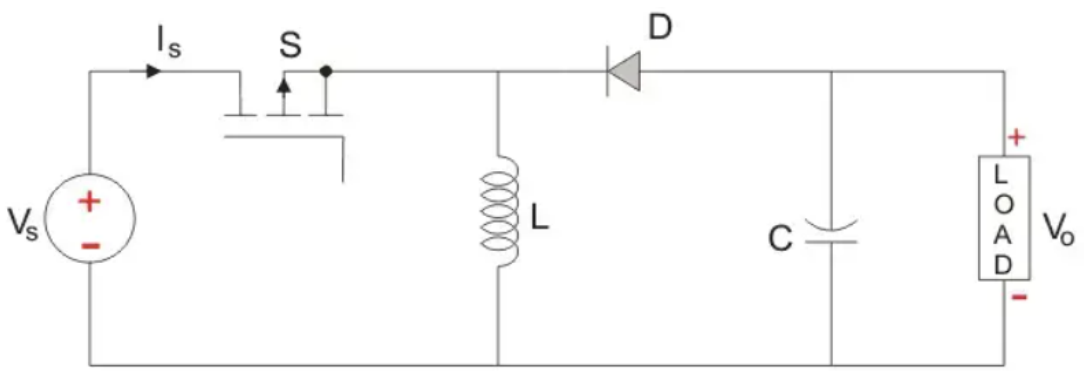

Figure 2.8 Buck-Boost Converter

During the on-state, the Buck Boost converter has two states: the on-state and the off-state are explained below.

- **On-state**

In the On-state, the input voltage source is directly connected to the inductor (L). This results in accumulating energy in L. In this stage, the capacitor supplies energy to the output load. The on-state circuit diagram of buck-boost is shown in figure 2.9.

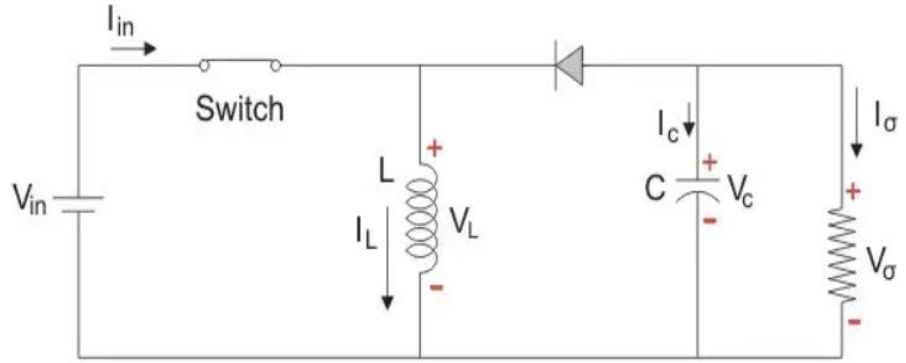

Figure 2.9 Buck-Boost Converter operation in on-state

Let, the switch is on for a time T_{ON} and off for time T_{OFF}.

We define the time period T as, $T = T_{ON} + T_{OFF}$

And the switching frequency, $f_{switching} = \frac{1}{T}$

The duty cycle, $D = \frac{T_{ON}}{T}$

$T_{ON} = DT$

$T_{OFF} = T - T_{OFF} = T - DT = (1 - D)T$

- Steady state operation for ON state by using KVL

$$V_{in} = V_L$$
$$V_L = L\frac{di_L}{dt} = V_{in}$$
$$\frac{di_L}{dt} = \frac{\Delta i_L}{\Delta t} = \frac{\Delta i_L}{DT} = \frac{V_{in}}{L}$$

So, $(\Delta i_L)_{ON} = \left(\frac{V_{in}}{L}\right) DT$ (15)

- **Off-state**

In the Off-state, the polarity of the inductor is reversed and the energy stored in the inductor is released and is ultimately dissipated in the load resistance and this helps to maintain the flow of current in the same direction through the load. The inductor is connected to the output load

and capacitor, so energy is transferred from L to C and R. The off-state circuit diagram of buck-boost is shown in figure 2.10.

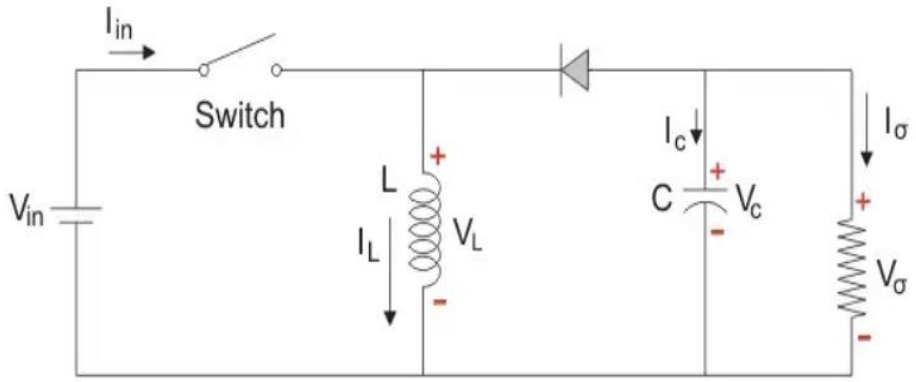

Figure 2.10 Buck-Boost converter operation in off-state

- Steady state operation for OFF state by using KVL

$$V_L = \mathrm{V_o}$$
$$\mathrm{V_L} = \mathrm{L}\frac{\mathrm{di_L}}{\mathrm{dt}} = V_o$$
$$\frac{\mathrm{di_L}}{\mathrm{dt}} = \frac{\Delta \mathrm{i_L}}{\Delta \mathrm{t}} = \frac{\Delta \mathrm{i_L}}{(1-\mathrm{D})\mathrm{T}} = \frac{V_{in} - \mathrm{V_o}}{\mathrm{L}}$$

So, $(\Delta i_L)_{OFF} = \left(\frac{\mathrm{V_o}}{\mathrm{L}}\right)(1-D)T$ (16)

We know, the net change of the inductor current over complete cycle is zero. So, equation (15) & (16) are combined and get equation (17)

$$(\Delta \mathrm{i_L})_{\mathrm{ON}} + (\Delta \mathrm{i_L})_{\mathrm{OFF}} = 0$$
$$\left(\frac{\mathrm{V_o}}{\mathrm{L}}\right)(1-\mathrm{D})\mathrm{T} + \left(\frac{-\mathrm{V_{in}}}{\mathrm{L}}\right)\mathrm{DT} = 0$$

Finally, $\frac{\mathrm{V_o}}{\mathrm{V_{in}}} = \frac{-D}{1-D}$ (17)

The relationship between the voltages and the duty cycle, D, can be seen in equation (17).

Conversion Ratio: $\mathbf{\frac{V_{out}}{V_{in}} = -\frac{D}{1-D}}$

When designing a Buck-Boost converter, the following equations are useful

Inductor current ripple: $\Delta i_L = \frac{V_{in} * DT}{L}$ (18)

Capacitor Ripple Voltage: $\Delta V_c = \frac{V_o\, DT}{RC}$ (19)

Critical Inductance: $L_c = \frac{(1-D)T * R}{2}$ (20)

Critical Capacitance: $C_c = \frac{DT}{2R}$ (21)

From the above equation (17) it can be seen that the polarity of the output voltage is always negative (because the duty cycle goes from 0 to 1), and that its absolute value increases with D, theoretically up to minus infinity when D approaches 1. If D > 0.5, the output voltage is larger than the input; and if D < 0.5, the output is smaller than the input. But if D = 0.5 the output voltage is equal to the input voltage. Apart from the polarity, this converter is either step-up (a boost converter) or step-down (a buck converter). Thus, it is named a buck-boost converter.

3

Bidirectional DC-DC Converter

3.1. Introduction

The study of bidirectional power converters has become a significant field of research in power electronics. Unlike conventional unidirectional converters, bidirectional converters allow power to flow in both directions, providing flexibility and making them widely used in applications such as electric vehicles (EVs), hybrid electric vehicles (HEVs), smart grids, uninterruptable power supplies (UPS), aerospace applications, and renewable energy systems like photovoltaic (PV) arrays, fuel cells (FCs), and wind turbines. These converters interface between power sources and energy storage elements, reducing system size and enhancing efficiency and performance by eliminating the need for separate converters for forward and reverse power flow. The general structure of bidirectional DC-DC converters is depicted in the figure 3.1. Depending on the location of the energy storage system, the converter operates as either a buck or boost type, with the control system regulating the system's voltage or current accordingly.

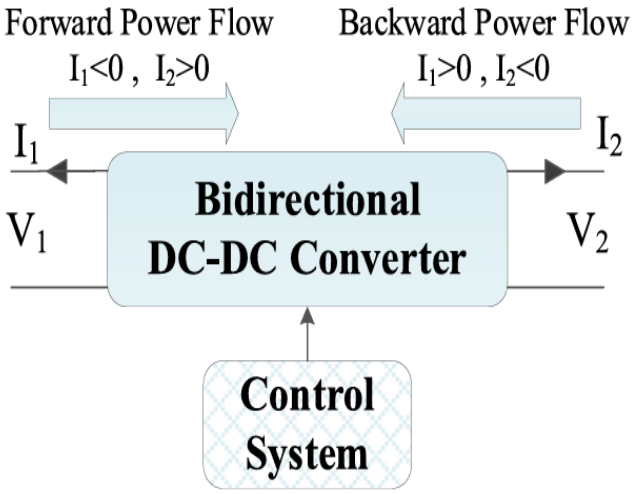

Figure 3.1 Structure of Bidirectional DC-DC converters

Due to its specific features, a bidirectional converter is suitable for systems requiring current supply in both directions based on the operating mode. A sample diagram of these applications in the powertrain of electric vehicles (EVs) is shown in the figure 3.2. To start, accelerate, or drive the vehicle uphill, extra power is needed to boost the high-voltage bus. This power can be provided by the auxiliary battery through a bidirectional DC-DC converter, which supplies the peak current from the battery when starting the motor. Unlike unidirectional topologies, bidirectional converters can reverse the direction of current and power. During deceleration, the auxiliary energy storage battery absorbs the regenerative energy fed back by the electric motor, enhancing efficiency and performance.

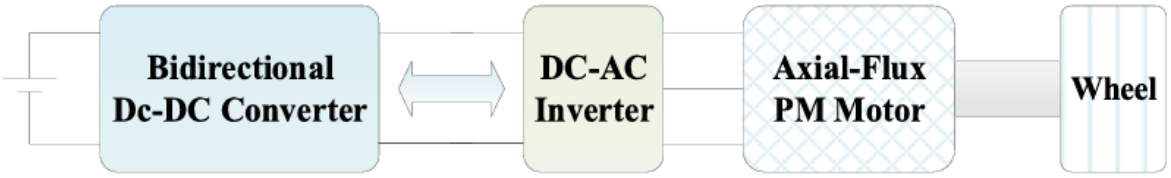

Figure 3.2 Block diagram of a Bidirectional DC-DC converter in EV powertrains

The application of bidirectional power converters extends beyond electric vehicles to include renewable energy systems, such as those based on fuel cells (FCs) or photovoltaic (PV) arrays. In these systems, bidirectional converters are used to supply either DC or AC loads via an inverter, as shown in the figure 3.3. To integrate multiple energy sources, a multi-input version of a unidirectional DC-DC converter may be employed to regulate the output DC voltage. Bidirectional DC-DC converters are necessary for managing power from batteries to the load during transient and overload conditions in the forward mode and for charging the battery pack in the reverse mode.

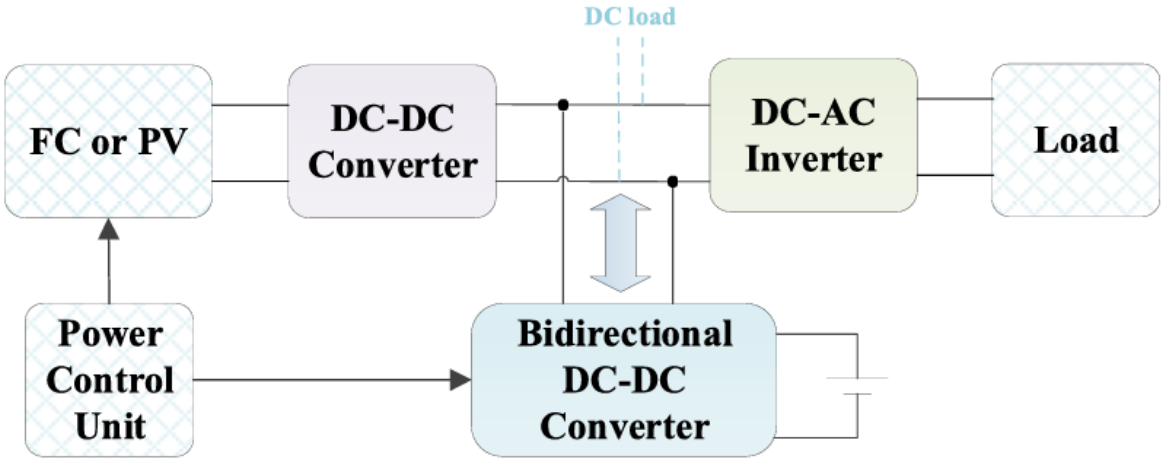

Figure 3.3 Block diagram of a Bidirectional DC-DC converter in FC or PV systems

The bidirectional DC-DC converter is also employed in smart grids and plug-in hybrid electric vehicle (PHEV) charging stations, as illustrated in the figure 3.4. In this vehicle-to-grid (V2G) architecture, bidirectional DC-DC converters are used to charge vehicles from the grid and to feed energy stored in PHEV batteries back to the grid when needed. Consequently, bidirectional DC-DC converters with low cost, high efficiency, and high reliability are crucial for these charging stations.

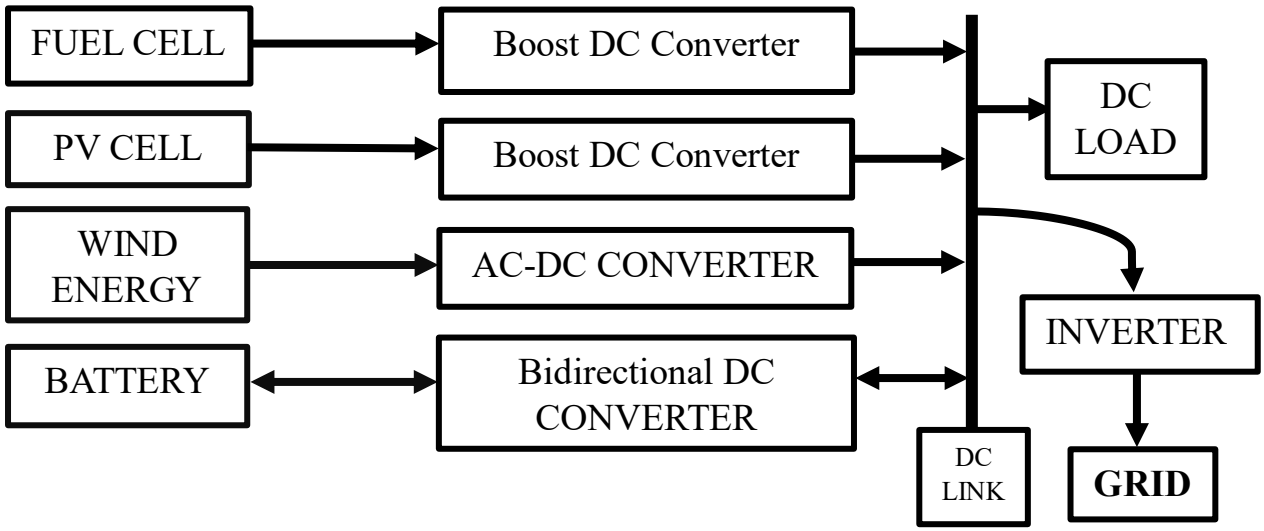

Figure 3.4 Block diagram of a Bidirectional DC-DC Converter connected with DC grid.

3.2. Types of Bidirectional Converter

There are two types of Bi-directional DC-DC converter on the basis of galvanic isolation provided between input and output.

1. Non-Isolated Bidirectional Dc to Dc Converter (NIBDC)

2. Isolated Bidirectional dc to dc Converter (IBDC)

3.2.1. Non-Isolated Bidirectional DC-DC Converter (NIBDC)

A non-isolated bidirectional converter is typically realized by adding an antiparallel diode to a switch (if not already present) and incorporating a controllable switch with a diode from a unidirectional converter topology. Non-isolated configurations include several basic DC-DC converters such as buck, boost, buck-boost, and CUK converters. Additionally, there are configurations based on voltage-boosting techniques like switched capacitor and interleaved multilevel converters. As a result, non-isolated configurations are categorized into eight distinct groups.

- Non isolated buck and boost derived Bidirectional DC-DC Converter.
- Non isolated buck-boost derived Bidirectional DC-DC Converter.
- Non isolated CUK derived Bidirectional DC-DC Converter.
- Non isolated SEPIC and ZETA derived Bidirectional DC-DC Converter.
- Cascaded Bidirectional DC-DC Converter.
- Switched capacitor Bidirectional DC-DC Converter.
- Interleaved Bidirectional DC-DC Converter.
- Multilevel Bidirectional DC-DC Converter.

（Ⅰ） Non isolated buck and boost derived Bidirectional DC-DC Converter

The fundamental bidirectional converter is based on the traditional buck and boost converters. As depicted in figure 3.5, this bidirectional topology evolves from the unidirectional buck and boost converters. By replacing the unidirectional switches of the traditional buck and boost converters with bidirectional power switches, a bidirectional buck-boost derived converter is created. In operation, the converter functions as a boost converter when stepping up from V_L to V_H and as a buck converter when operating in the reverse direction.

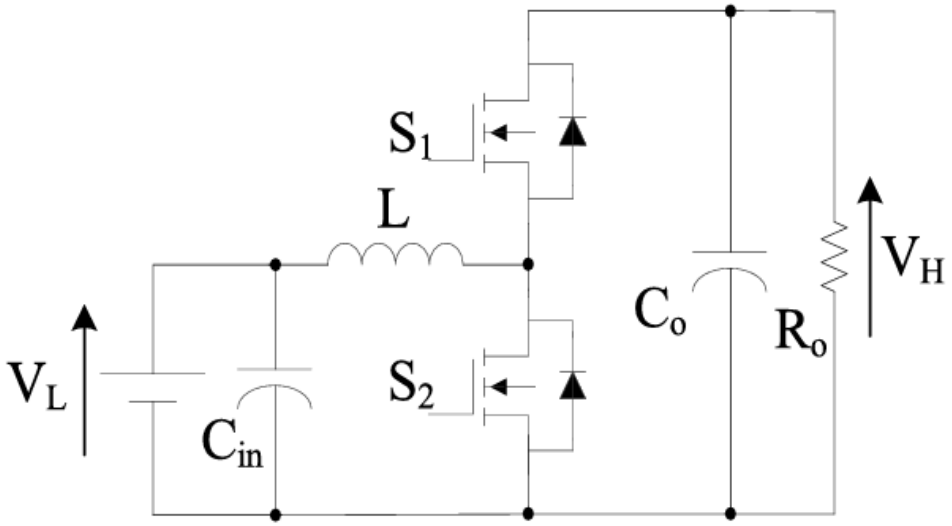

Figure 3.5 Circuit diagram of Non isolated buck and boost derived Bidirectional DC-DC Converter.

（Ⅱ） Non isolated buck-boost derived Bidirectional DC-DC Converter

Using the same approach applied to evolve unidirectional converters into bidirectional ones, a bidirectional buck-boost converter can be derived by replacing any unidirectional switches in its topology with bidirectional switches, as illustrated in figure 3.6. This bidirectional buck-boost converter retains the fundamental feature of the traditional buck-boost converter, which allows for voltage bucking or boosting. Additionally, it provides the capability to perform these functions in both directions of power flow, including with a negative output voltage.

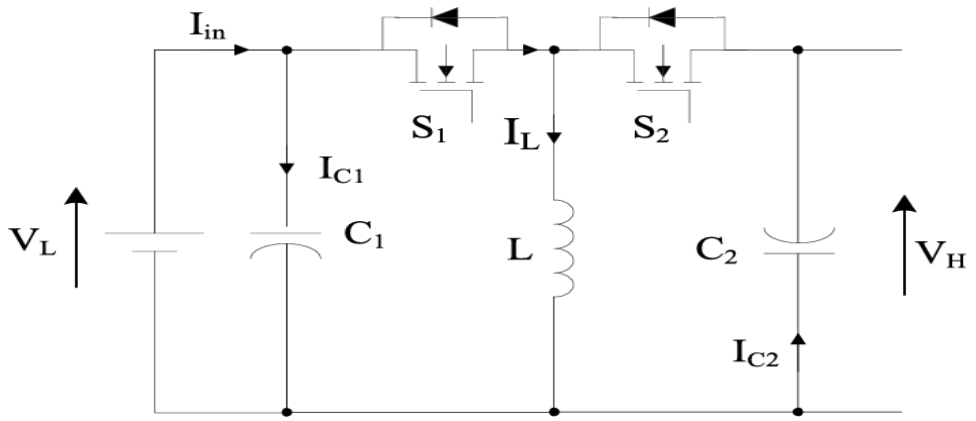

Figure 3.6 Circuit diagram of Non isolated buck-boost derived Bidirectional DC-DC Converter.

（Ⅲ） Non isolated CUK derived Bidirectional DC-DC Converter

The CUK converter, known for its continuity input and output currents, can be adapted to a bidirectional topology by replacing the original power switch and diode with two bidirectional power switches, as shown in figure 3.7. Variations of the bidirectional CUK converter include the coupled inductor version, which was originally developed for the unidirectional CUK converter to eliminate input/output current ripples. This technique has also been applied to the bidirectional CUK converter, serving as the foundation for further research into the control of bidirectional coupled-inductor CUK converters.

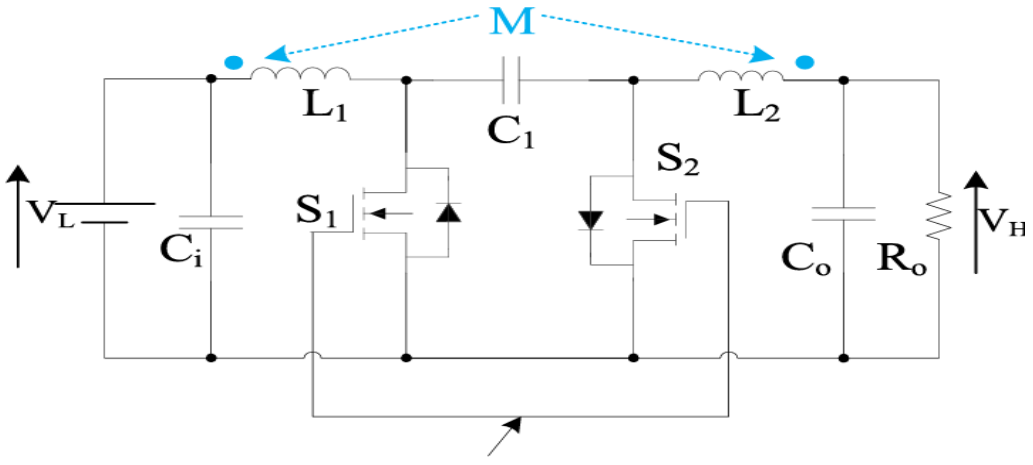

Figure 3.7 Circuit diagram of Non isolated CUK derived Bidirectional DC-DC Converter.

（Ⅳ） Non isolated SEPIC and ZETA derived Bidirectional DC-DC Converter

The Single-Ended Primary-Inductor Converter (SEPIC) and Zeta converters can be derived from the CUK converter by rearranging its elements to achieve a positive output voltage. As illustrated in figure 3.8, the bidirectional SEPIC/Zeta DC-DC converter functions as a SEPIC converter when power flows from V_L to V_H and as a Zeta converter when power flows from V_H to V_L. An auxiliary branch highlighted in this converter design creates a new direct power delivery path between the input and output, which helps reduce current ripples.

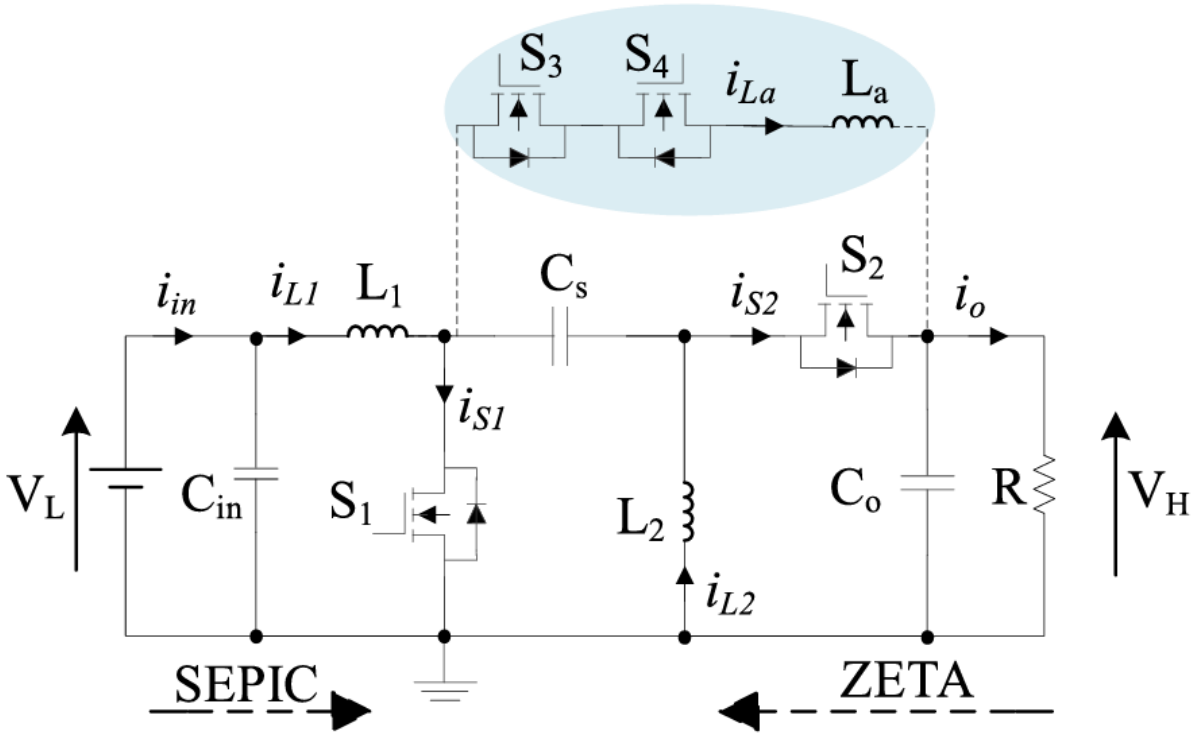

Figure 3.8 Circuit diagram of Non isolated SEPIC and ZETA derived Bidirectional DC-DC Converter.

（Ⅴ）Cascaded Bidirectional DC-DC Converter

To enhance the voltage boost capability of a converter and reduce current stress, multiple converters can be connected in a cascaded formation. Figure 3.9 illustrates the basic cascaded non-isolated bidirectional DC-DC converter, originally designed for electric vehicle (EV) applications. This converter results from cascading two buck-boost bidirectional converters. While it uses more components than a basic bidirectional buck-boost converter, this configuration achieves a higher voltage gain ratio with the same switch duty cycle. Additionally, it reduces current ripples and stress on inductors, switches, capacitors, and diodes, allowing the converter to handle higher power ratings.

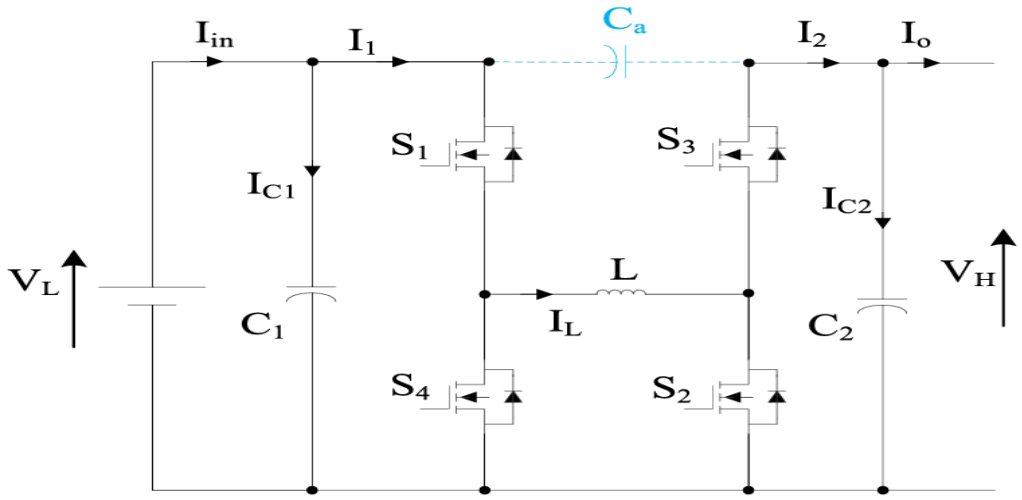

Figure 3.9 Circuit diagram of Cascaded Bidirectional DC-DC Converter.

(Ⅵ) Switched capacitor Bidirectional DC-DC Converter.

The switched-capacitor (SC) cell enhances the voltage boosting capability of converters by utilizing a bidirectional configuration, as shown in figure 3.10. This design evolves from a unidirectional SC cell to achieve bidirectional energy transfer, eliminating the need for inductors and thus avoiding the associated magnetic utilization and weight. Despite the absence of inductors, the converter can maintain a continuous input current by paralleling two similar strings of SC cells operating in anti-phase, with the potential for further extension by adding more cells. This approach results in an efficient, lightweight, and scalable solution for high voltage conversion ratios.

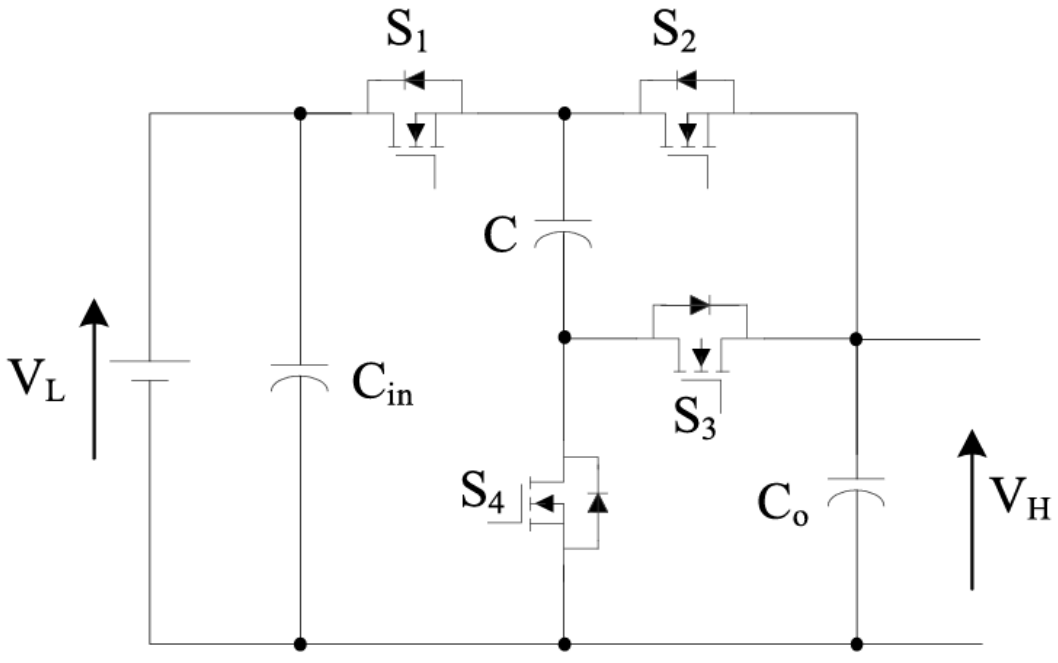

Figure3.10 Circuit diagram of Switched capacitor Bidirectional DC-DC Converter.

(Ⅶ) Interleaved Bidirectional DC-DC Converter

Figure 3.11 depicts a bidirectional DC-DC converter that employs the interleaving technique to cancel switching frequency current ripple, leading to a smaller EMI filter. In multi-stage bidirectional interleaved topologies for automotive applications, interleaving significantly reduces filter size, enhances dynamic response, and improves thermal management. Variations of interleaved converters include topologies with coupled inductors in either direct or reverse configurations, aimed at minimizing current ripple and boosting the converter's dynamic performance.

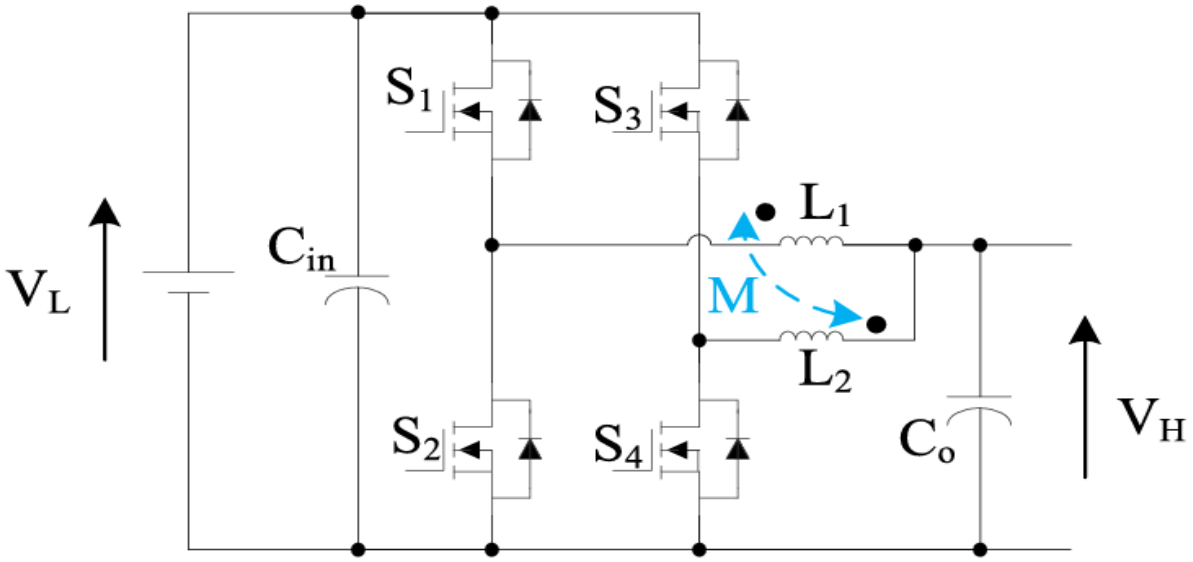

Figure 3.11 Circuit diagram of Interleaved Bidirectional DC-DC Converter.

(Ⅷ) Multilevel Bidirectional DC-DC Converter

Figure 3.12 shows a multilevel bidirectional DC-DC converter that uses a repeating switching module pattern at each level to achieve high voltage gain. Initially designed for dual voltage automotive systems, this converter avoids inductors, resulting in significantly reduced weight and size compared to converters with magnetic elements.

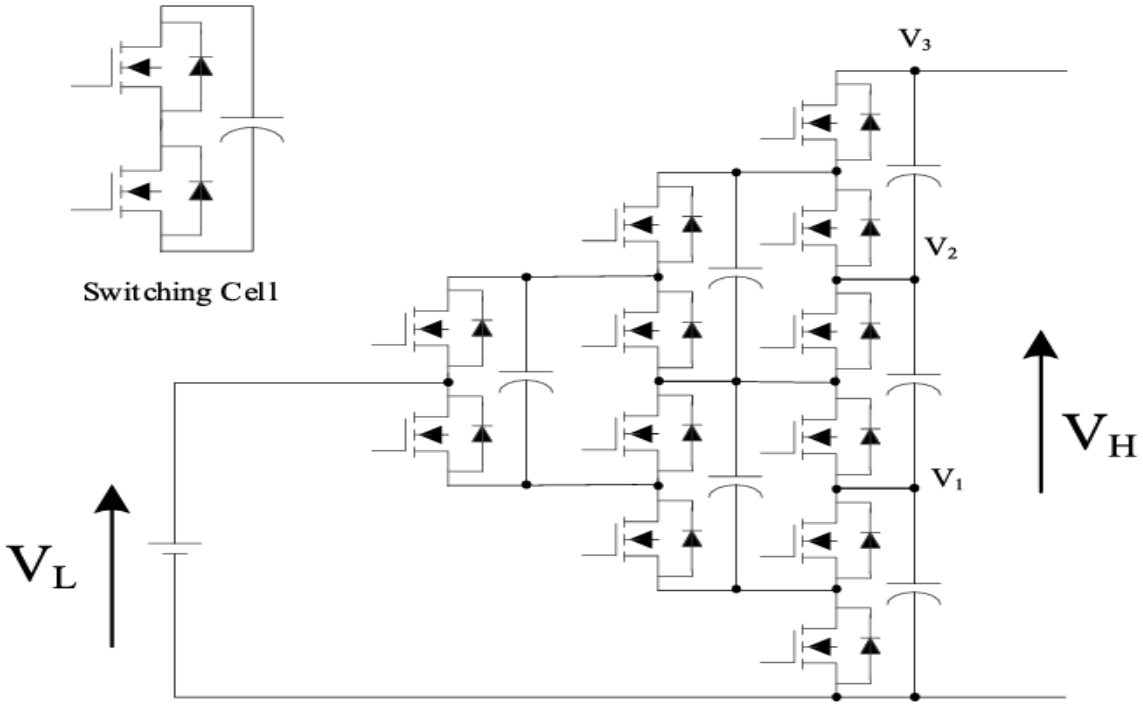

Figure 3.12 Circuit diagram of Multilevel Bidirectional DC-DC Converter.

.

3.2.2 Isolated Bidirectional DC-DC Converter (IBDC)

Galvanic isolation enhances power converters by allowing for high gain through adjustable turn ratios of windings, which makes them ideal for applications requiring wide input voltage ranges and precise load regulation. Besides offering high voltage gain, this isolation facilitates the development of multi-input and multi-output topologies, and provides crucial protection for sensitive loads against faults and noise. It also improves safety in critical systems such as aircraft, electric vehicles, and renewable energy sources. Isolated bidirectional converters, which are well-suited for these applications, leverage these benefits by maintaining isolation between input and output, thus ensuring reliable and safe operation. These topologies are classified and summarized as below.

- Bidirectional Flyback Converter
- Isolated CUK & SEPIC/ZETA Bidirectional DC-DC Converter.
- Push-Pull Bidirectional DC-DC Converter.
- Forward Bidirectional DC-DC Converter
- Dual Active Bridge (DAB) Bidirectional DC-DC Converter.
- Dual Half-Bridge Bidirectional DC-DC Converter.
- Half Bridge-Full Bridge Bidirectional DC-DC Converter.
- Multiport DAB Bidirectional DC-DC Converter.

（Ⅰ） Bidirectional Flyback Converter

To achieve a higher voltage boost in buck-boost converters without isolation, various methods can be employed. However, when magnetic isolation is required, the Flyback converter is a popular choice, where a transformer replaces the inductor in the buck-boost configuration. By applying volt-second and charge-second balance principles, the voltage gain in forward power flow matches the voltage gain ratio of the Flyback converter. It is important to carefully design the transformer and incorporate a voltage clamp snubber to suppress leakage currents. The circuit diagram of bidirectional flyback converter is shown in figure 3.13.

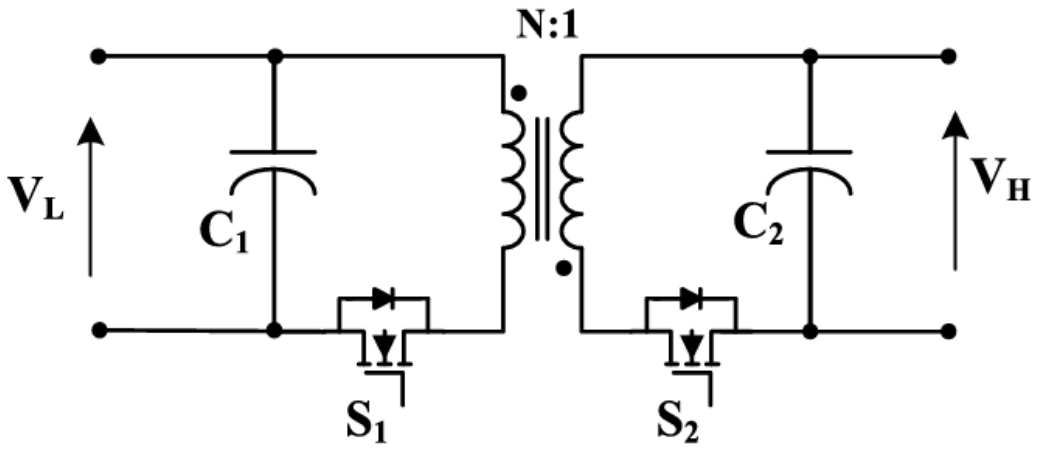

Figure 3.13 Circuit diagram of Bidirectional Flyback Converter

（II）Isolated CUK & SEPIC/ZETA Bidirectional DC-DC Converter

Based on the non-isolated bidirectional CUK converter, an isolated bidirectional CUK converter was realized to introduce the benefits of magnetic isolation to the original version. Hence, the new converter, which is depicted in figure 3.14 shown a continuous input/output current and provides isolation between input-output sides with a high voltage gain ratio that incorporates the turn ratio of the transformer.

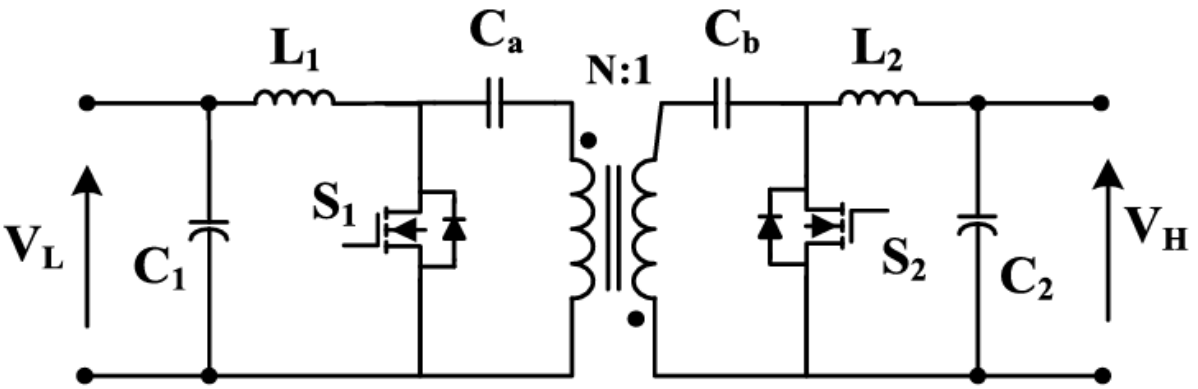

Figure 3.14 Circuit diagram of Isolated CUK & SEPIC/ZETA Bidirectional DC-DC Converter

（III）Push-Pull Bidirectional DC-DC Converter

The bidirectional push-pull converter is shown in figure 3.15, an extension of the unidirectional push-pull converter, enables power to flow in both directions rather than just one. It employs a multi-winding transformer similar to the unidirectional version for power conversion. For high-power applications, a three-phase variant of the bidirectional push-pull converter has been proposed, which utilizes a three-phase power system to handle increased power levels and improve performance while maintaining the fundamental principles of the push-pull topology.

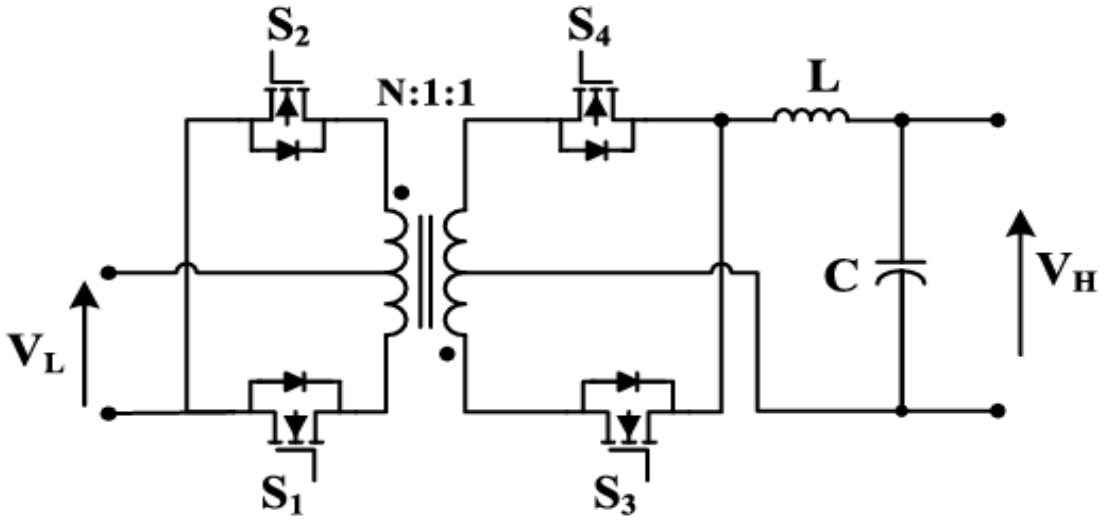

Figure 3.15 Circuit diagram of Push-Pull Bidirectional DC-DC converter.

（IV）Forward Bidirectional DC-DC Converter

The bidirectional forward converter is shown in figure 3.16, an advancement of the unidirectional forward converter, enables power flow in both directions and can achieve zero voltage switching through the use of a clamped circuit. Further research into the bidirectional forward DC-DC converter has introduced a resonant version that leverages the transformer's leakage inductance as the resonant inductor, enhancing its performance and efficiency.

Hybrid configurations of isolated topologies, such as Forward-Flyback, Push-pull Forward, and Flyback-Push-pull converters, have been explored in the literature. In these hybrids, the primary side of the transformer is based on one of these isolated topologies, while the secondary side utilizes a different one. The secondary can be either current-fed or voltage-fed, depending on the specific application and desired features.

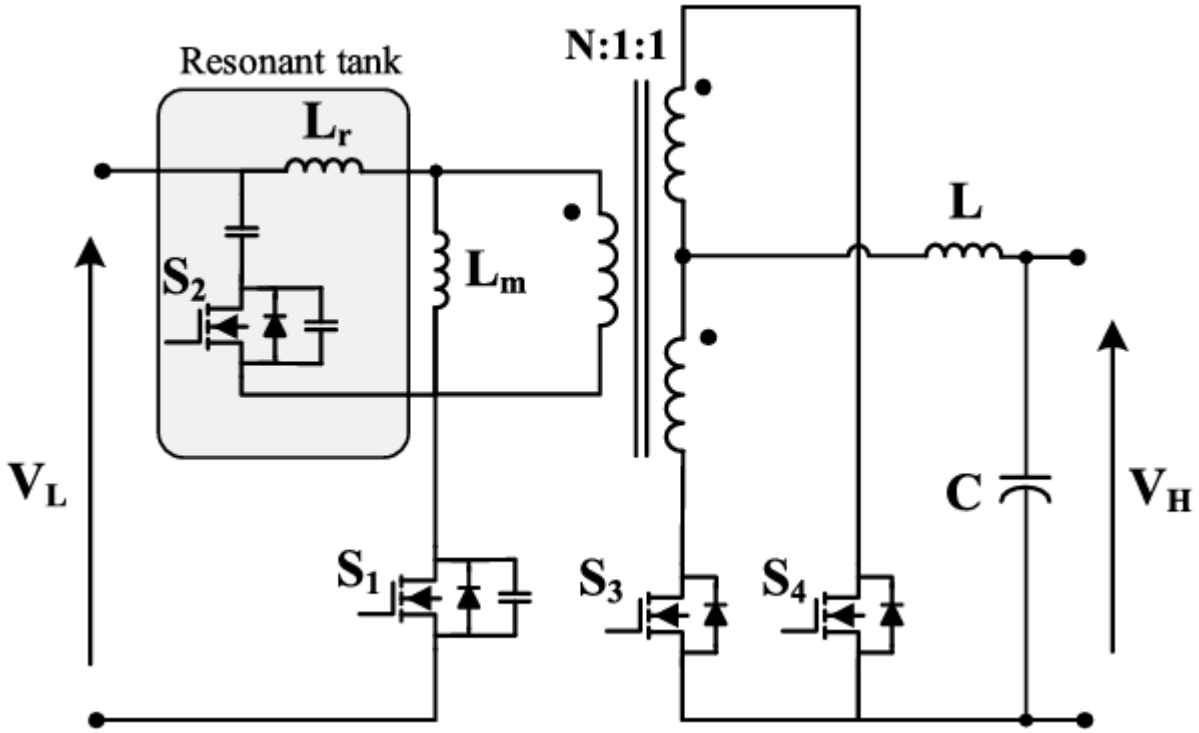

Figure 3.16 Circuit diagram of Forward Bidirectional DC-DC Converter

（V）Dual Active Bridge (DAB) Bidirectional DC-DC Converter

One popular technique for high-power applications involves using back-to-back bidirectional topologies isolated by a high-frequency transformer. These converters can be either voltage-fed or current-fed, and configured as half-bridge or full-bridge. Figure 3.17 illustrates the basic topology of the Dual Active Bridge (DAB) converter, which utilizes two full-bridge circuits on both sides of the transformer. With eight power switches and galvanic isolation, this topology is ideal for high-power, high voltage gain applications like automotive systems. Although the large number of switches can lead to losses, this can be mitigated by using low-loss silicon carbide (SiC) or gallium nitride (GaN) power switches. Energy transfer is controlled by adjusting the phase shift between the AC voltage waveforms of the transformer's primary and secondary windings, making control schemes crucial for optimizing efficiency.

As DAB (Dual Active Bridge) topologies are among the most popular isolated bidirectional converters, extensive reviews have been conducted on DAB-derived configurations. The general layout of a DAB-derived converter is illustrated in Figure 3.17. The converter consists of three stages: a) In the first stage, depending on the application, either a voltage-fed or current-fed full-bridge is used for DC-AC conversion; b) In the second stage, a high-frequency transformer steps up the AC voltage while providing galvanic isolation. A resonant tank may be incorporated with the transformer to achieve Zero Voltage Switching (ZVS) or Zero Current Switching (ZCS), thereby enhancing efficiency; c) In the third stage, based on the application requirements, either a voltage-fed or current-fed full-bridge is used for AC-DC rectification.

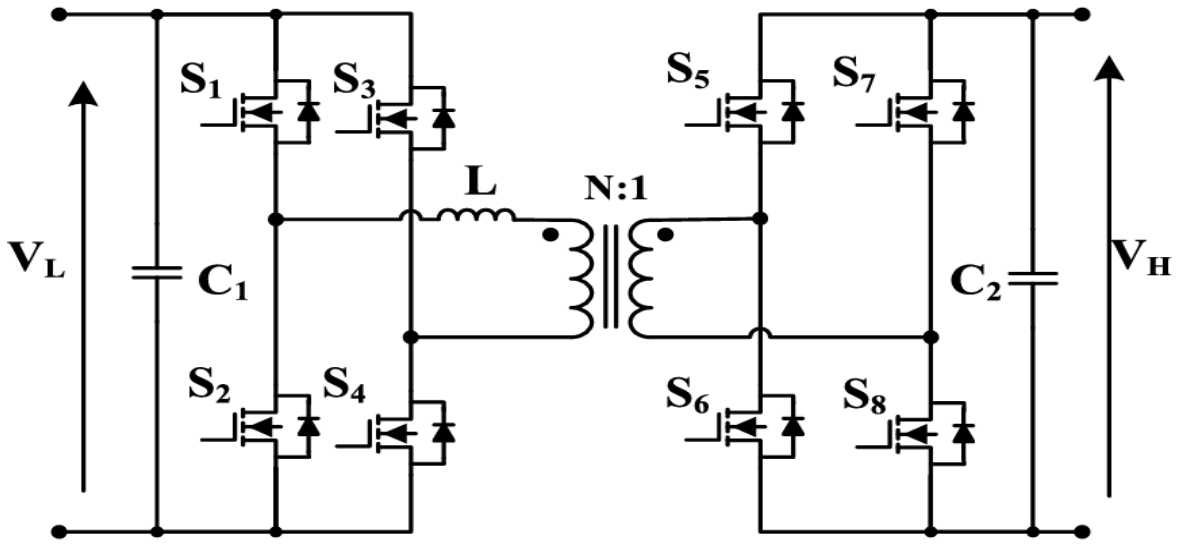

Figure 3.17 Circuit diagram of Dual Active Bridge (DAB) Bidirectional DC-DC Converter.

（VI）Dual Half-Bridge Bidirectional DC-DC Converter

In comparison to the Dual Active Bridge (DAB) topology, the half-bridge topology is advantageous for lower power applications, reducing the number of power switches from eight to four. The figure 3.18 illustrates a bidirectional isolated converter employing voltage-fed half-bridge topologies on both sides of the transformer. The absence of an inductor in this design eliminates the right half-plane zero (RHPZ), simplifying the controller design due to the converter's minimum-phase behaviour. The converter is based on the dual half-bridge concept, originally featuring a current-fed half-bridge on the primary side and a voltage-fed half-bridge on the secondary side of the transformer. Another variant uses a voltage-fed topology on the primary side and a current-fed topology on the secondary side, enabling a continuous current waveform desirable in certain applications. Further studies on dual half-bridge converters, such as the interleaved dual half-bridge topology, aim to enhance voltage boost capability, reduce the transformer ratio, and decrease current stress.

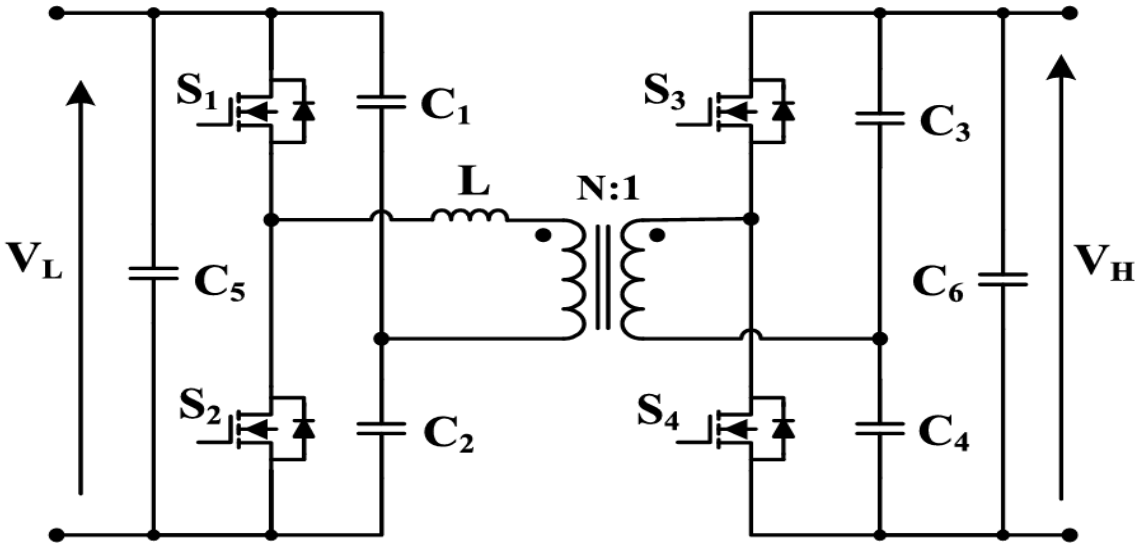

Figure 3.18 Circuit diagram of Dual Half-Bridge Bidirectional DC-DC Converter.

（VII）Half Bridge-Full Bridge Bidirectional DC-DC Converter

In the context of UPS design, an isolated bidirectional DC-DC converter using a voltage-fed half-bridge topology on the primary side and a voltage-fed full-bridge topology on the secondary side of the transformer has been proposed. This configuration, depicted in Figure 3.19, simplifies control requirements compared to the Dual Active Bridge (DAB) due to the reduced number of switches. It is particularly suitable for integrating a two-switch buck-boost converter in the half-bridge side, resulting in a comprehensive UPS topology. Other variants of this configuration include the full-bridge half-bridge bidirectional DC-DC converter, which has been combined with impedance networks to enhance performance.

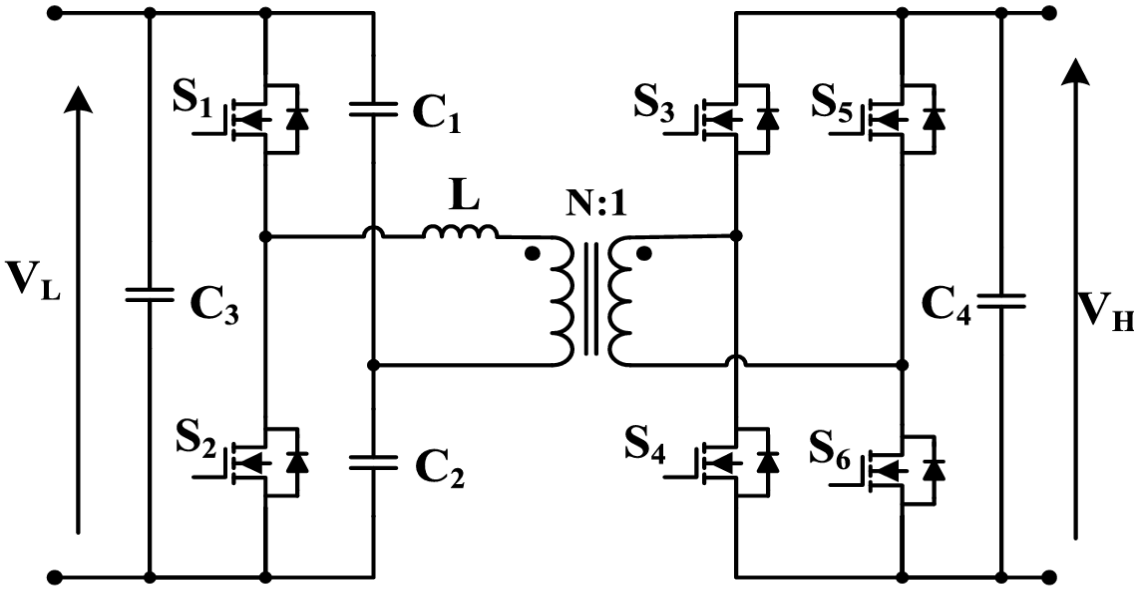

Figure 3.19 Circuit diagram of Half Bridge-Full Bridge Bidirectional DC-DC Converter.

（VIII）Multiport DAB Bidirectional DC-DC Converter

Multi-input converters are an excellent choice for integrating multiple input voltage sources in renewable energy systems and hybrid electric vehicles. One such example is an isolated multi-input bidirectional DC-DC converter based on the Dual Active Bridge (DAB) topology, utilizing a multi-winding transformer along with decoupled power flow management. This configuration, illustrated in the figure 3.20, enables efficient control of power flow.

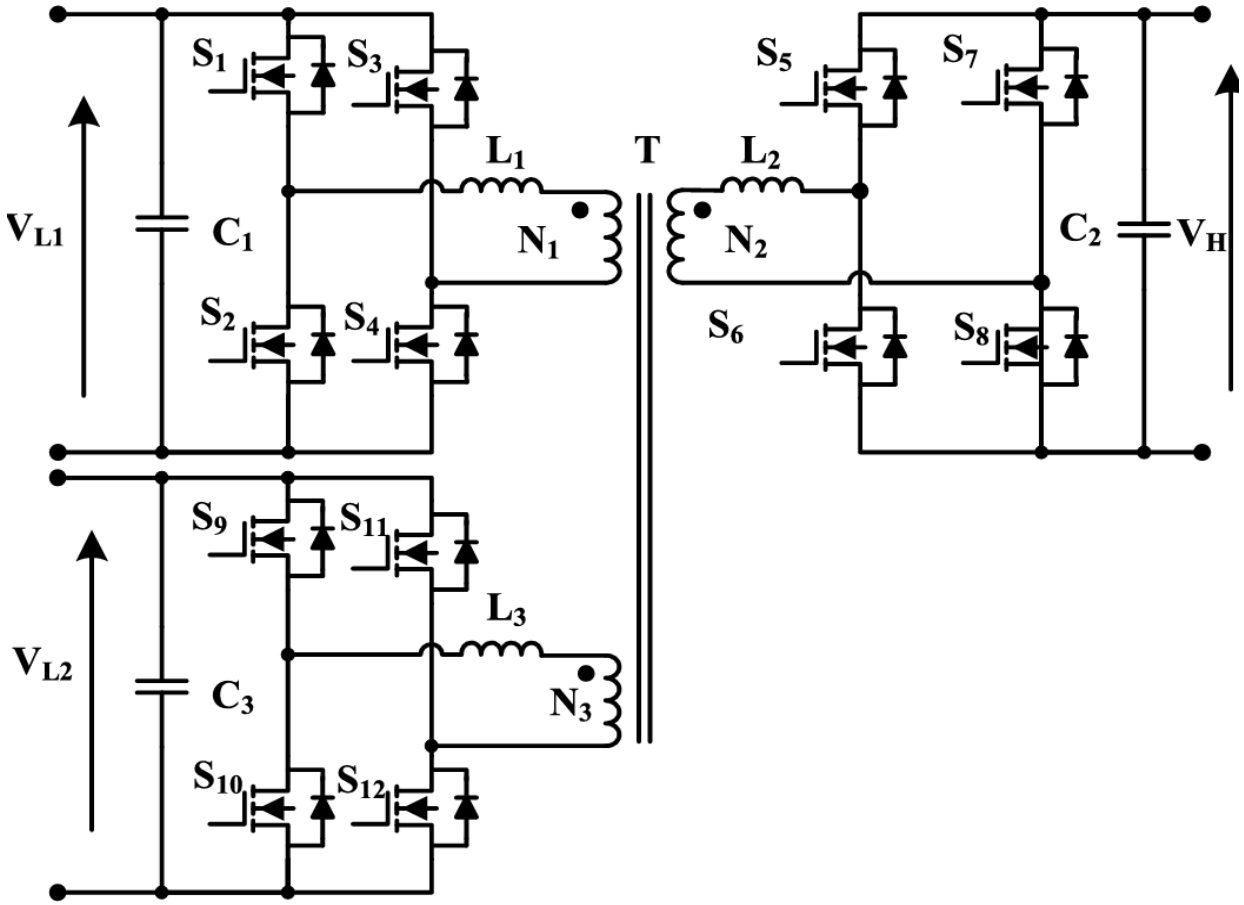

Figure 3.20 Circuit diagram of Multiport DAB Bidirectional DC-DC Converter.

3.3 Comparison of Non-isolated bidirectional converters

Topology	V_H/V_L	Inductors	Capacitors	Switches	Application
Basic buck & boost Figure 3.5	$\frac{1}{1-D}$	1	2	2	Photovoltaic system, Uninterruptable Power Supply
Buck-Boost Figure 3.6	$\frac{-D}{1-D}$	2	2	2	Electric Vehicle
CUK Figure 3.7	$\frac{-D}{1-D}$	2	3	4	Battery storage system
SEPIC/Zeta Figure 3.8	$\frac{D}{1-D}$	2	3	2	Distributed Power system
Cascaded Figure 3.9	$\frac{1}{1-D}$	1	2	4	Electric Vehicle, Smart Grid
Switched Capacitor Figure 3.10	2	0	3	4	Distributed Energy Resources
Interleaved Figure 3.11	$\frac{1}{1-D}$	n=2	2	2n=4	High Power applications, Distributed Energy storages
Multilevel Figure 3.12	n=3	0	$\frac{n(n+1)}{2}$ =6	n(n+1) =12	Dual voltage Architecture (Automotive systems)

3.4 Comparison of Isolated bidirectional converters

Topology	V_H/V_L	Inductors	Capacitors	Switches	Windings	Application
Flyback Figure 3.13	$\frac{ND}{1-D}$	0	2	2	2	Uninterruptable Power Supply, Low-Medium Power Application
CUK Figure 3.14	$\frac{ND}{1-D}$	2	4	2	2	Low Power Application, Photovoltaic System
Push-Pull Figure 3.15	ND	1	1	4	4	Medium Power (2φ) – High Power (3 φ) Application
Forward Figure 3.16	ND	1	1	3	3	Low-Medium Power Application
DAB Figure 3.17	Varies w.r.t Control Scheme	0 (V-fed)	2	8	2	High Power Application, Automotive Application
Dual Half-Bridge Figure 3.18	Varies w.r.t Control Scheme	0 (V-fed)	6	4	2	Automotive, Fuel cell, Battery
Half-Full Bridge Figure 3.19	Varies w.r.t Control Scheme	0 (V-fed)	4	6	2	Uninterruptable Power Supply, Electric Vehicle
Multiport-DAB Figure 3.20	Varies w.r.t Control Scheme	0 (V-fed)	n=3	4n=12	n=3	Multi Sustainable Sources Generation System

4

The Proposed High Gain Bidirectional DC-DC Converter (HGBDC)

The proposed high-gain bidirectional converter (HGBDC) features a straightforward design, utilizing only four active power switches. This simplicity in construction contributes to its effectiveness. The converter achieves high voltage gain through the careful selection of duty cycles and the design of appropriate inductor and capacitor values. Operating the converter at a lower duty ratio helps mitigate core saturation issues in the inductor.

Additionally, the converter design allows the input current to be distributed among multiple inductors, which reduces their size and eliminates the need for a separate clamping circuit to supply energy to the load. Performance analysis conducted with MATLAB/Simulink has demonstrated the converter's viability for interfacing energy storage devices with the DC link in electric vehicles. The converter effectively manages power flow during both forward motoring and regenerative braking, ensuring efficient energy transfer between the energy source and the motor.

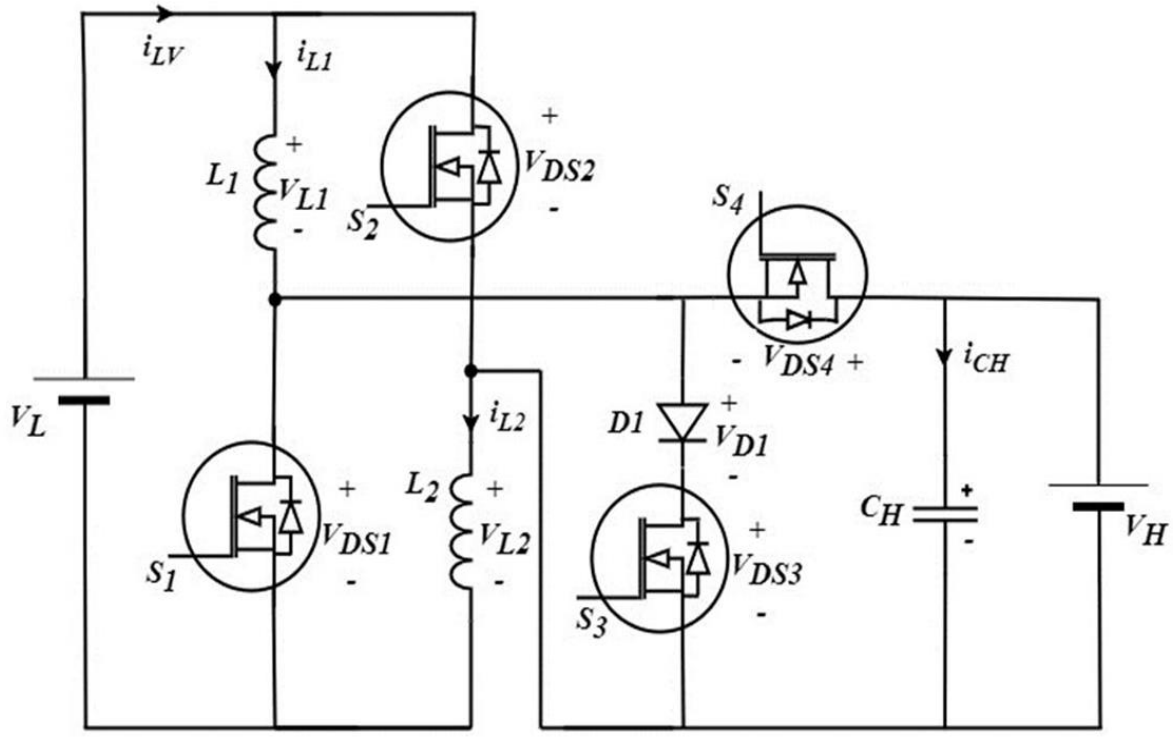

Figure 4.1 Proposed high gain bidirectional DC-DC converter (HGBDC)

The proposed HGBDC shown in figure 2.1 has four active power switches (S1, S2, S3, and S4), two identical inductors (L1 and L2), a diode (D1), and a capacitor (C_H) at the high voltage side. Diode D1 helps in blocking the reverse voltage V_L appearing across the MOSFET while the switches S1 and S2 are conducting in boost mode. A switching frequency of fs is used by the switches S1, S2, S3, and S4. During boost mode, switches S1 and S2 have a duty ratio of d_1, and switch S3 has a duty ratio of d_2. The duty ratio of the switch S4 is (1- d_1- d_2) during boost mode and it is d_b during buck mode of operation of the converter.

4.1 Operating Principle of proposed Bidirectional DC-DC Converter

A. Boost Mode:

The boost operation of the proposed converter is operated in three different mode. Mode1, Mode2 and Mode3. The current flow path of the proposed HGBDC operating in boost mode in explained in figure 2.2. During this mode, the energy is transferred from the low voltage side to the high voltage side of the converter with the help of controlled switches S1, S2, S3 and S4. The switches S1, S2, S3 and S4 are operated through PWM control.

- **Mode 1:**

The switches S1 and S2 are turned on in this mode, while the switches S3 and S4 are turned off for the duration of $d_1 T_s$. Energy flow from the battery to inductor L1, L2 which are connected in parallel, are shown in figure 4.2. The energy stored in the capacitor (C_H) is released to the load.

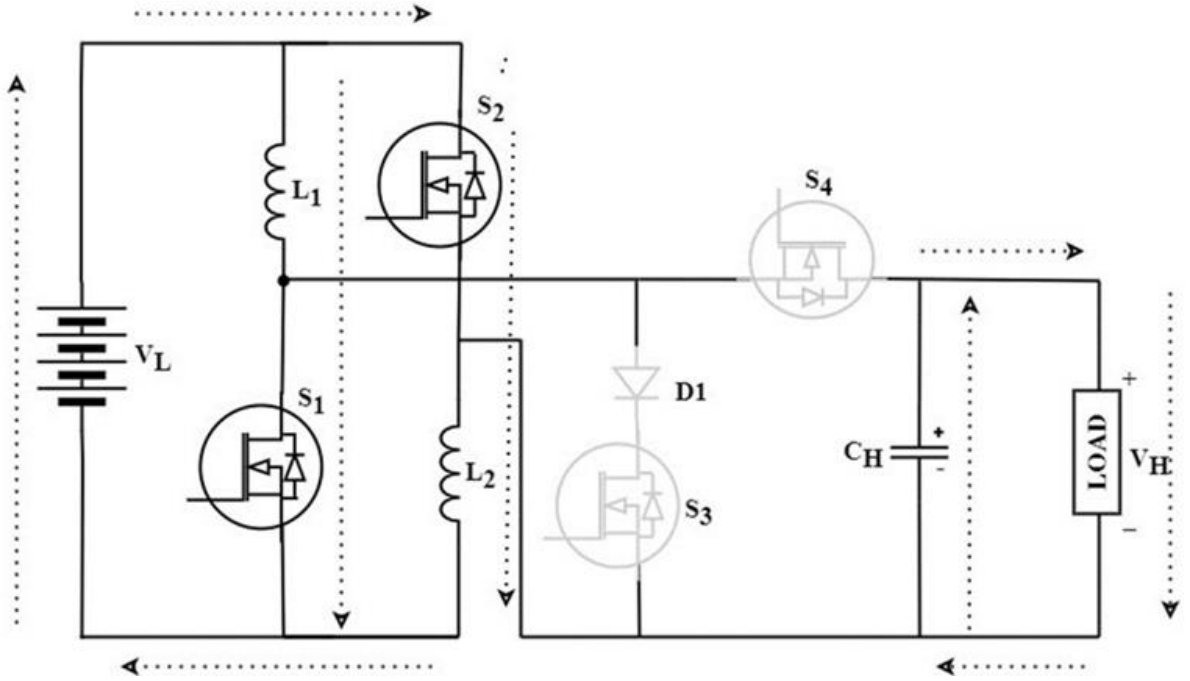

Figure 4.2 Proposed HGBDC in boost mode 1

The voltage across the inductors is expressed in following equations.

$$V_{L1} = V_{L2} = V_L \quad (1)$$

$$L_1 \frac{di_{L1}}{dt} = L_1 \frac{di_{L2}}{dt} = L \frac{di_L}{dt} \quad (2)$$

$(\because\ L_1 = L_2 = L)$

$$L \frac{di_L}{dt} = V_L$$

$$\therefore\ \frac{di_L}{dt} = \frac{V_L}{L} \quad (3)$$

- **Mode 2:**

Switch S3 is active for the duration of $d_2 T_s$, while switches S1 and S2 are turned off in Mode2. As shown in figure 4.3, current flow is through L1, D1, S3 and L2. The energy from the source is delivered to the inductors. The load receives the energy that is stored in the capacitor (C_H). Source is in series with the inductors in this mode.

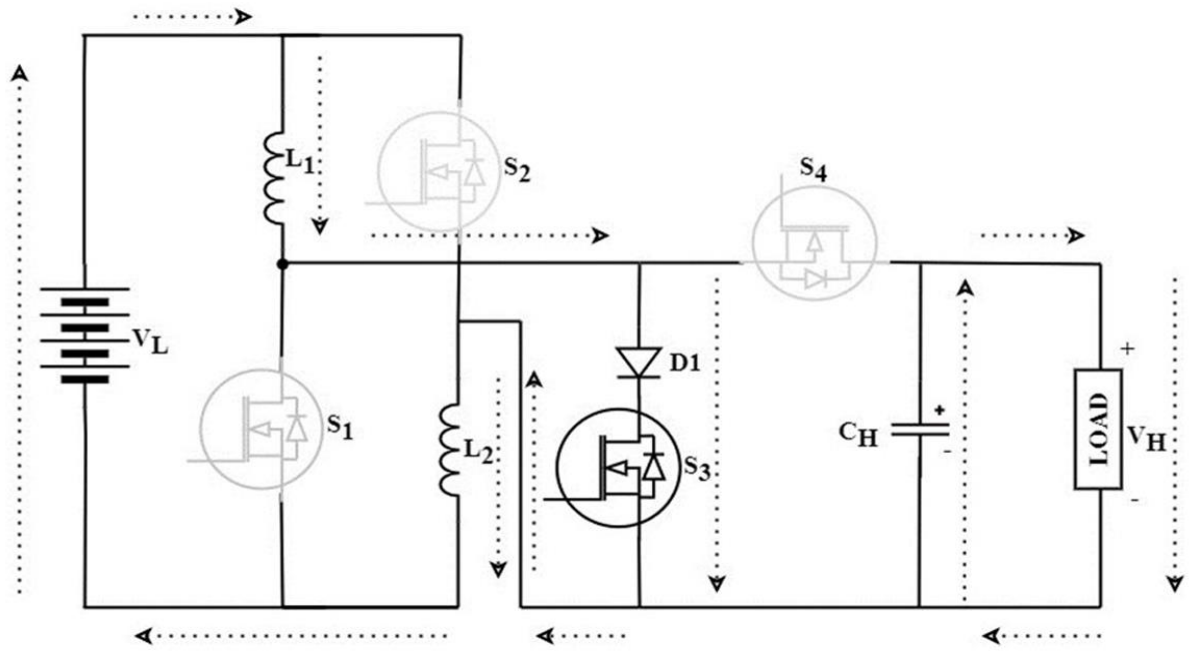

Figure 4.3 Proposed HGBDC in boost mode 2

The currents flowing through and the voltages across the inductors expressed in following equations.

$$i_{L1} = i_{L2} = i_L \quad (4)$$

$$V_{L1} = V_{L2} = L\frac{di_L}{dt} \quad (5)$$

$(\because\ L_1 = L_2 = L)$

$$V_{L1} + V_{L2} = V_L \quad (6)$$

$$2L\frac{di_L}{dt} = V_L$$

$$\therefore \frac{di_L}{dt} = \frac{V_L}{2L} \quad (7)$$

- **Mode 3:**

The switches S1, S2 and S3 are turned off in this mode. whereas the body diode of the MOSFET S4 conducts during $(1 - d_1 - d_2)T_s$. Diode D1 is reverse biased. The load is supplied by both the source and the inductors as depicted in figure 4.4. The capacitor $C_H$is in charging mode as the body diode of S4 is forward biased. The inductors are connected in series to the source.

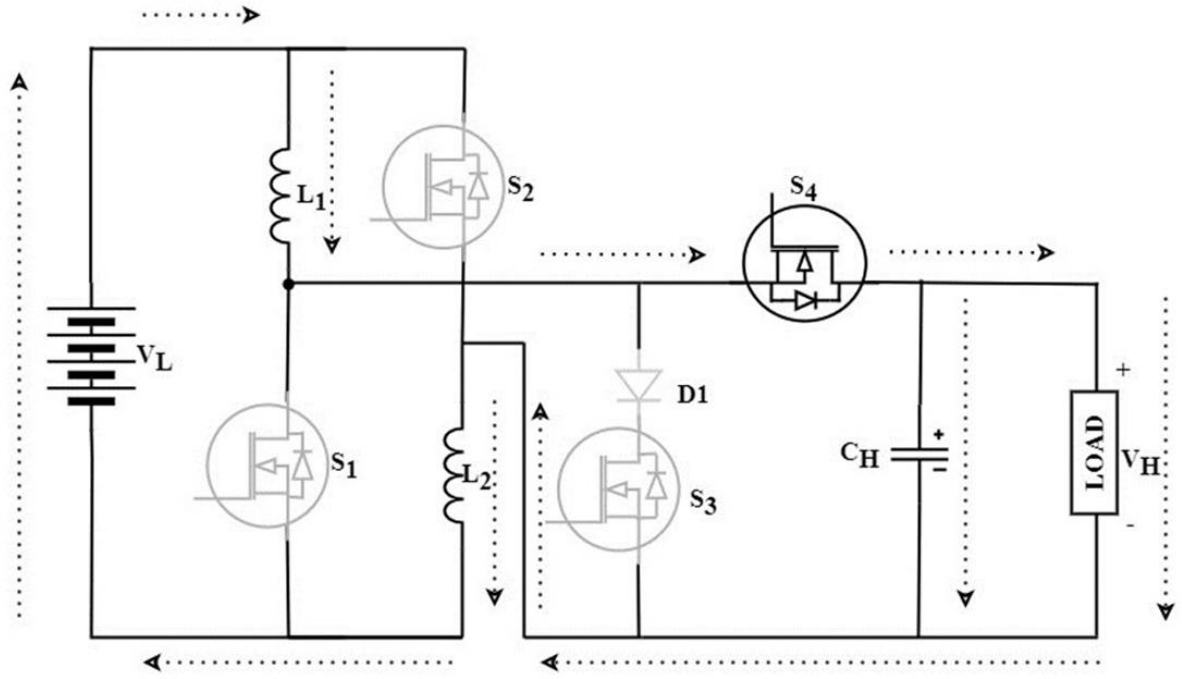

Figure 4.4 Proposed HGBDC in boost mode 2

The current through and the voltage across the inductors are given in equations.

$$i_{L1} = i_{L2} \quad (8)$$

$$V_{L1} = V_{L2} = L\frac{di_L}{dt} \quad (9)$$

$$V_{L1} + V_{L2} = V_L - V_H \quad (10)$$

$$2L\frac{di_L}{dt} = V_L - V_H$$

$$\therefore \frac{di_L}{dt} = \frac{V_L - V_H}{2L} \quad (11)$$

(3), (7), and (11) are combined to get (12) using the state space averaging technique:

$$\int_0^{d_1 T_s}\left(\frac{di_L}{dt}\right)dt + \int_0^{d_2 T_s}\left(\frac{di_L}{dt}\right)dt + \int_0^{(1-d_1-d_2)T_s}\left(\frac{di_L}{dt}\right)dt = 0 \quad (12)$$

$$\frac{V_L}{L}d_1 T_s + \frac{V_L}{2L}d_2 T_s + \frac{V_L - V_H}{2L}(1 - d_1 - d_2)T_s = 0$$

$$\frac{T_S}{L}\left[V_L d_1 + \frac{V_L}{2}d_2 + \frac{V_L - V_H}{2}(1 - d_1 - d_2)\right] = 0$$

$$V_L\left(d_1 + \frac{1}{2} - \frac{d_2}{2}\right) - V_H\left(\frac{1}{2} - \frac{d_1}{2} - \frac{d_2}{2}\right) = 0$$

$$V_L\left(\frac{d_1}{2} + \frac{1}{2}\right) = \frac{V_H}{2}(1 - d_1 - d_2)$$

$$V_L(d_1 + 1) = V_H(1 - d_1 - d_2)$$

$$\therefore \frac{V_H}{V_L} = \frac{1 + d_1}{1 - d_1 - d_2} \quad (13)$$

The resulting voltage gain in boost mode of proposed converter is given by equation no (13). A desired output voltage can be produced by controlling the power switch of the proposed HGBDC converter with pulse width modulation.

B. Buck mode:

The buck operation of the converter is explained in two different mode during the same switching cycle. The current flow path of the proposed HGBDC operating in buck mode is explained in figure 2.3. Energy is transferred from the high voltage side to the low voltage side with the help of controlled switches S4, S1 andS2 in this mode. The switchS4 is operated through the PWM control with a duty ratio of d_b.

- **Mode 1:**

In this mode, S4 is turned on and S1, S2, S3 are turned off for a duration of $d_b T_s$. The inductors L1 and L2, which are connected in series with the load and the battery, facilitate the transfer of energy from the high voltage side to the low voltage side of the converter as shown in figure 4.5.

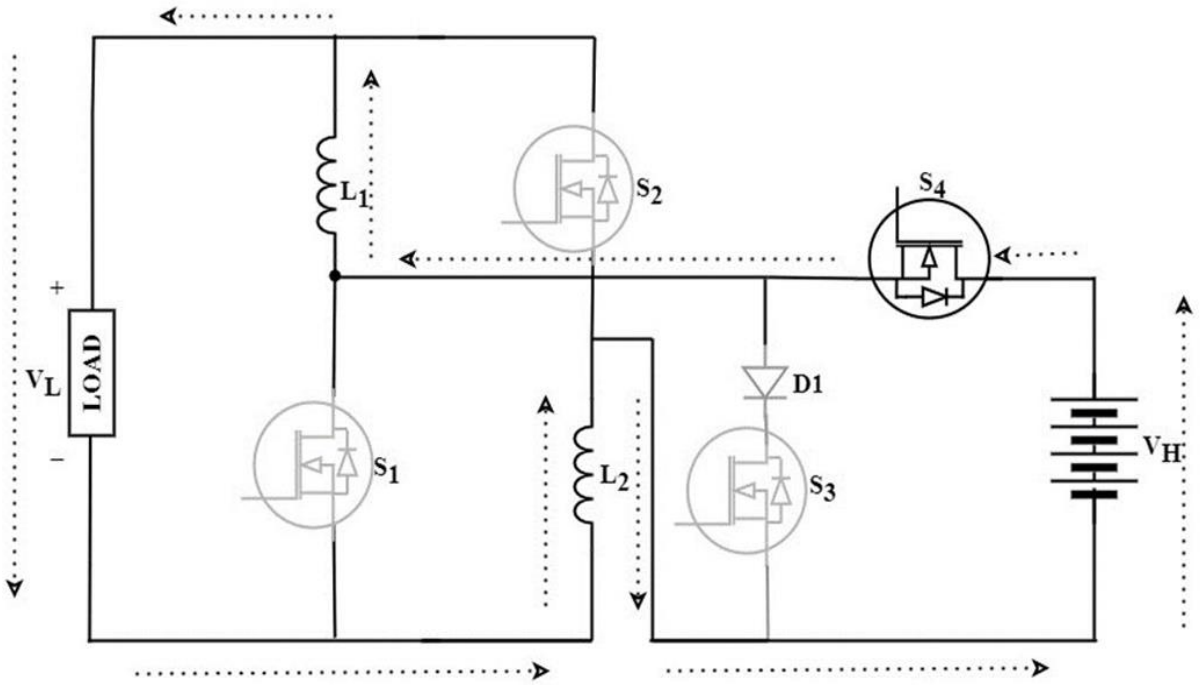

Figure 4.5 Proposed HGBDC in buck mode 1

The current flowing through and the voltage across the inductors are given in following equations.

$$i_{L1} = i_{L2} \quad (14)$$

$$V_{L1} + V_{L2} = V_H - V_L \quad (15)$$

$$V_{L1} = V_{L2} = L\frac{di_L}{dt}$$

$$2L\frac{di_L}{dt} = V_H - V_L$$

$$\therefore \frac{di_L}{dt} = \frac{V_H - V_L}{2L} \quad (16)$$

- **Mode 2:**

The body diodes of the S1 and S2 conduct for a duration of $(1 - d_b)T_S$ in this mode, while the S4 is turned off. The current flow path inductors L1 and L2 discharge their stored energy to the load on low voltage side in shown in figure 4.6.

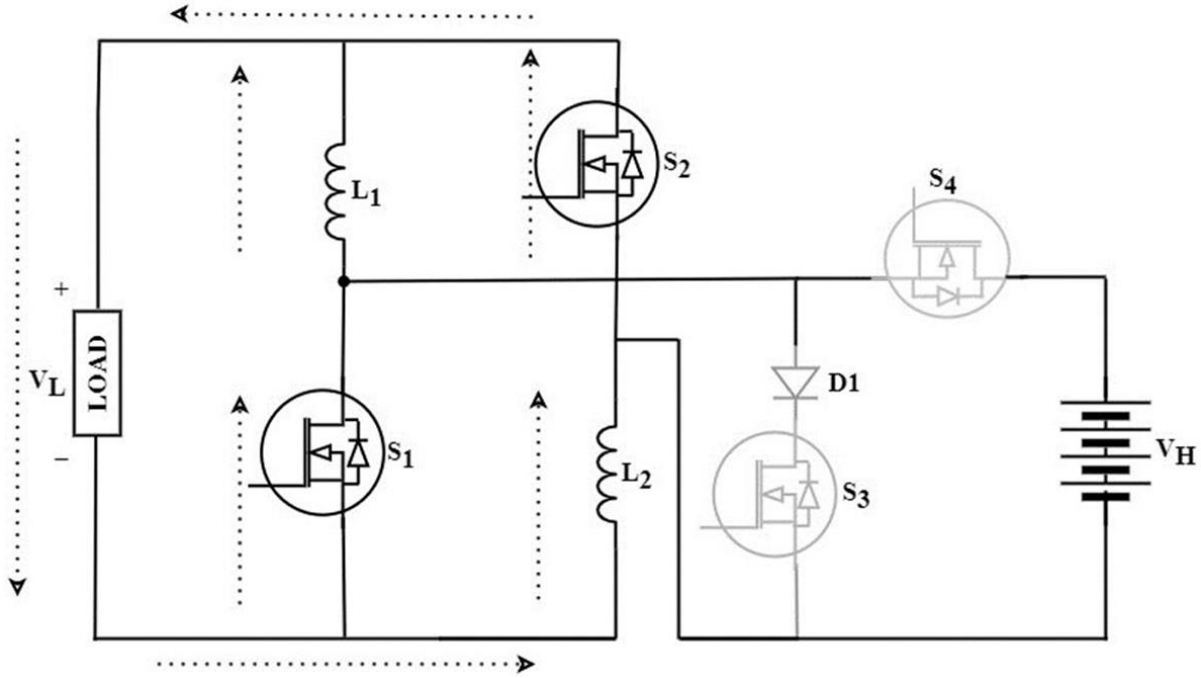

Figure 4.6 Proposed HGBDC in buck mode 2

The voltage across inductors are given in following equations.

$$V_{L1} + V_{L2} = -V_L \quad (17)$$

$$L_1\frac{di_{L1}}{dt} = L_1\frac{di_{L2}}{dt} = -V_L \quad (18)$$

$$\therefore \frac{di_L}{dt} = \frac{-V_L}{L} \quad (19)$$

Equations (16) and (19) are combined to get (20) using the state space averaging technique.

$$\int_0^{d_b T_s}\left(\frac{di_L}{dt}\right)dt + \int_0^{(1-d_b)T_s}\left(\frac{di_L}{dt}\right)dt = 0 \qquad (20)$$

$$\frac{V_H - V_L}{2L} d_b T_s + \left(\frac{-V_L}{L}\right)(1-d_b)T_s = 0$$

$$\frac{T_S}{L}\left[\left(\frac{V_H - V_L}{2}\right)d_b - V_L(1-d_b)\right] = 0$$

$$\frac{V_H}{2}d_b - \frac{V_L}{2}d_b - V_L + V_L d_b = 0$$

$$\frac{V_H}{2}d_b = V_L - \frac{V_L}{2}d_b$$

$$V_H d_b = V_L(2-d_b)$$

$$\therefore \frac{V_L}{V_H} = \frac{d_b}{2-d_b} \qquad (21)$$

The resulting voltage gain in buck mode is given by equation no (21), where d_b is the duty ratio of the converter in buck mode of operation. A desired output voltage can be produced by controlling the power switch of the proposed HGBDC converter with pulse width modulation.

4.2 Theoritical operational waveforms of HGBDC

A. Boost mode

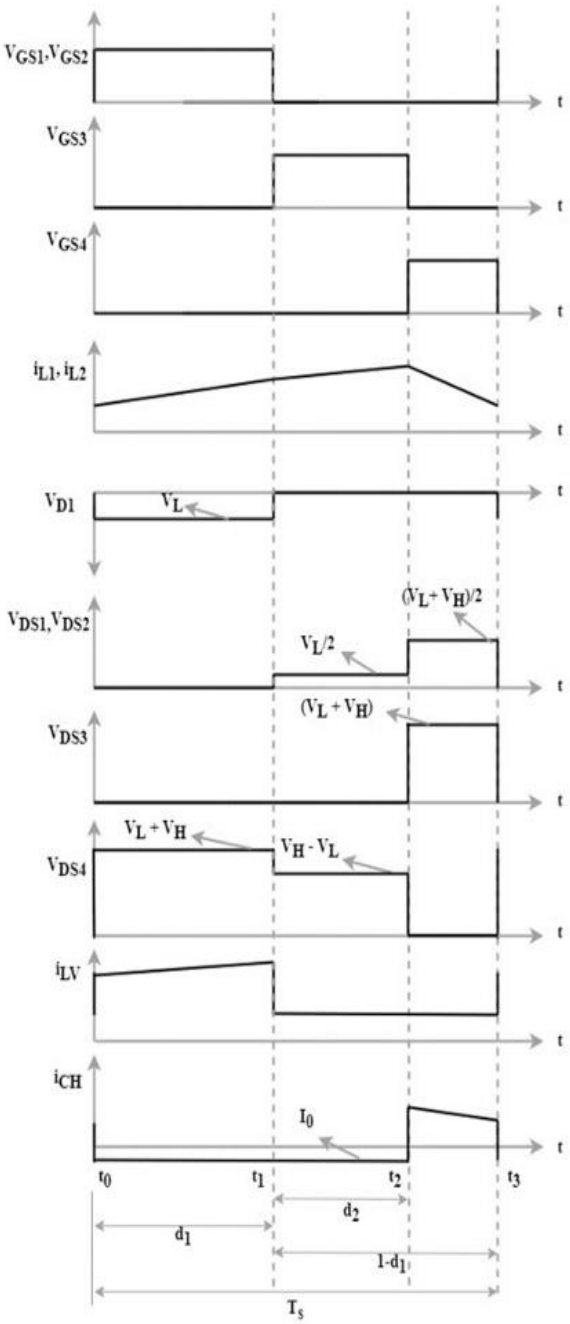

Fig.4.7(a)

B. Buck mode

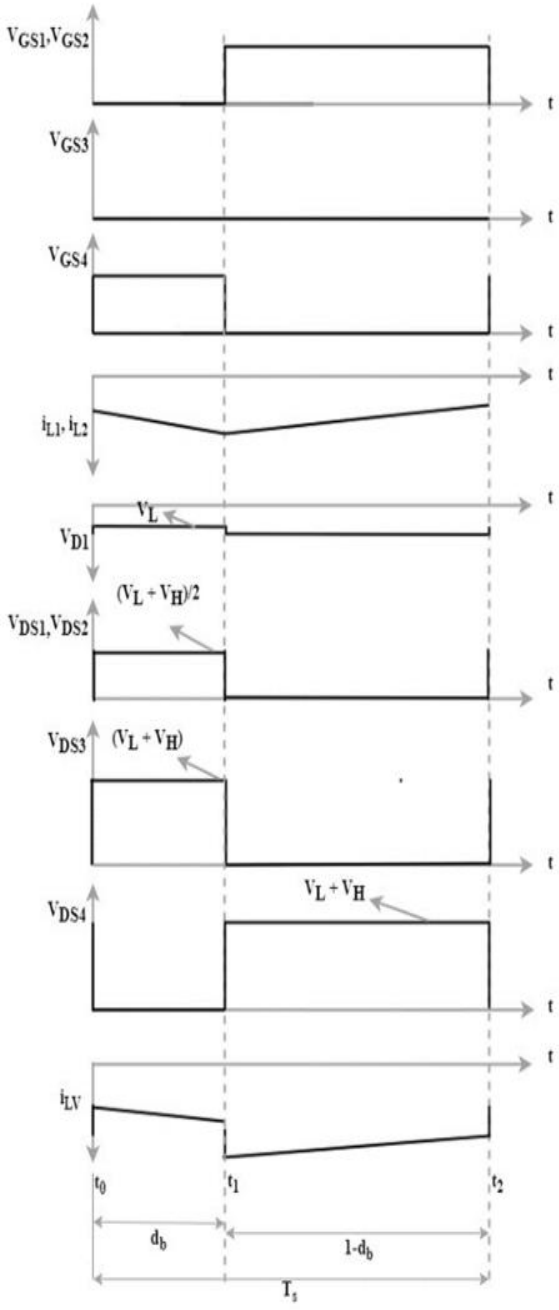

Fig.4.7(b)

Figure 4.7(a) Operational waveforms of Proposed HGBDC in boost mode.

Figure 4.7(b) Operational waveforms of Proposed HGBDC in buck mode.

4.3 Proposed Bidirectional DC-DC converter connected to battery source and a DC motor load

The proposed High Gain Bidirectional DC-DC Converter (HGBDC) is being evaluated for potential use in electric vehicles (EVs) by integrating it into a basic DC motor drive system. This evaluation involves operating the converter in continuous conduction mode to assess its performance in both forward motoring and regenerative braking scenarios. As illustrated in figure 5.8, the HGBDC is connected to a battery and a DC motor load. DC motors are commonly used in the light electric vehicle industry due to their straightforward design, making them a suitable choice for testing the converter's functionality.

Lithium-ion batteries are considered a strong candidate for future EV battery technology due to their impressive attributes, including high power density, high energy density, long cycle life, lack of memory effect, and overall superior energy efficiency. During regenerative braking, the proposed bidirectional DC converter enables power transfer from the motor back to the battery, effectively recapturing energy. Conversely, when the vehicle is in motion, the converter supplies power from the battery to the DC motor.

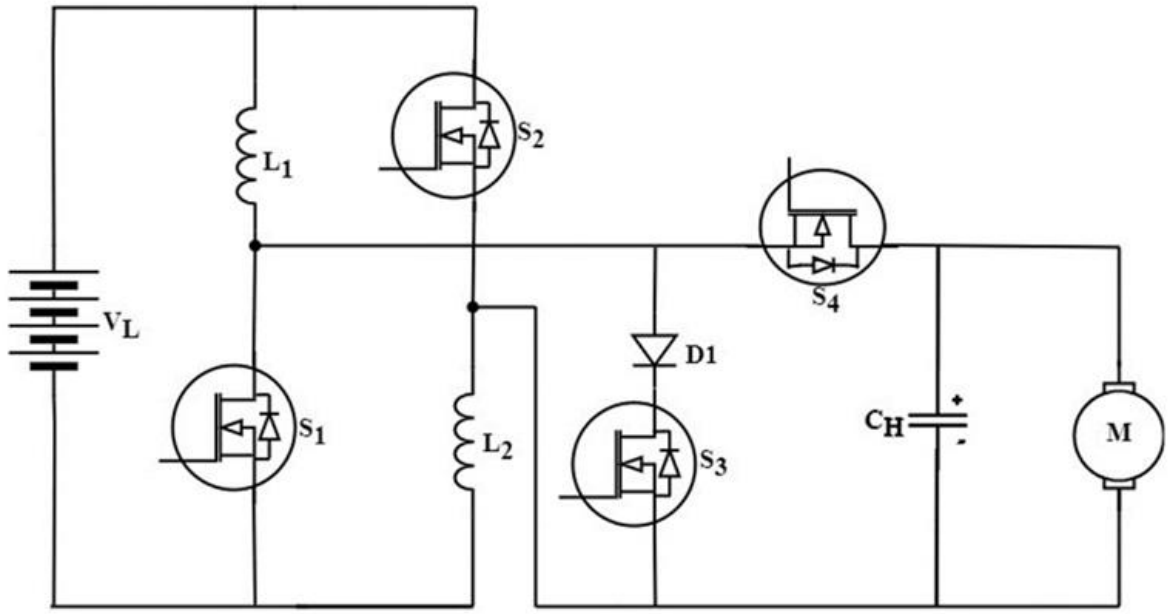

Figure 4.8 Proposed converter connected to battery source and a DC motor load

Two different cases are considered for analysing the proposed bidirectional DC-DC converter fed DC motor drive for an electric vehicle.

I. a step change in speed during forward motoring.
II. transition of the motor operation from forward motoring to regenerative braking.

These two cases are analysed by modelling and simulation using MATLAB / Simulink for a duration of 10 seconds.

5

Modelling and Simulation

5.1 Proposed HGBDC in boost mode with resistive load

5.1.1 Simulation of Proposed converter in boost mode

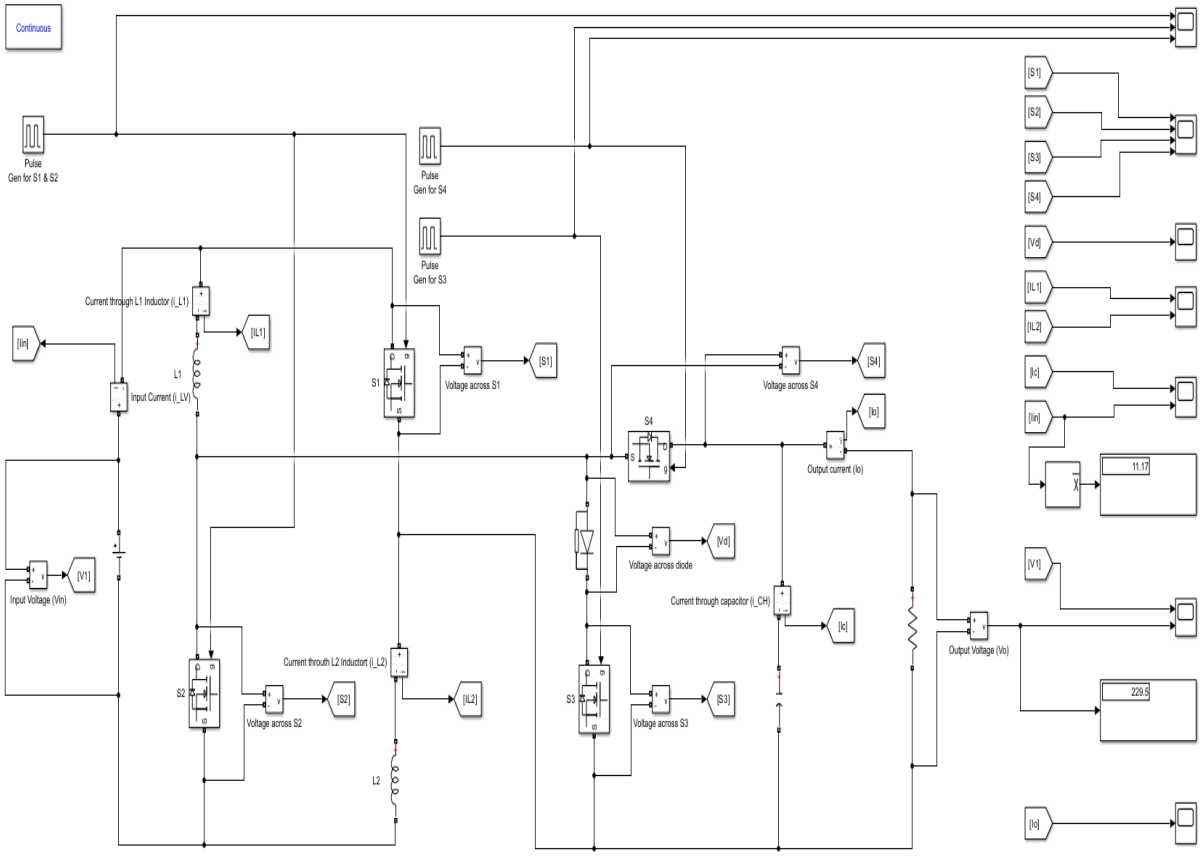

Figure 5.1 Simulation of Proposed converter in boost mode

Converter specification

Parameter	Value / Specification
Input Voltage	48 volts
Output voltage	229.3 volts
Switching frequency	50 kHz
Inductor (L1, L2)	200 μH
Capacitor (C_H)	300 μF
Load (Resistive)	100 Ohm

5.1.2 Opertational Waveforms in boost mode

- **Switching for S1, S2, S3 and S4**

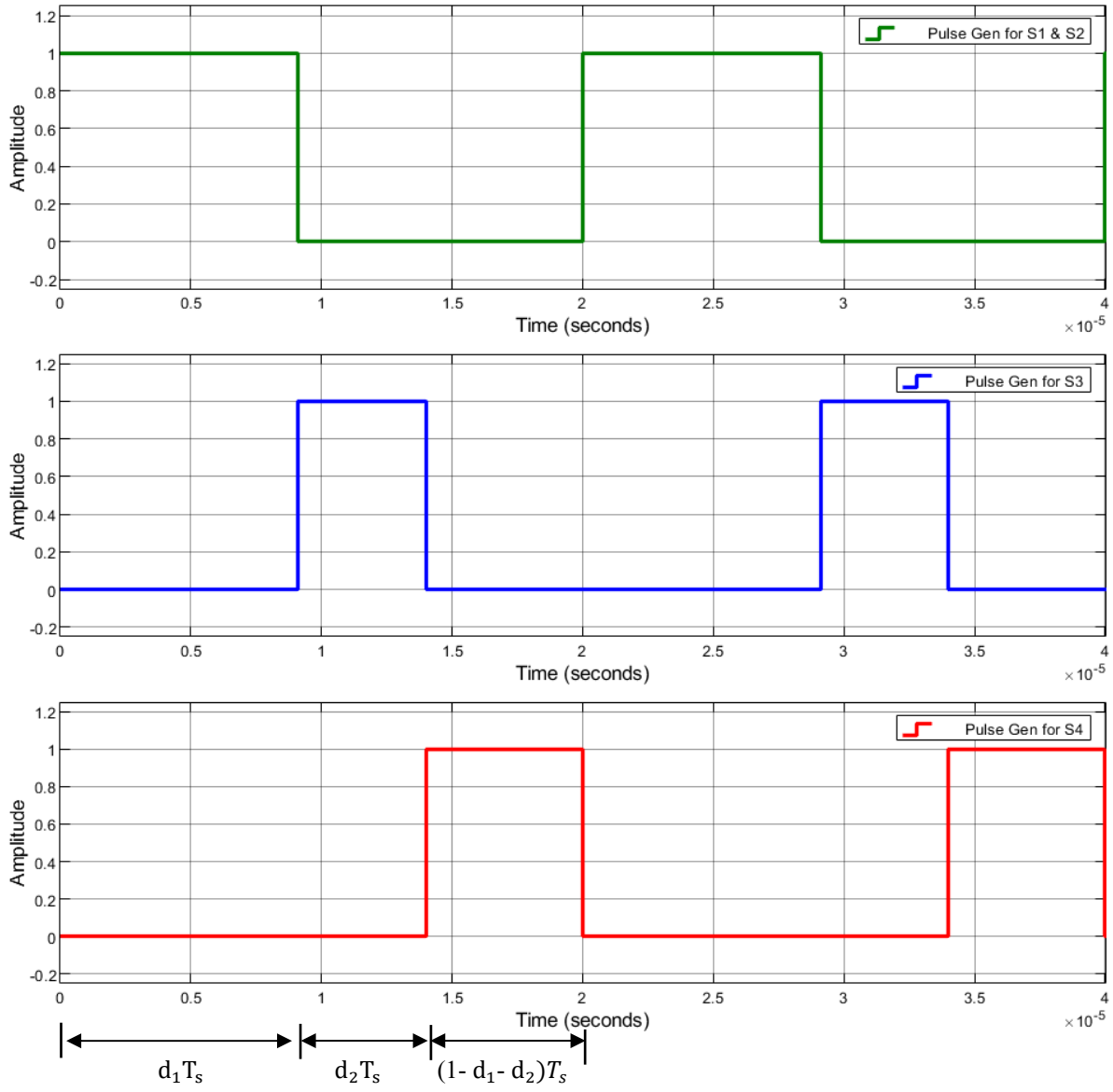

Figure 5.2 Switching pulse for MOSFETs S1, S2, S3 and S4

The switches S1 and S2 are turned on in this mode, while the switches S3 and S4 are turned off for the duration of d_1T_s as shown in green colour waveform in figure 5.2.

Switch S3 is active for the duration of d_2T_s, while switches S1 and S2 are turned off as shown in blue colour waveform in figure 5.2.

The switches S1, S2 and S3 are turned off in this mode. The body diode of the MOSFET S4 conducts during $(1- d_1- d_2)T_s$ for a certain limit of load, otherwise required a gate pulse to active MOSFET S4 as shown in red colour waveform in figure 5.2.

- **Voltage across S1, S2, S3, S4 and diode**

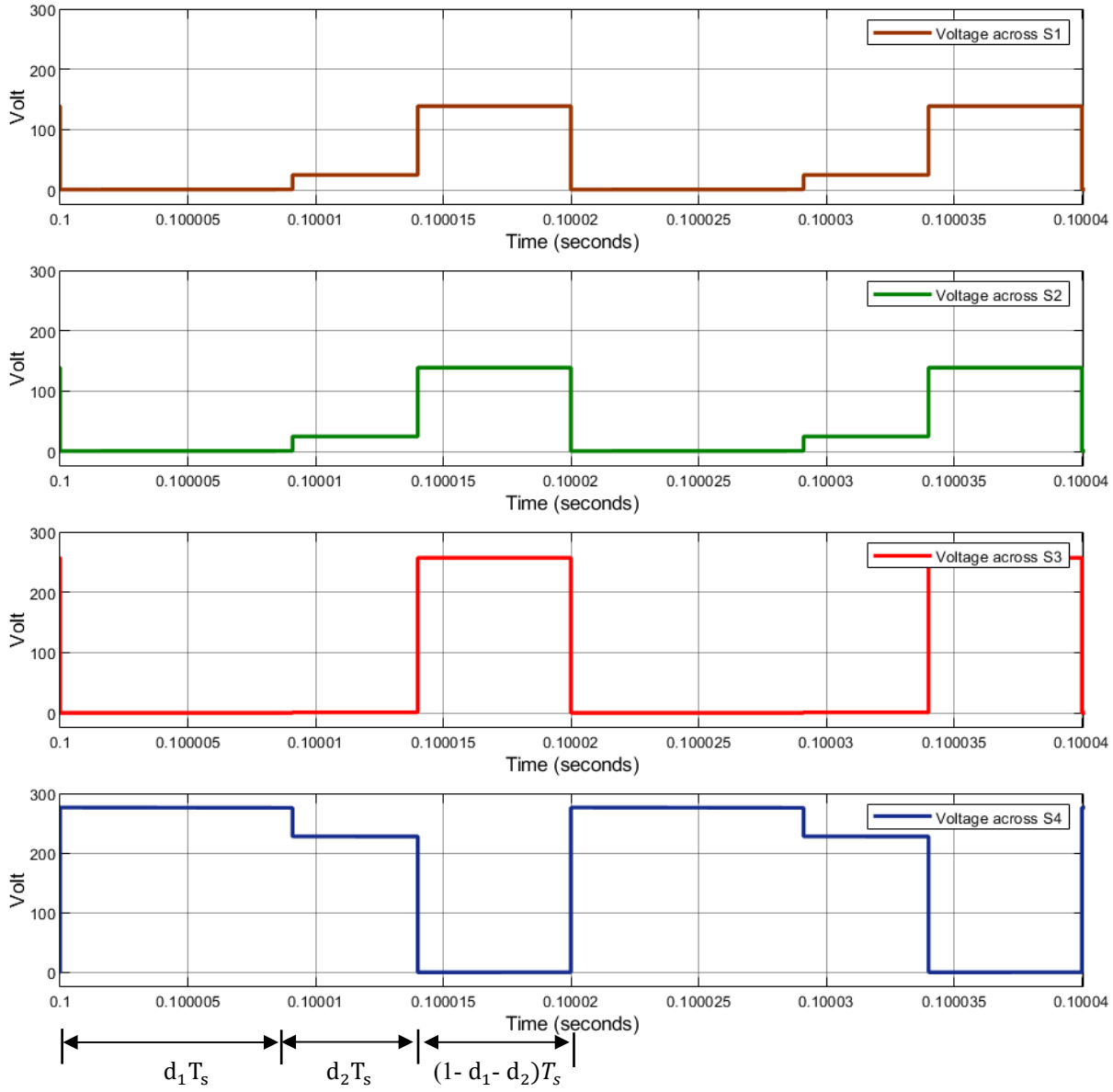

Figure 5.3 Waveform of Voltage across MOSFETs S1, S2, S3 and S4

For d_1T_s time duration voltage across S1 and S2 is zero, voltage across S3 also zero, voltage across S4 is $(V_L + V_H)$

For d_2T_s time duration voltage across S1 and S2 is $\frac{V_L}{2}$, voltage across S3 is zero, voltage across S4 is $(V_H - V_L)$

For $(1- d_1- d_2)T_s$ time duration voltage across S1 and S2 is $\frac{(V_L+V_H)}{2}$, voltage across S3 is $(V_L + V_H)$, voltage across S4 is zero.

Here, V_L = Low voltage side voltage or Input voltage or V_{in}

V_H = High voltage side voltage or Output voltage or V_O

- **Voltage across diode (V_d)**

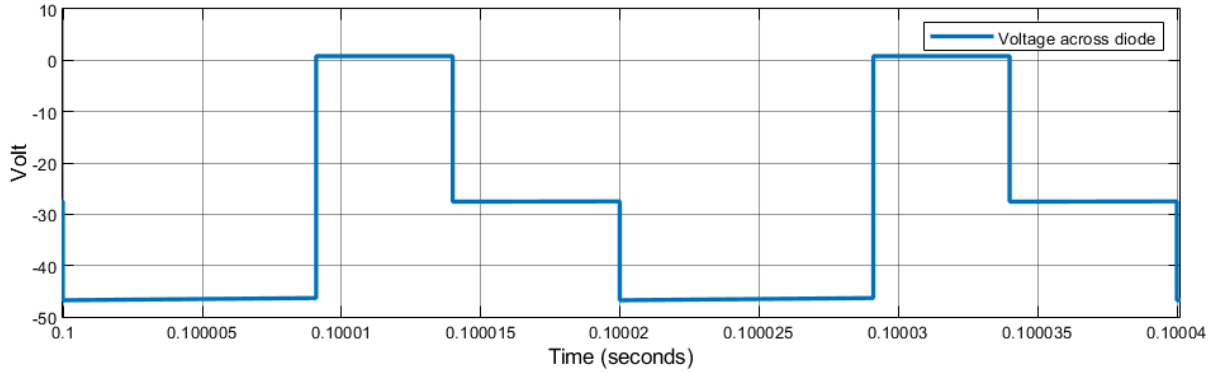

Figure 5.4 Waveform of Voltage across diode

- **Current through inductor L1 (i_{L1}) and inductor L2 (i_{L2})**

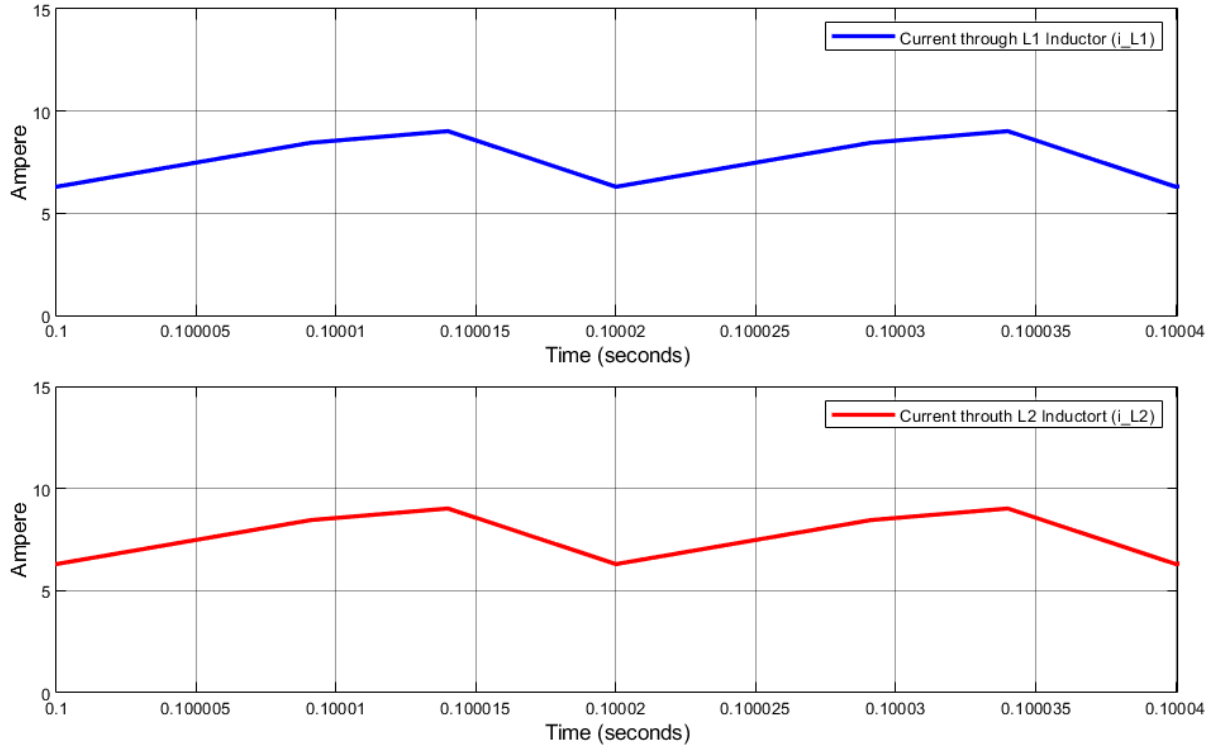

Figure 5.5 Waveform of Current through inductors L1 and L2 (I_{L1} & I_{L2})

In boost mode, the inductor current increases when the first three switches S1, S2 and S3 are turned on, whereas the current through the inductor decreases when the switch S4 is turned on. In figure 5.5, blue waveform shows current through inductor L1 and red waveform shows current through inductor L2.

- **Charing current (I_{CH}) and Input current (I_{LV})**

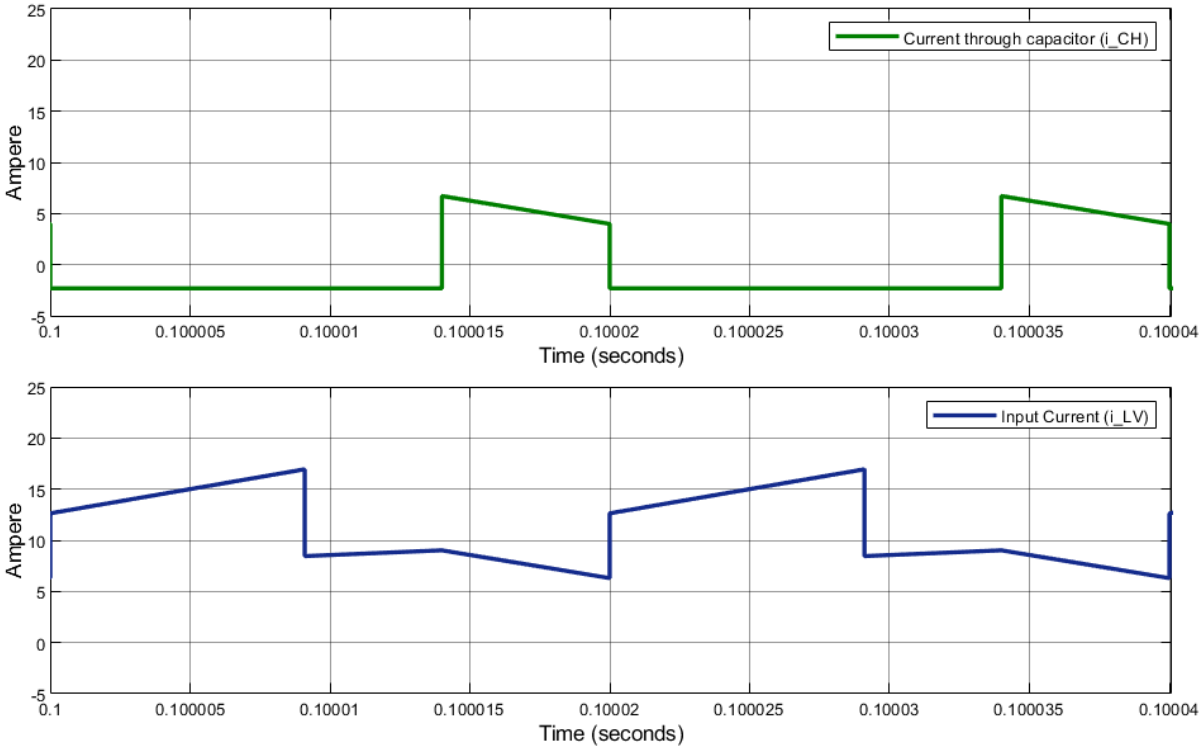

Figure 5.6 Waveform of Charing current (I_{CH}) and Input current (I_{LV})

- **Output current (I_O or I_{HV})**

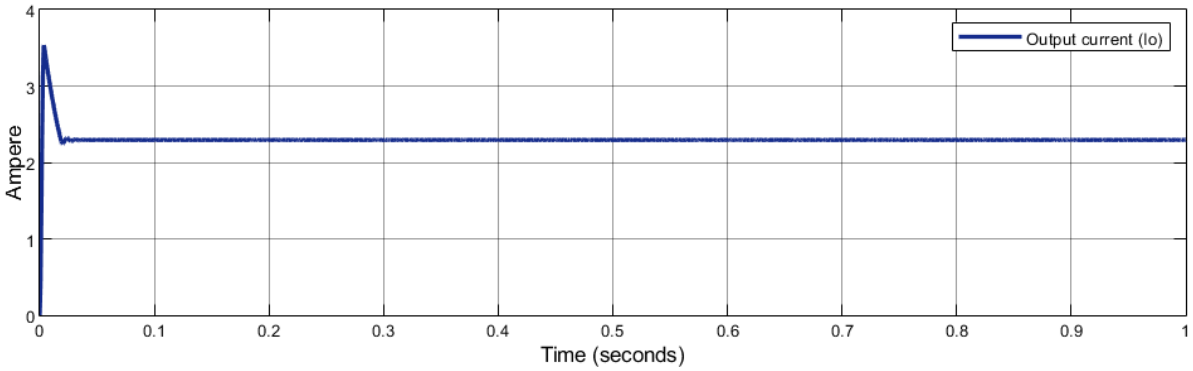

Figure 5.7 Waveform of output current (I_O)

- **Input voltage (Vin), Output voltage (Vo)**

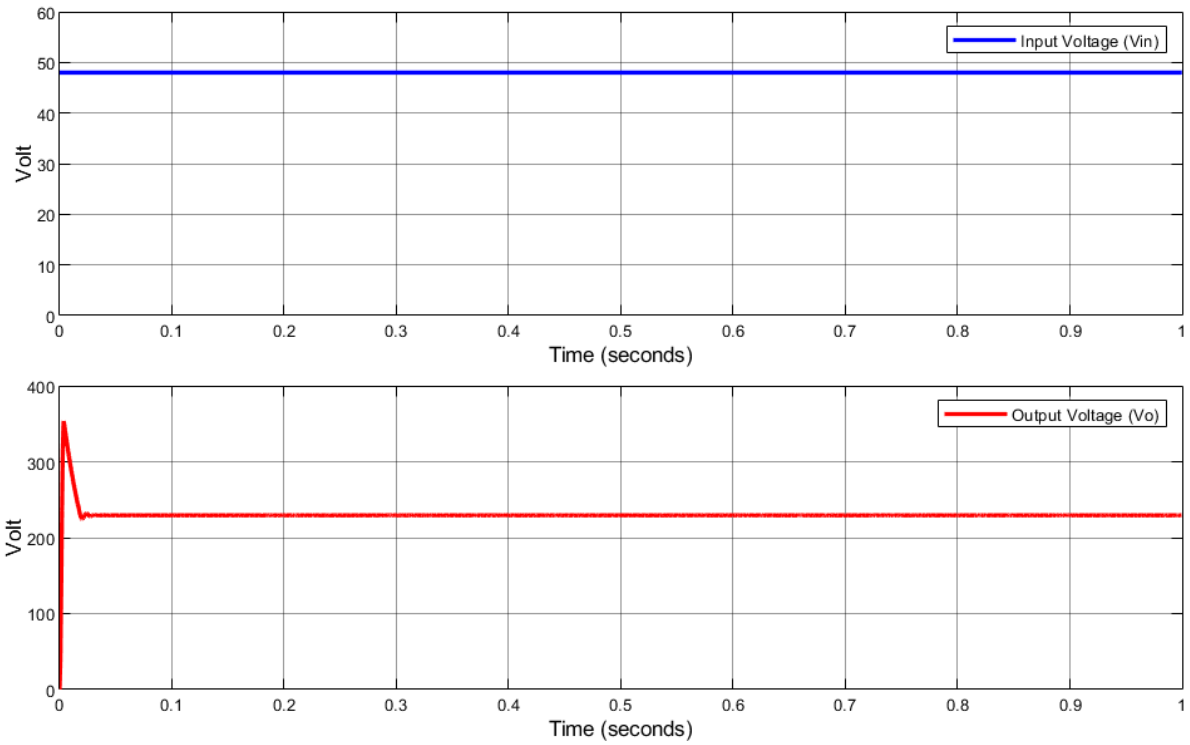

Figure 5.8 Waveform of Input voltage and output voltage

In boost mode, low voltage side volage (V_L) as input voltage (V_{in}) is given 48volt by a battery as per blue colour waveform in figure 5.8. The converter gives High voltage side voltage (V_H) as output voltage (V_O) is equal to 229.3volt as per red colour waveform in figure 5.8.

5.2 Proposed HGBDC in buck mode with resistive load

5.2.1 Simulation of Proposed converter in buck mode

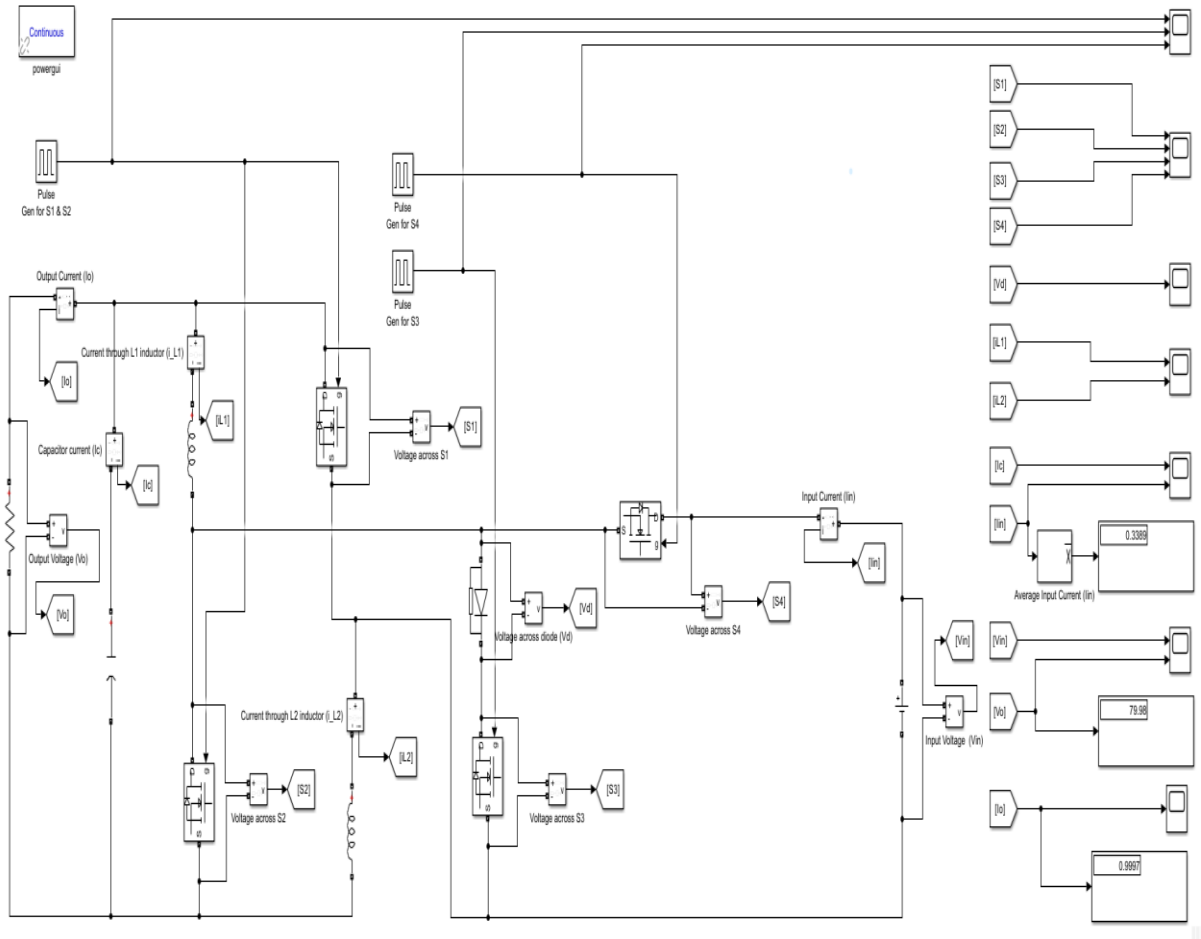

Figure 5.9 Simulation of Proposed converter in buck mode

Converter specification

Parameter	Value / Specification
Input Voltage	240 volts
Output voltage	79.98 volts
Switching frequency	50 kHz
Inductor (L1, L2)	200 μH
Capacitor (C_H)	300 μF
Load (Resistive)	80 Ohm

5.2.2 Operational waveform in buck mode

- **Switching for S1, S2, S3 and S4**

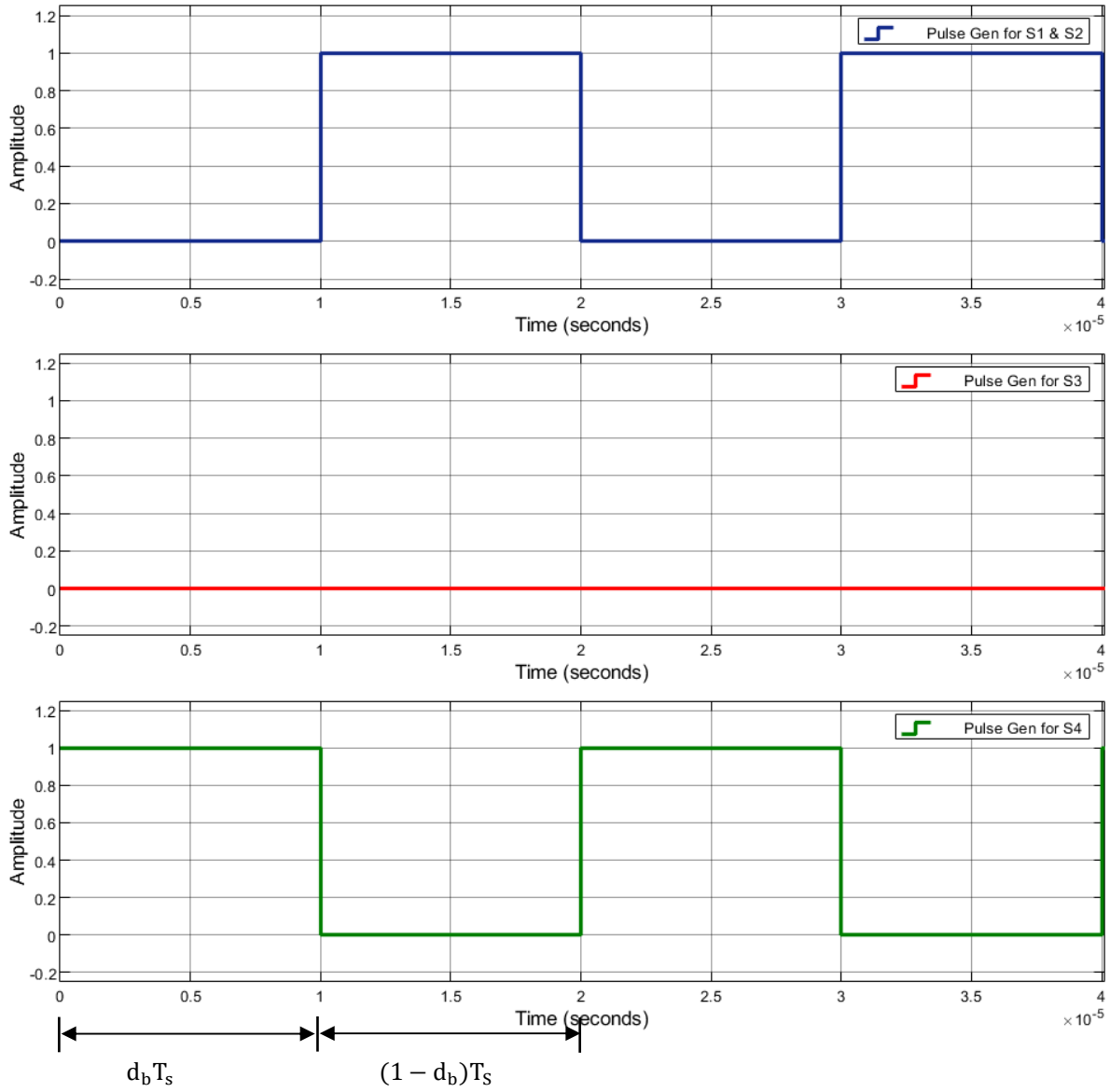

Figure 5.10 Switching of MOSFET S1, S2, S3 and S4

In buck mode, the MOSFET S4 is turned on and the MOSFETs S1, S2, S3 are turned off for a duration of d_bT_s as shown in green colour waveform in figure 5.10.

For a duration of $(1-d_b)T_S$, the MOSFETs S1 and S2 conduct and the MOSFET S4 is turned off the as shown in blue colour waveform in figure 5.10.

No gate pulse required for MOSFET S3 in buck mode operation as shown in red waveform in figure 5.10.

- **Voltage across MOSFET S1, S2, S3, S4**

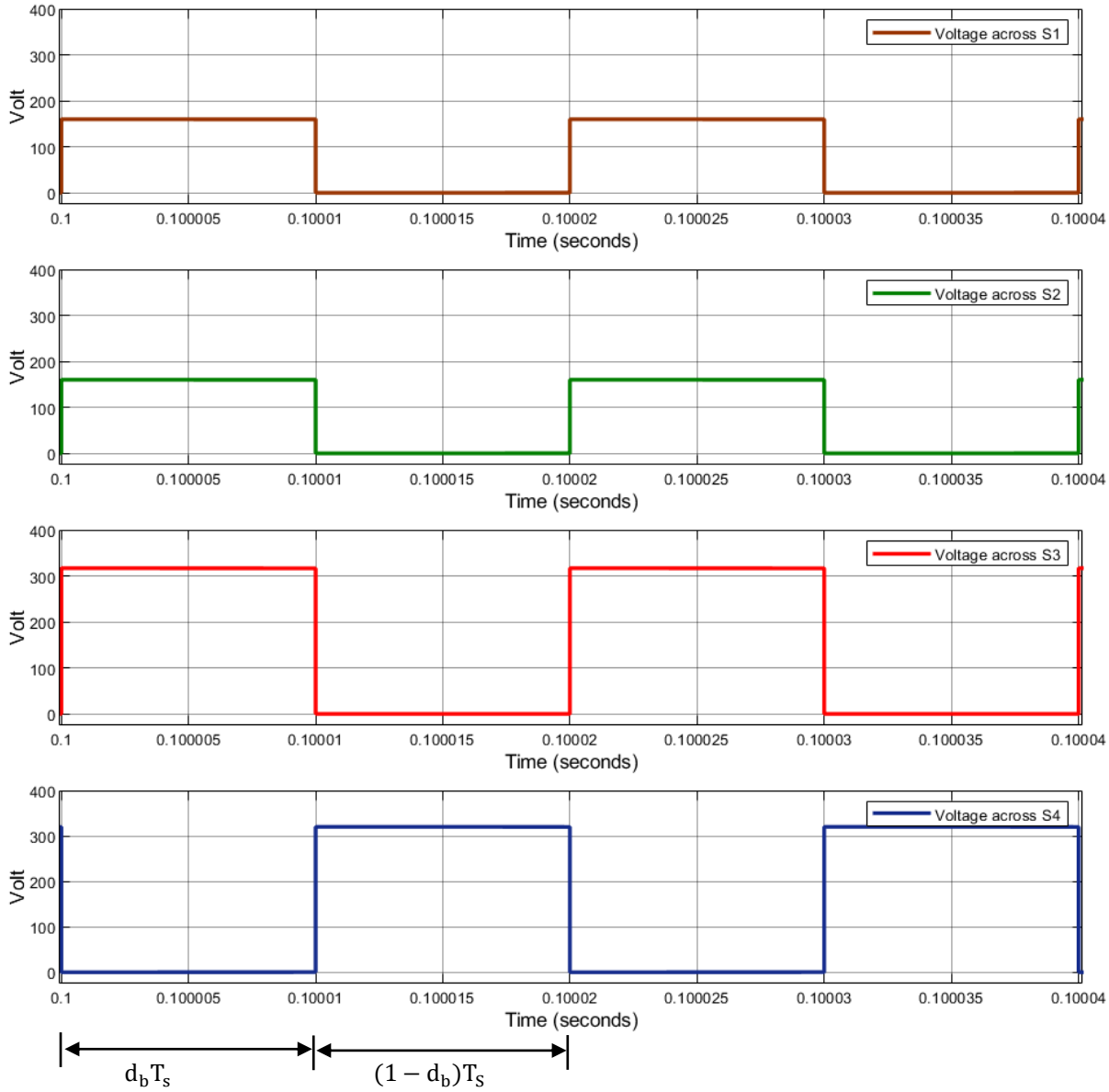

Figure 5.11 Waveform of voltage across MOSFET S1, S2, S3, S4

For d_bT_s time duration voltage across S1 and S2 is $\frac{(V_L+V_H)}{2}$, voltage across S3 also $(V_L + V_H)$, voltage across S4 is zero.

For $(1 - d_b)T_S$ time duration voltage across S1 and S2 is zero, voltage across S3 is zero, voltage across S4 is $(V_L + V_H)$

Here, V_H = Voltage at High voltage side or Input voltage or V_{in}

V_L = Voltage at Low voltage side or Output voltage or V_O

- **Voltage across diode (V_d)**

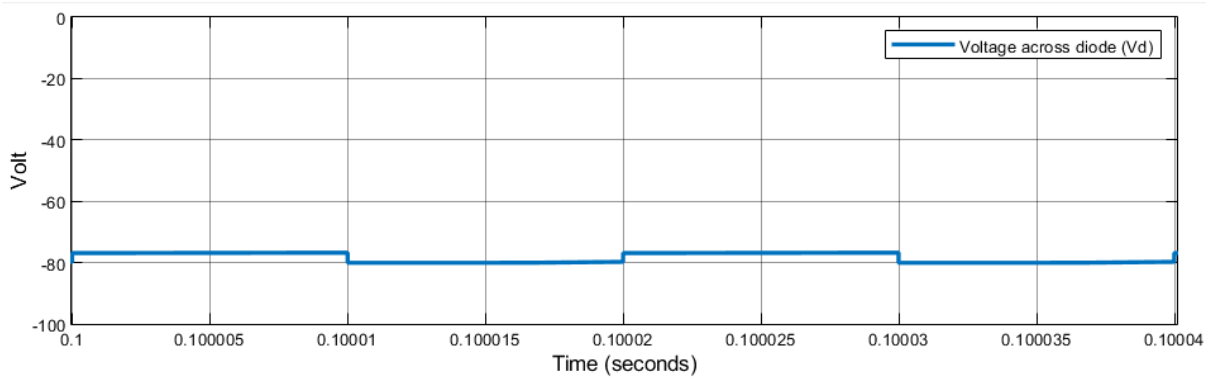

Figure 5.12 Waveform across Voltage across diode

- **Current through inductor L1 (i_{L1}) and inductor L2 (i_{L2})**

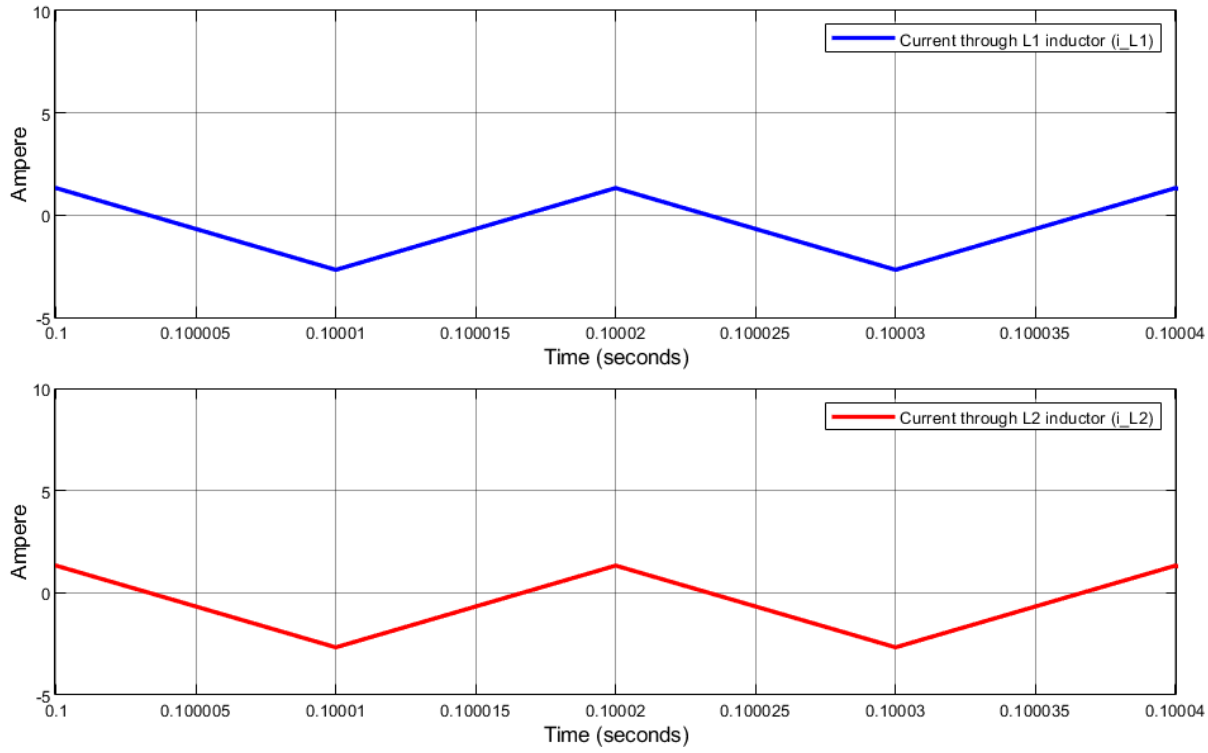

Figure 5.13 Waveform of current through inductor L1 and inductor L2

In buck mode, the inductor current decreases when the MOSFETs S1, S2 are turned off and the MOSFET S4 turned on, whereas the current through the inductor increases when the MOSFETs S1 & S2 are conduct and the MOSFETs S4 is turned off. In figure 5.13, blue waveform shows current through inductor L1 and red waveform shows current through inductor L2.

- **Output Current (I_{LV} or I_O)**

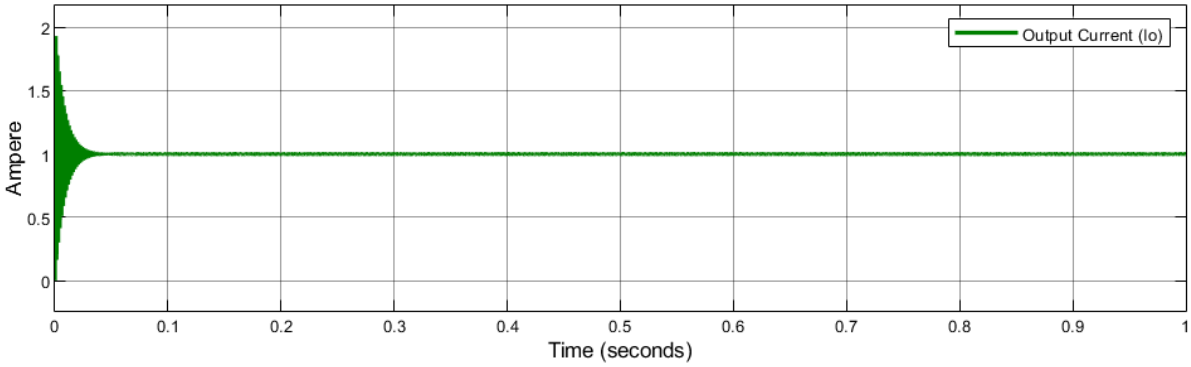

Figure 5.14 Waveform of output current

- **Input voltage (V_{in}), Output voltage (V_O)**

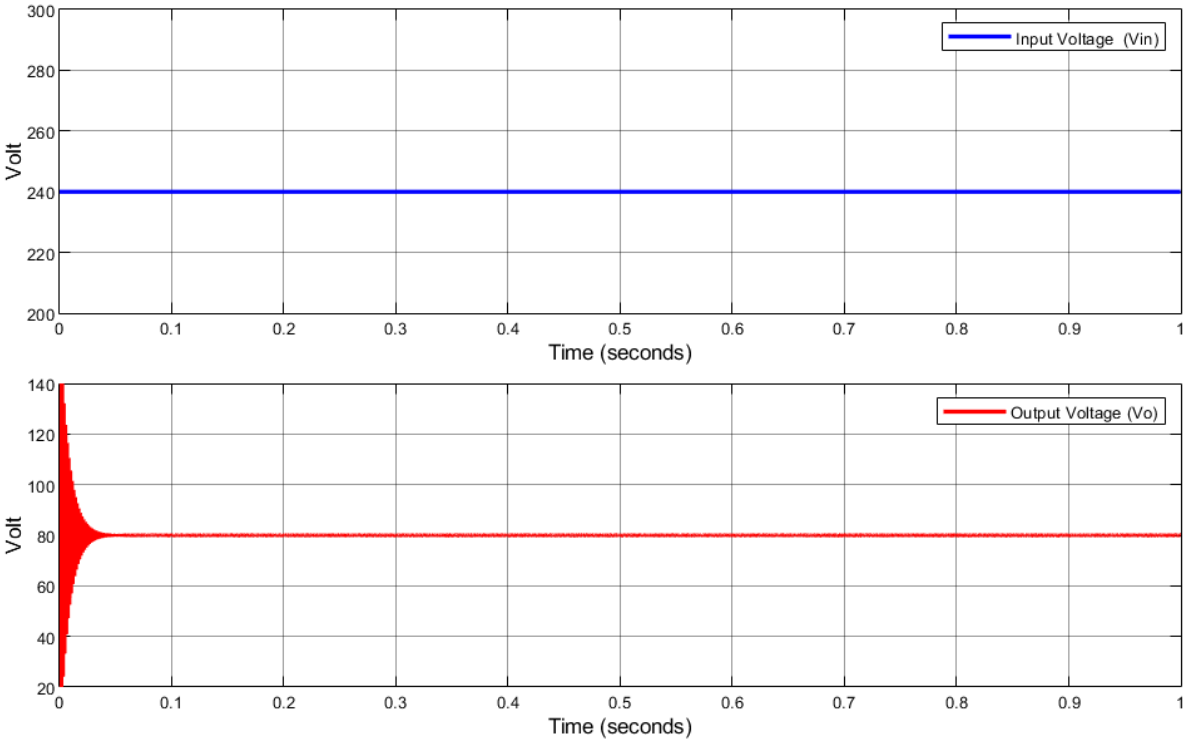

Figure 5.15 Waveform of Input voltage and output voltage

In buck mode, Voltage at High voltage side (V_H) as input voltage (V_{in}) is given 240volt by a battery as per blue colour waveform in figure 5.15. The converter gives output voltage (V_O) at Low voltage side (V_H) is equal to 79.98 volt as per red colour waveform in figure 5.15.

5.3 Simulation of Proposed Bidirectional DC-DC converter connected to battery source and a DC motor load

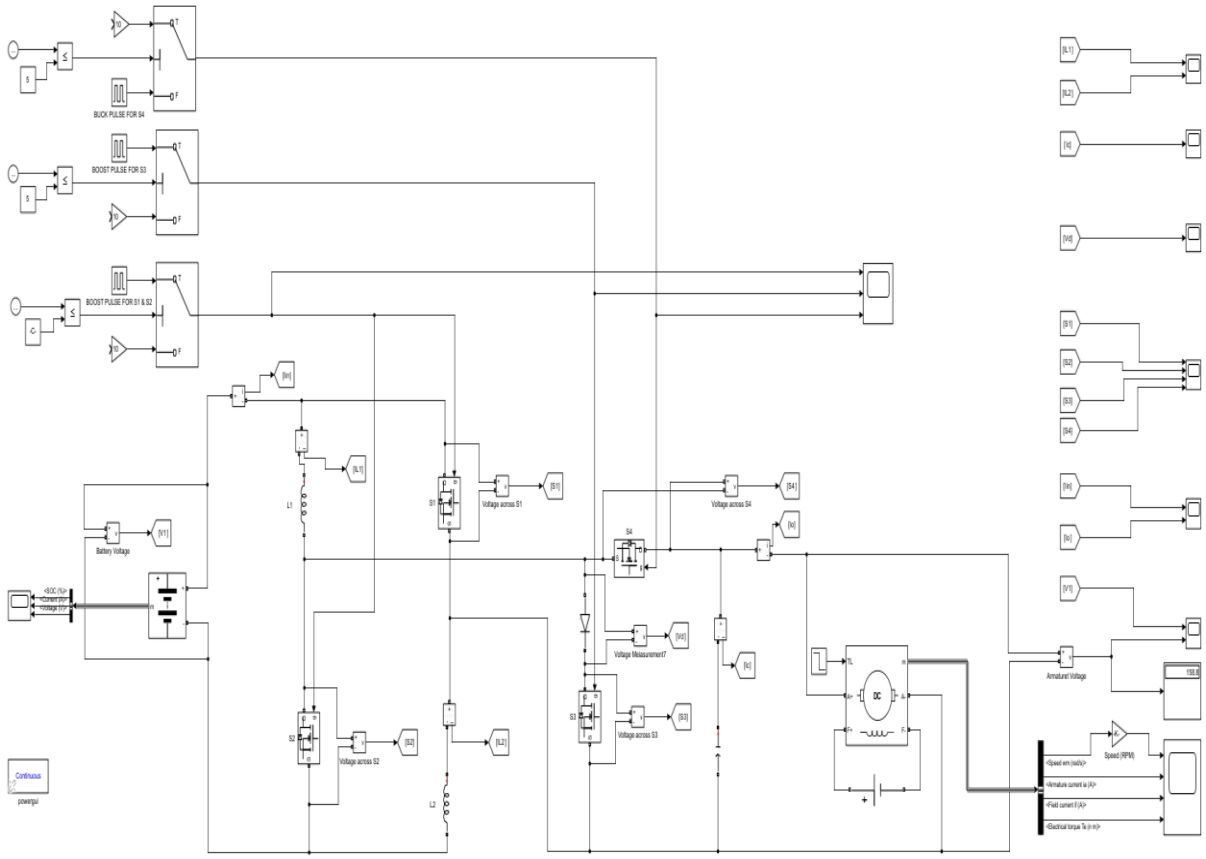

Figure 5.16 Simulation of Proposed Bidirectional DC-DC converter with motor load

Converter specification

Parameter	Value / Specification
Input Voltage	48 volts
Switching frequency	50 kHz
Inductor (L1, L2)	200 μH
Capacitor (C_H)	300 μF
Load (Separately excited DC Motor)	5 HP, 240 volts, 1750 RPM Field voltage 150 volt

Battery specification

Parameter	Value / Specification
Type	Li-ion
Nominal Voltage	48 volts
Initial % SOC	80%
Capacity	140 Ah

5.3.1 Case 1: A step change in speed during forward motoring

A step change in motor speed from 1250 RPM to 1750 RPM at constant torque constitutes the second instance of transient operation done in this system.

- **DC motor response for a step change in speed during forward motoring**

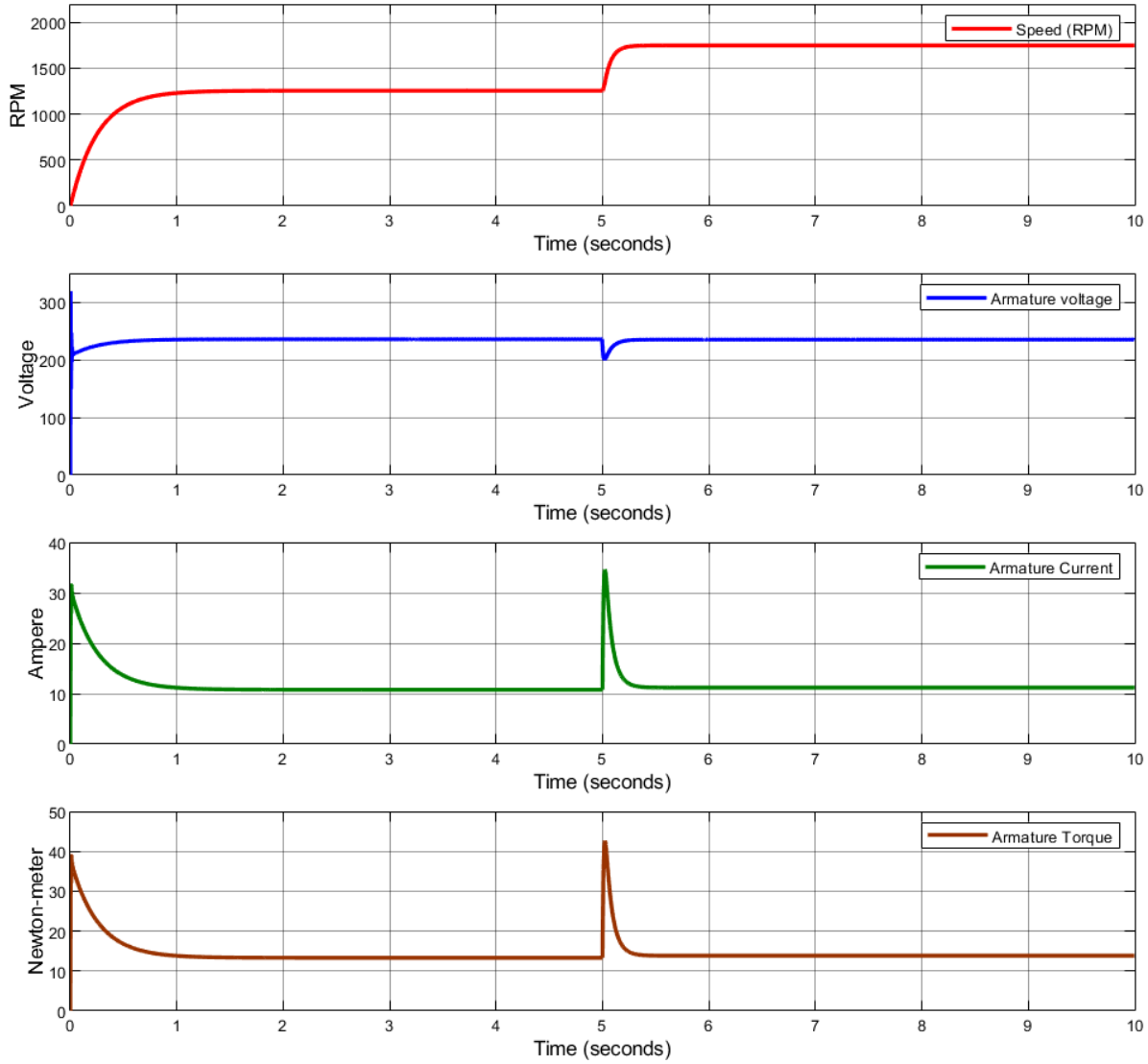

Figure 5.17 DC motor response for a step change in speed during forward motoring

The red colour waveform depicts the DC motor speed waveform for a duration of 10 seconds and shows a step change in motor speed at 5 second from 1250 RPM to 1750 RPM. The change in armature voltage with respect to the change in motor speed is depicted in blue waveform in figure 5.17. The characteristics of Armature current that is identical to that of Armature torque is shown in green and brown waveform respectively in figure 5.17.

- **Battery response for a step change in speed during forward motoring**

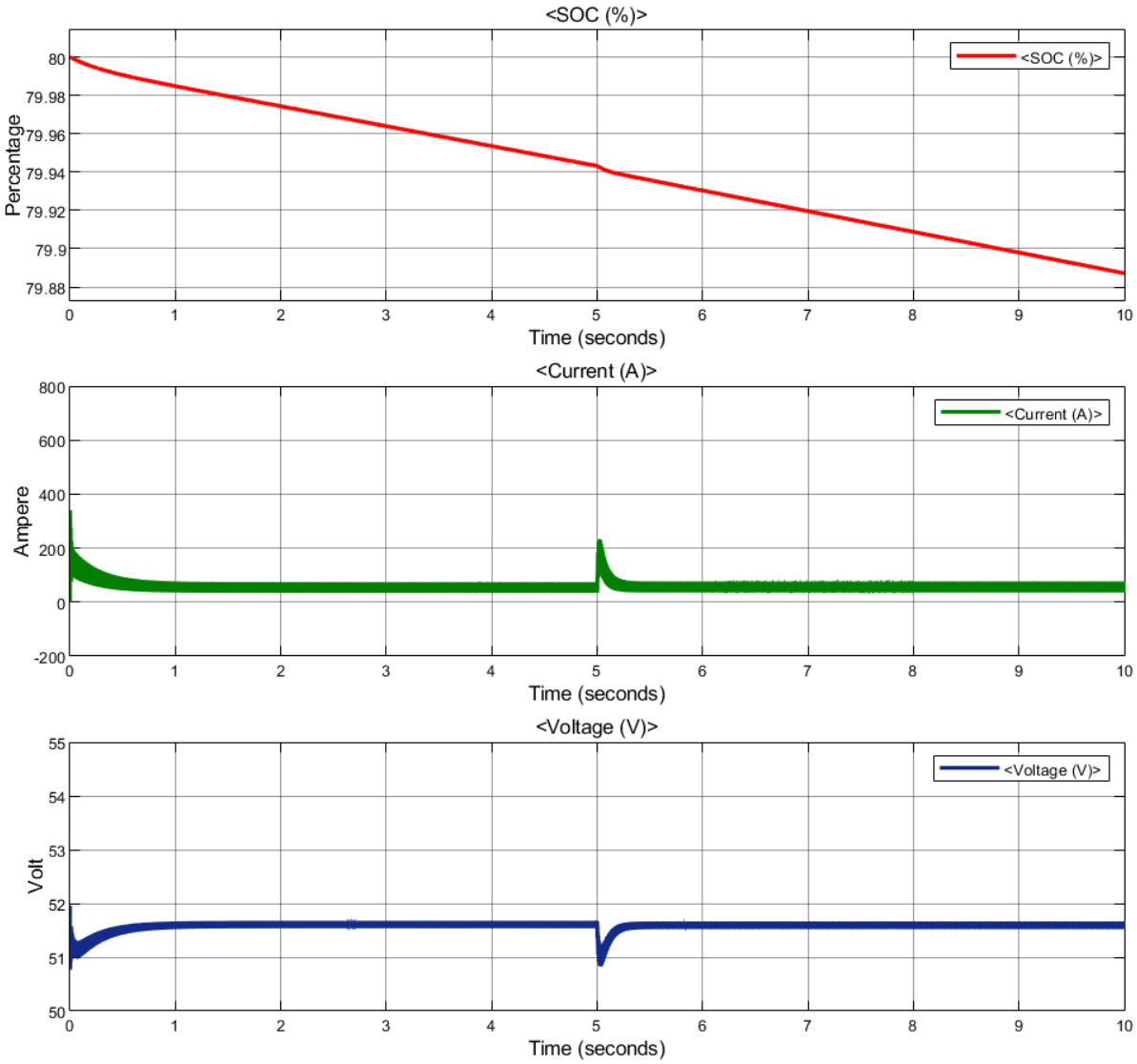

Figure 5.18 Battery response for a step change in speed during forward motoring

As seen in figure 5.18, when the speed increases, the motor draws more energy from the source, resulting in a fall in the SOC from 80% to 79.885%. The battery voltage and current during this phase are depicted blue and green colour waveform respectively in figure 5.18.

5.3.2. Case2: Transition of the motor operation from forward motoring to regenerative braking

- **DC motor response during transition of the motor operation from forward motoring to regenerative braking**

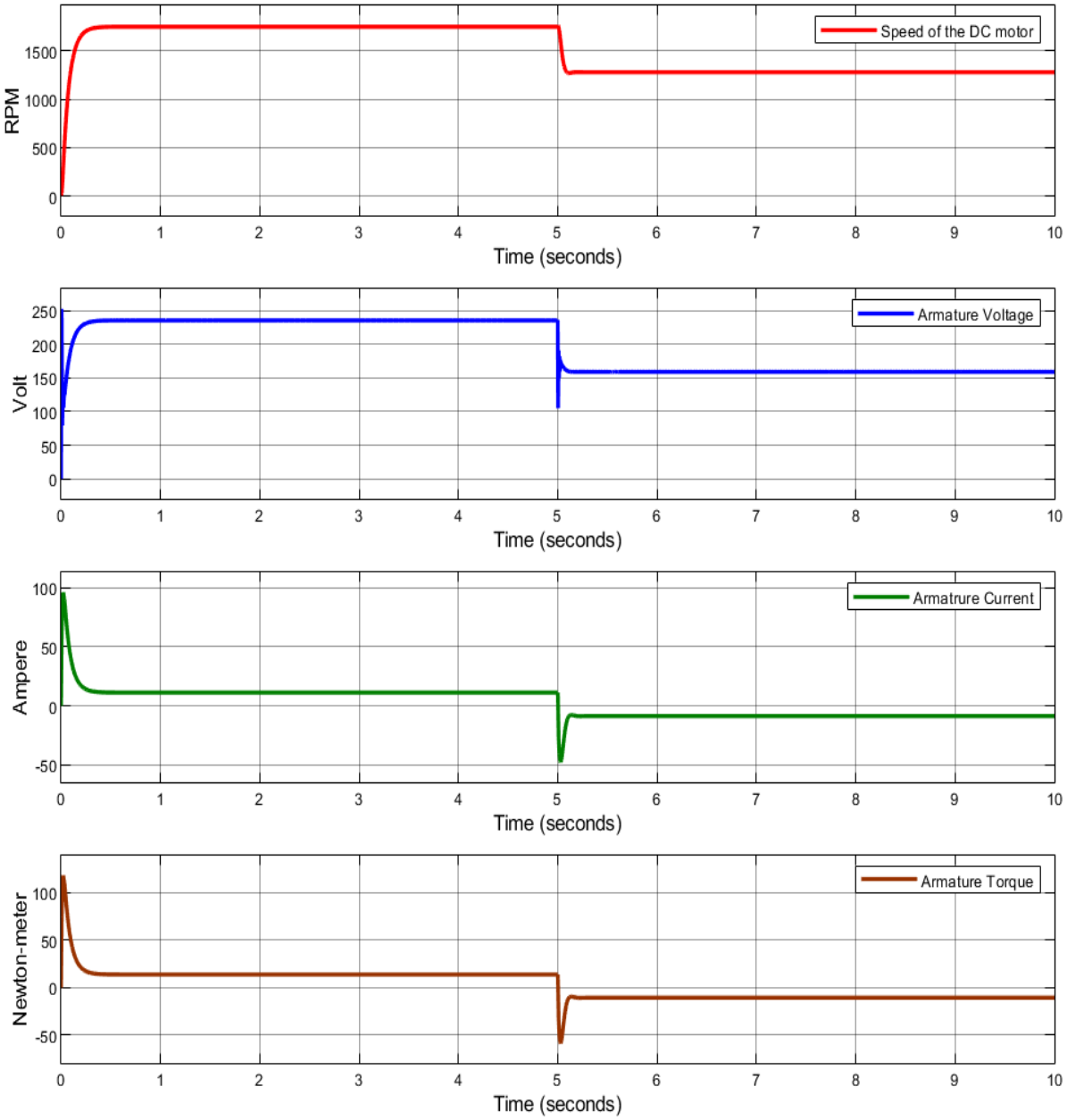

Figure 5.19 DC motor response during transition of the motor operation from forward motoring to regenerative braking

In figure 5.19 shows DC motor response during transition of the motor operation from forward motoring (0 – 5 sec) to regenerative braking (5 – 10 sec). The red colour waveform is Speed of the DC motor, blue colour waveform is Armature voltage, green colour waveform is Armature current, brown colour waveform is Armature torque.

- **Battery response during transition of the motor operation from forward motoring to regenerative braking**

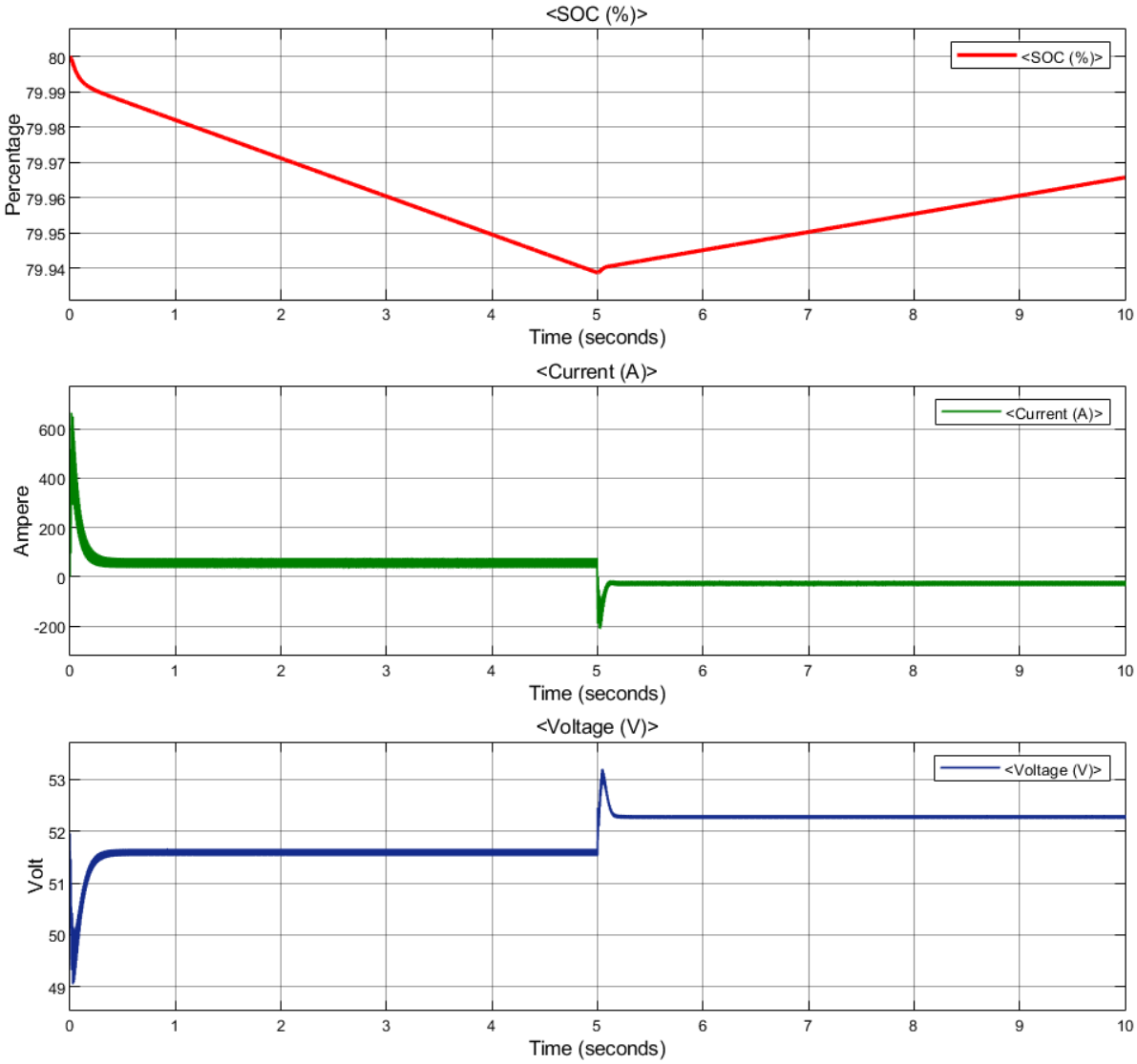

Figure 5.20 Battery response during transition of the motor operation from forward motoring to regenerative braking

In figure 5.20 shows Battery response during transition of the motor operation from forward motoring (0 – 5 sec) to regenerative braking (5 – 10 sec).

The red colour waveform shows SOC decreases from 80% to 79.94% during forward motoring mode and SOC increases from 79.94% to 79.965% during regenerating braking of the DC motor.

The green colour waveform shows battery current or input current changes during transition of the motor operation from forward motoring to regenerative braking.

The blue colour waveform shows battery voltage or input voltage changing during transition of the motor operation from forward motoring to regenerative braking.

6

Analysis of the results of Simulation

6.1 Proposed bidirectional DC-DC converter with resistive load in boost mode

The converter is modelled and simulated using MATLAB/Simulink for a duration of 1 second. The simulated circuit diagram as shown in figure 5.1. The steady-state inductor current and the gate drive pulses of the MOSFET switches for boost mode of operations of the converter are shown in figure 5.5 and 5.2 respectively. In boost mode, the inductor current increases when the first three switches S1, S2 and S3 are turned on, whereas the current through the inductor decreases when the switch S4 is turned on. The duty ratio of the PWM pulses generated, d1 and d2 for the switches S1/S2 and S3 respectively are 0.455 and 0.245. The input voltage and output voltage waveforms are shown in figure 5.8.

Theorical converter gain = $\frac{1+d_1}{1-d_1-d_2} = \frac{1+0.455}{1-0.455-0.245} = \frac{1.455}{0.3} = 4.85$

- **Result of the simulated converter in boost mode**

Input voltage (V_L)	48 V
Output voltage (V_H)	229.5 V
Input Current (I_{LV})	11.17 A
Output Current (I_{HV})	2.295 A

Simulated Converter gain = $\frac{V_H}{V_L} = \frac{229.5}{48} = 4.78$

Efficiency of simulated converter, $\eta = \frac{P_o}{P_{in}} \times 100\%$

$= \frac{V_o I_o}{V_{in} I_{in}} \times 100\%$

$= \frac{229.5 \times 2.295}{48 \times 11.17} \times 100\%$

$= \frac{526.7}{536.16} \times 100\%$

$= 98.24\%$

6.2 Proposed bidirectional DC-DC converter with resistive load in buck mode

The converter is modelled and simulated using MATLAB/Simulink for a duration of 10 seconds. The gate drive pulses of the MOSFET switches for buck mode of operations of the converter are shown in figure 5.10. The duty ratio of the PWM pulses generated, d_b the switch S4 operates with a duty ratio d_b which is 0.5. The input voltage and output voltage waveforms are shown in figure 5.15.

Theorical converter gain = $\frac{d_b}{2-d_b} = \frac{0.5}{2-0.5} = \frac{0.5}{1.5} = 0.3333$

- **Result of the simulated converter in buck mode**

Input voltage (V_H)	240 V
Output voltage (V_L)	79.98 V
Input Current (I_{HV})	0.3389 A
Output Current (I_{LV})	0.9997 A

Simulated converter gain = $\frac{V_L}{V_H} = \frac{79.98}{240} = 0.33325$

Efficiency of simulated converter, $\eta = \frac{P_o}{P_{in}} \times 100\%$

$= \frac{V_o I_o}{V_{in} I_{in}} \times 100\%$

$= \frac{79.98 \times 0.9997}{240 \times 0.3389} \times 100\%$

$= \frac{79.956}{81.336} \times 100\%$

$= 98.30\%$

6.3 Proposed Bidirectional DC-DC converter connected to battery source and DC motor load

The circuit diagram of proposed Bidirectional DC-DC converter connected to battery source and DC motor load as shown in figure 4.8 and the simulated circuit diagram as shown in figure 5.16. Two different cases are analysed for the proposed work which are mentioned at 4.3 in previous chapter.

6.3.1 Case1: Analysis for a step change in speed during forward motoring

The converter is modelled and simulated using MATLAB/Simulink for a duration of 10 seconds. Figure 5.17 shows the DC motor response for this case, i.e the waveform of motor speed, armature torque, armature current, armature voltage (output voltage V_H) of the converter and figure 5.18 shows the battery response for this case, i.e the waveform of battery SOC, battery voltage, battery current. At 5 second step change in motor speed from 1250 RPM to 1750 RPM at constant torque. when the speed increases, the motor draws more energy from the source, resulting in a fall in the SOC from 80% to 79.885%.

6.3.2 Case2: Analysis for Transition of the motor operation from forward motoring to regenerative braking

The converter is modelled and simulated using MATLAB/Simulink for a duration of 10 seconds. This simulated circuit is shown in figure 5.16. The converter is made to operate in boost (forward motoring) mode from 0-5 seconds and in buck (regenerative braking) mode from 5-10 seconds. Figure 5.19 shows the DC motor response for this case, i.e the waveform of motor speed, armature torque, armature current, armature voltage (output voltage V_H) of the converter, and figure 5.20 shows the battery response for this case, i.e the waveform of battery SOC, battery voltage, battery current. Simulations are carried out for the braking action with a speed change from 1750 rpm to 1280 rpm when the motor current and torque exhibit a reversal characteristic as shown in figure 5.19. The change in directions of current and torque during the transition from motoring mode to regenerative braking mode indicates the reversal of power flow.

There is a dip in battery voltage and reduction in SOC of the battery during forward motoring (0 to 5 seconds). But the battery voltage and SOC of the battery increases during regenerative braking as observed in figure 5.20. The SOC of the battery increases from 79.94% to 79.965% during a short span of 5 second in regenerative braking mode.

7

Conclusion

The thesis presents a high gain bidirectional converter designed for electric vehicle applications, with a particular focus on enabling efficient battery charging during regenerative braking. Through performance analysis conducted in MATLAB/Simulink, the effectiveness of converter in both motoring and regenerative braking modes is demonstrated. The following key points have been concluded here.

The converter is noted for its ability to balance high voltage gain with a manageable number of components. This is important because a simpler design with fewer components tends to be more reliable and cost-effective.

Although the introduction of soft switching could further improve efficiency by reducing switching losses, it would introduce additional complexity and increase the number of components. Thus, while the proposed converter is effective and straightforward, any potential enhancements must carefully consider the trade-offs between performance gains and design complexity.

The converter excels in controlling power flow direction by seamlessly transitioning between motoring and regenerative braking modes, which is essential for optimizing energy efficiency. During forward motoring, the converter powers the motor using energy stored in the battery. Conversely, in regenerative braking mode, the motor operates as a generator, and the converter transfers the recovered energy back to the battery for storage. This bidirectional capability enhances overall energy efficiency by ensuring that energy is effectively utilized and stored, thereby optimizing the performance of the electric vehicle and extending the range.

Transient analysis helps to optimize the performance of a converter by minimizing overshoot and ripple, ensuring system stability, assessing component stress for reliability, and implements effective protection measure. There is ample scope of research to study the transient performance of the proposed converter. Also, variations in inductance and saturation characteristics of inductor in the converter can affect the efficiency and performance of the converter. The performance of the proposed converter can be analysed with above non-idealities of inductor in future.

8

References

[1]. S. A. Gorji, H. G. Sahebi, M. Ektesabi and A. B. Rad, "Topologies and Control Schemes of Bidirectional DC–DC Power Converters: An Overview," in *IEEE Access*, vol. 7, pp. 117997-118019, 2019, doi: 10.1109/ACCESS.2019.2937239.

[2]. D. Flores Cortez, G. Waltrich, J. Fraigneaud, H. Miranda and I. Barbi, "DC–DC Converter for Dual-Voltage Automotive Systems Based on Bidirectional Hybrid Switched-Capacitor Architectures," in *IEEE Transactions on Industrial Electronics*, vol. 62, no. 5, pp. 3296-3304, May 2015, doi: 10.1109/TIE.2014.2350454.

[3]. Z. Wang, P. Wang, B. Li, X. Ma and P. Wang, "A Bidirectional DC–DC Converter With High Voltage Conversion Ratio and Zero Ripple Current for Battery Energy Storage System," in *IEEE Transactions on Power Electronics*, vol. 36, no. 7, pp. 8012-8027, July 2021, doi: 10.1109/TPEL.2020.3048043.

[4]. Y. Zhang, Y. Gao, L. Zhou and M. Sumner, "A Switched-Capacitor Bidirectional DC–DC Converter With Wide Voltage Gain Range for Electric Vehicles With Hybrid Energy Sources," in *IEEE Transactions on Power Electronics*, vol. 33, no. 11, pp. 9459-9469, Nov. 2018, doi: 10.1109/TPEL.2017.2788436.

[5]. A. Kumar, X. Xiong, X. Pan, M. Reza, A. R. Beig and K. A. Jaafari, "A Wide Voltage Gain Bidirectional DC–DC Converter Based on Quasi Z-Source and Switched Capacitor Network," in *IEEE Transactions on Circuits and Systems II: Express Briefs*, vol. 68, no. 4, pp. 1353-1357, April 2021, doi: 10.1109/TCSII.2020.3033048.

[6]. Y. Zhang, W. Zhang, F. Gao, S. Gao and D. J. Rogers, "A Switched-Capacitor Interleaved Bidirectional Converter With Wide Voltage-Gain Range for Super Capacitors in EVs," in *IEEE Transactions on Power Electronics*, vol. 35, no. 2, pp. 1536-1547, Feb. 2020, doi: 10.1109/TPEL.2019.2921585.

[7]. Y. Zhang, Y. Gao, J. Li and M. Sumner, "Interleaved Switched-Capacitor Bidirectional DC-DC Converter With Wide Voltage-Gain Range for Energy Storage Systems," in *IEEE Transactions on Power Electronics*, vol. 33, no. 5, pp. 3852-3869, May 2018, doi: 10.1109/TPEL.2017.2719402.

[8]. Y. Zhang, Q. Liu, Y. Gao, J. Li and M. Sumner, "Hybrid Switched-Capacitor/Switched-Quasi-Z-Source Bidirectional DC–DC Converter With a Wide Voltage Gain Range for Hybrid Energy Sources EVs," in *IEEE Transactions on Industrial Electronics*, vol. 66, no. 4, pp. 2680-2690, April 2019, doi: 10.1109/TIE.2018.2850020.

[9]. L. -S. Yang and T. -J. Liang, "Analysis and Implementation of a Novel Bidirectional DC–DC Converter," in *IEEE Transactions on Industrial Electronics*, vol. 59, no. 1, pp. 422-434, Jan. 2012, doi: 10.1109/TIE.2011.2134060.

[10]. M. Lakshmi and S. Hemamalini, "Non isolated High Gain DC–DC Converter for DC Microgrids," in *IEEE Transactions on Industrial Electronics*, vol. 65, no. 2, pp. 1205-1212, Feb. 2018, doi: 10.1109/TIE.2017.2733463.

[11]. C. P. Ragasudha and S. Hemamalini, "Performance Analysis of a High Gain Bidirectional DC-DC Converter Fed Drive for an Electric Vehicle with Battery Charging Capability During Braking," in *IEEE Access*, vol. 12, pp. 14499-14511, 2024, doi: 10.1109/ACCESS.2024.3357726.

[12]. A. R. N. Akhormeh, K. Abbaszadeh, M. Moradzadeh and A. Shahirinia, "High-Gain Bidirectional Quadratic DC–DC Converter Based on Coupled Inductor With Current Ripple Reduction Capability," in *IEEE Transactions on Industrial Electronics*, vol. 68, no. 9, pp. 7826-7837, Sept. 2021, doi: 10.1109/TIE.2020.3013551.

[13]. M. A. Salvador, T. B. Lazzarin and R. F. Coelho, "High Step-Up DC–DC Converter With Active Switched-Inductor and Passive Switched-Capacitor Networks," in *IEEE Transactions on Industrial Electronics*, vol. 65, no. 7, pp. 5644-5654, July 2018, doi: 10.1109/TIE.2017.2782239.

[14]. Y. Zhang, H. Liu, J. Li and M. Sumner, "A Low-Current Ripple and Wide Voltage-Gain Range Bidirectional DC–DC Converter With Coupled Inductor," in *IEEE Transactions on Power Electronics*, vol. 35, no. 2, pp. 1525-1535, Feb. 2020, doi: 10.1109/TPEL.2019.2921570.

[15]. V. Rathore, K. Rajashekara, P. Nayak and A. Ray, "A High-Gain Multilevel dc–dc Converter for Interfacing Electric Vehicle Battery and Inverter," in *IEEE Transactions on Industry Applications*, vol. 58, no. 5, pp. 6506-6518, Sept.-Oct. 2022, doi: 10.1109/TIA.2022.3185183.

[16]. S. B. Santra, D. Chatterjee and T. -J. Liang, "High Gain and High-Efficiency Bidirectional DC–DC Converter With Current Sharing Characteristics Using Coupled Inductor," in *IEEE Transactions on Power Electronics*, vol. 36, no. 11, pp. 12819-12833, Nov. 2021, doi: 10.1109/TPEL.2021.3077584.